

國立臺灣大學醫學院藥理學研究所



博士論文

Graduate Institute of Pharmacology

College of Medicine

National Taiwan University

Doctoral Dissertation

MPT0E028在人類大腸直腸癌與B細胞淋巴癌之
抗癌機轉探討

Evaluation of the anticancer mechanisms of MPT0E028
in human colorectal cancer and B-cell lymphoma

黃瀚立

Han-Li Huang

指導老師: 鄧哲明 博士, 潘秀玲 博士

Advisor: Che-Ming Teng, Ph.D., Shioh-Lin Pan, Ph.D.

中華民國 104 年 3 月

March 2015

Contents



口試委員會審定書.....	i
誌謝.....	ii
Abbreviations.....	iv
中文摘要.....	1
Abstract	3
Chapter 1 Introduction.....	5
1.1 Research Motivation and Aim.....	5
1.2 Literature Reviews.....	7
Chapter 2 Materials and Methods.....	39
2.1 Materials.....	39
2.2 Methods.....	40
Chapter 3 Anticancer Activity of MPT0E028, a Novel Potent Histone Deacetylase Inhibitors, in Human Colorectal Cancer HCT116 Cells <i>in vitro</i> and <i>in vivo</i>	
中文摘要.....	52
Abstract.....	53
3.1 Results.....	54
3.2 Discussion.....	59
Chapter 4 Novel Histone Deacetylase Inhibitor, MPT0E028, Displays Potent Growth-Inhibitory Activity against Human B-cell Lymphoma <i>in vitro</i> and <i>in vivo</i>	
中文摘要.....	76
Abstract.....	77
4.1 Results.....	78

4.2 Discussion.....	85
Chapter 5 Conclusion and Perspectives.....	105
Publications.....	113
References.....	114





國立臺灣大學博士學位論文
口試委員會審定書

探討 MPT0E028 在人類大腸直腸癌與 B 細胞淋巴癌之抗
癌機轉

Evaluation of the anticancer mechanisms of MPT0E028 in
human colorectal cancer and B-cell lymphoma

本論文係黃瀚立君 (F98443009) 在國立臺灣大學藥理學研究所完
成之博士學位論文，於民國 104 年 3 月 9 日承下列考試委員審查通過
及口試及格，特此證明

口試委員：

鄧哲明

(指導教授)

陳育玲

(指導教授)

顏茂雄

陳慶士

劉景平

黃德富

系主任 (所長)

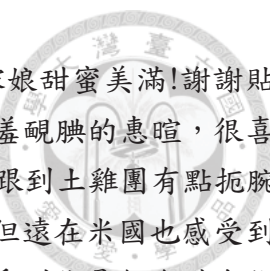
林瓊瓊

致謝



時光飛逝，轉眼間加入實驗室已滿六個年頭，想當初剛進實驗室的青澀無知，很幸運地在許多人的幫助下讓我一路成長到現在，心裡滿是感謝。感謝實驗室大家長 鄧哲明老師，對於老師在國家生技產業投入的心力熱忱，及不吝提攜後進為人師表的風骨印象非常深刻，很感謝能在這樣值得一生學習的好老師下接受指導，鄧老師謝謝您。謝謝年輕美麗的師母，在佳節時刻總能品嚐到您的好手藝，謝謝貼心的您讓我們有家的溫暖。感謝開朗熱情的阿潘學姊，感謝您在我對實驗或未來失去方向時，總是幫我點燈解惑指引方向，謝謝您的支持鼓勵與信任，也謝謝您讓實驗室總是充滿了歡笑。謝謝 陳慶士老師，非常感謝您給予寶貴的機會到 OSU 體驗學習，也感謝您在實驗及生活上給予的協助。謝謝 劉景平老師，感謝您提供的化合物讓我能順利完成這份論文。感謝口試委員 黃德富老師與 顏茂雄老師，感謝你們寶貴的意見讓這篇論文更臻完善。

感謝藥理所所有老師的指導，也謝謝所辦兩位年輕貌美的梁姐姐與沈姐姐，謝謝你們總是熱情的迎接與叮嚀提醒，讓我不用為繁瑣的行政程序煩惱。謝謝明快俐落的雅玲學姊，在您的打點下實驗室總是衣食無缺設備齊全，謝謝您平時在生活上給予的鼓勵與幫助，和學姊聊天真的很開心。謝謝大家閨秀婕妤學姊，感謝妳帶領我學習實驗，學姊修理電子產品的英姿真是令人崇拜!謝謝開朗健談的姿璇學姊，謝謝妳都會順路帶我回家，和健談的學姊聊天很有趣。謝謝聰明蓋世又熱心的輝隆學長，謝謝你總是能提出精闢的建議幫助我完成實驗，也謝謝你在 OSU 的照顧。謝謝認真貼心的岸圻學姊，妳的小禮物跟明信片讓人在異鄉的我們都溫暖了起來，妳認真努力的身影是我學習的榜樣。謝謝阿莎力鄰居思穎學姊，謝謝妳總會一針見血提供我意見和我分享心情，我很愛妳幫我買的包包唷。謝謝幽默風趣的美全學姊，每次聽學姊分享事情都好生動有如身歷其境，學姊做實驗俐落的身影也是我努力的目標，感謝學姊也總是在實驗上給予很多的幫助。謝謝謹慎細心的俊翰學長，謝謝學長在實驗上給予的建議，你的觀察入微與細膩也是我學習的典範。謝謝貼心的儷薰學姊，謝謝妳每次都耐心回答忍受我的蠢問題，也謝謝妳都會像姊姊一樣聽我分享心情。謝謝美麗大方的清裕學姊，謝謝妳都很熱心的幫我解決問題，和妳聊天聽妳精闢的分析總是很開心，祝清清幸福美滿!謝謝貼心的惠珍學姊，謝謝妳聽我分享心情提供我意見，祝學姊之後能一切順心。謝謝氣質優雅的之雅學姊，感謝你在實驗上的幫助，祝福你和學長甜蜜蜜有個世紀婚禮!謝謝俐落大方又可愛的敏吾學姊，感謝妳一直以來在實驗及生活上的幫助，很開心能和妳一起在 OSU 度過兩年受到妳許多照顧也從妳身上學到許多待人處事，也謝謝妳幫我矯正我的審美觀給我很多意見，很喜歡和妳聊天分享心情，對妳有說不盡的感謝!謝謝又 man 又帥氣的皇儒學長，感謝你忍受我當兩年的電燈泡，真的很感謝你的照顧，也謝謝你磨練出我堅強的意志，對學長也有說不盡的感謝，要好好疼咪咪喔!謝謝率性活潑的俐婷學姊，感謝你在實驗上的幫助，祝福你幸福美滿喔!謝謝很強但總是很謙虛的佑維學長，祝福你和之雅學姊甜蜜蜜!謝謝文靜氣質的憶菽學姊，很開心在美國有學姊的陪伴與幫忙，受了妳很多照顧也給妳添了很多麻煩，很懷念

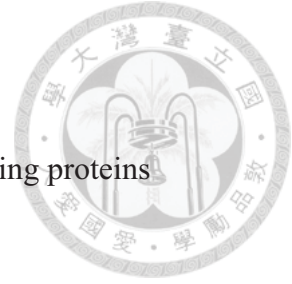


一起到處玩的日子，祝學姊一帆風順喔!謝謝實驗夥伴鐘琺，祝福新嫁娘甜蜜美滿!謝謝貼心活潑的雅琪，很喜歡和你逛街聊天大笑，成為人妻後變超美的!謝謝害羞靦腆的惠暄，很喜歡你的天然萌，祝福你能一路實現你的夢想!謝謝土雞城小開嘉華，沒機會跟到土雞園有點扼腕，祝你在業界發光發熱!謝謝活力十足的玨衡，雖然跟你相處時間不多，但遠在米國也感受到你的熱情與可愛!謝謝帥氣又搞笑的和穎，雖然和你接觸不多，但可以感受到你是個充滿自信又受學姊們關愛的有趣學弟!謝謝超上相的子涵，凡事認真的你做什麼都是游刃有餘。謝謝努力的俊璋，趁你畢業前要多向你討教好吃好玩的資訊。謝謝美麗的強人琪琪、氣質的子瑩、正妹人妻幸蓉、文靜的思淨、靦腆的于傑、可愛的怡琳，謝謝你們在實驗上的幫助!感謝在美國認識的學長姊們及實驗室夥伴們，謝謝你們給予的幫助，很幸運能認識你們和你們有過一段回憶。謝謝羿如學姊的教導與陪伴，很喜歡和你分享心情一同逛街，謝謝你就像大姊姊一樣照顧我。謝謝曉菁學姊、志謙學長，在你們身上學到好多做實驗的技巧，有你們在的實驗室也總是有歡笑。謝謝運動好夥伴明臻學姊，謝謝你給予實驗上的指導，很懷念和你一起去運動到處去吃美食的日子。謝謝氣質優雅的張琳老師，謝謝你像姊姊一樣照顧我陪我聊天分享心情，祝福張老師能一切順利。謝謝裕洲宥庭夫婦及柏廷，和你們聊天出遊真的很開心，希望有機會大家再相聚。謝謝一起出發的好夥伴俊升，祝福 high 咖又三八的你順順利利。謝謝身邊好朋友們的陪伴與照顧，謝謝佳怡、小野、仁芳、范范，有你們分擔心情一同享樂，讓我每天都有愉悅的心情繼續努力。

最後，感謝一直支持鼓勵我陪伴我的爸爸媽媽與姐姐，謝謝你們讓我能無後顧之憂追求理想，謝謝你們不求回報的付出，對你們有無盡的感謝。謝謝瑞賢一路的陪伴與支持，謝謝你不辭辛勞地陪伴我進出晚上與假日的實驗室還遠赴美國，謝謝你陪我度過許多歡笑與淚水，對你也有說不盡的感謝。

再次感謝一路上曾經給予指導幫助的師長與家人朋友。謹以感恩的心獻上本論文，獻給摯愛的家人、師長與朋友們予以惠存，謝謝你們豐富我的人生。

Abbreviations



4E-BPs	Eukaryotic translation initiation factor 4E-binding proteins
Ac-Histone H3	Acetyl-Histone H3
Ac- α -tubulin	Acetyl- α -tubulin
BID	BH3 interacting-domain death agonist
c-Myc	V-myc myelocytomatosis viral oncogene homolog (avian)
CTCL	Cutaneous T-cell lymphoma
DMSO	Dimethyl sulfoxide
eIF4E	Eukaryotic translation initiation factor 4E
ELISA	Enzyme-linked immunosorbent assay
FBS	Fetal bovine serum
GSK3 β	Glycogen synthase kinase 3 beta
HDAC	Histone deacetylase
HUVEC	Human umbilical vein endothelial cell
MM	Multiple Myeloma
MTT	3-(4,5-dimethylthiazol-2-yl)-2,5-diphenyltetrazolium bromide
mRNA	Messenger ribonucleic acid
mTOR	Mammalian target of rapamycin
P70S6K	Ribosome protein s6 kinase
PARP	Poly (ADP-ribose) polymerase
PI	Propidium iodide
PBS	Phosphate buffer saline
PI3K	Phosphatidylinositol-4,5-bisphosphate 3-kinase

PTCL	Peripheral T-cell lymphoma
RT-PCR	Reverse transcription polymerase chain reaction
SAHA	Suberoylanilide hydroxamic acid
siRNA	Small interfering ribonucleic acid
SRB	Sulforhodamine B
STAT	Signal transducers and activators of transcription



中文摘要

隨著人民平均壽命延長及生活習慣的改變，癌症發生率仍持續上升，根據台灣衛生福利部國民健康署統計，癌症已為國人十大死因之首達三十二年。為有效治療癌症，藥物開發在癌症領域中仍是相當重要的課題，其中組蛋白去乙酰酶 (histone deacetylase, HDAC) 為近期相當重要的藥物作用標的。本實驗室和台北醫學大學劉景平教授及潘秀玲副教授合作發展一個新穎的組蛋白去乙酰酶抑制劑 MPT0E028，本篇論文即在探討MPT0E028在人類大腸直腸癌及B細胞淋巴瘤之抗癌機轉。

本篇論文第一部分，我們著重在探討MPT0E028在人類大腸直腸癌中的抗癌機轉及HDAC抑制效果。MPT0E028可以抑制許多癌細胞的生長，尤其對於HCT116細胞最為敏感。相對於第一個被FDA認可的HDAC抑制劑SAHA，MPT0E028可產生較強的細胞凋亡作用及HDAC抑制效果。在HCT116異體移植體內實驗中，MPT0E028可延緩並抑制腫瘤生長，相對於SAHA也具有較強的抑癌效果。

本篇論文第二部分，我們著重在探討MPT0E028在人類B細胞淋巴瘤中的抗癌機轉及MPT0E028作用下，HDAC及Akt之間的關係。根據kinome diversity screen實驗結果發現，MPT0E028具有可直接接合並抑制Akt的能力；而我們也發現，HDAC及Akt皆對MPT0E028所引發的細胞凋亡作用具有貢獻，並且為獨立作用，並顯示相對於SAHA具有較強的效果。除體外實驗，B細胞淋巴瘤動物模式體內實驗中也發現MPT0E028可以延長存活率並且抑制腫瘤生長。

綜合而言，我們的結果顯示MPT0E028具獨特性而有潛力成為癌症治療的新選擇。

關鍵字: MPT0E028, 組蛋白去乙酰酶 (HDAC), Akt, 大腸直腸癌, B細胞淋巴瘤, 細胞凋亡



Abstract



The incidence rate of cancer is increasing as more people live to an old age and as lifestyle changes. According to Health Promotion Administration, Ministry of Health and Welfare in Taiwan, cancer has been the first place of ten leading deaths for thirty-two years. In order to cure cancer efficaciously, drug development is still an important issue in cancer therapy. Histone deacetylase inhibitor (HDAC) has been an important drug target in recent years. Our lab cooperates with Professor Jing-Ping Liou (Taipei Medical University) and Associate Professor Shioh-Lin Pan (Taipei Medical University) to develop a novel HDAC inhibitor MPT0E028. In this thesis, we investigated the anticancer mechanism of MPT0E028 in human colorectal cancer and B-cell lymphoma.

In the first part of this thesis, we focus on the antiproliferation effect and the anti-HDAC potency of MPT0E028 in human colorectal carcinoma. MPT0E028 can inhibit a panel of cancer cells, especially most potent in HCT116 cells. MPT0E028 can induce stronger apoptosis effect and HDAC enzyme inhibition *in vitro* compared to SAHA, the first therapeutic HDAC inhibitor approved by FDA. HCT116 xenograft tumor growth was delayed and inhibited under treatment of MPT0E028 *in vivo*, which also showed a better antitumor efficacy than SAHA.

In the second part of this thesis, we focus on the antitumor effect of MPT0E028 in human B-cell lymphoma and the relationship between HDACs and Akt under the treatment of MPT0E028. According to kinome diversity screen data, MPT0E028 was found to exhibit direct Akt targeting ability. We revealed that both its inhibitory activity on HDAC and Akt contribute to MPT0E028-induced apoptosis, which functioned independently and showed stronger effect than SAHA. Besides *in vitro* experiment, *in vivo* study also showed that MPT0E028 may prolong the survival rate and inhibit tumor

growth in B-cell lymphoma model.

Taken together, our results demonstrated that MPT0E028 has unique properties and may be a potential and promising anti-cancer therapeutic option.



Keywords: MPT0E028, histone deacetylase (HDAC), Akt, colorectal cancer, B-cell lymphoma, apoptosis

Chapter 1 Introduction

1.1 Research Motivation and Aim



Cancer has been an increasing and threatening disease among the world as more people live to an old age and lifestyle changes. Although people spent decades trying to fight cancer, the outcome seems not so satisfied. Traditional chemotherapy can kill cancer cells efficiently; however, it may also target normal cells, which lead to severe side effect. How to cure cancer efficiently and safely is a throne problem in recent years. To date, people are still looking for appropriate cancer treatment option. Drug development is an important issue and urgent medical need in cancer therapy. Therefore, our main goal is to develop a novel, promising, and safe drug for cancer treatment.

Small molecule target therapy has been a promising therapeutic option in cancer and many different drug targets are under investigated. HDACs are one of the promising drug targets since they are overexpressed in cancer cells, which control chromosome condensation to regulate gene expression. We cooperate with Professor Jing-Ping Liou (Taipei Medical University) and Associate Professor Shio-Lin Pan (Taipei Medical University) to develop MPT0E028, a small molecule designed as a HDAC inhibitor. Our specific aim is trying to develop MPT0E028 as a potential therapeutic option in cancer therapy.

First, we need to figure out the antitumor and HDAC inhibition effect of MPT0E028, comparing to the first HDAC inhibitor, SAHA. In the first part of this thesis, we tried to determine whether MPT0E028 as truly a HDAC inhibitor. Second, since HDAC inhibitors exhibit their antitumor effect especially against T-cell

lymphoma, we also want to know whether MPT0E028 may be effective in B-cell lymphoma. In the second part of this thesis, we tried to determine the antitumor effect of MPT0E028 against human B-cell lymphoma. In addition to HDAC inhibition effect, we also tried to find out other possible mechanisms of MPT0E028.

Since there are no local designed and developed new drugs in Taiwan, the main goal of this thesis is to discover and develop novel anticancer compound, MPT0E028, to become a promising anticancer agent.

1.2 Literature Reviews



Colorectal Cancer

Colorectal cancer is the third most common type of cancer diagnosed and common cause of cancer-related death in Taiwan (Fig. 1-1) and in the United States. According to the report published by American Cancer Society in 2014, an estimated 96,830 cases of colon and 40,000 cases of rectal cancer are expected to be diagnosed in 2014; while an estimated 50,310 deaths from colorectal cancer are expected to occur in 2014, accounting for about 8% of all cancer deaths (Siegel, Ma et al. 2014) (Fig. 1-2). The histological progression of colorectal cancer from adenoma to carcinoma has been correlated to sequence of genetic mutations (Fearon and Vogelstein 1990) (Boland and Goel 2005), which involves genes such as aberrant crypt foci (*APC*), *K-RAS*, and *TP53* (Fearhead, Wilding *et al.* 2002) (Fig. 1-3). The *APC* gene is the most commonly mutated gene in colorectal cancer, which may result in the deregulation of Wnt-APC- β -catenin signaling pathway. Disruption of the TGF- β IIR/SMAD4 pathway and mutations in mismatch repair genes (e.g. *hMLH1*, *hMSH2*) and cyclin-dependent kinase inhibitors (e.g. *CDKN2A*) have all been identified as key factors in the development and progression of colorectal cancer.

Surgery is the most common treatment for early-stage colorectal cancer. Chemotherapy (anticancer drugs) alone, or combination therapy with monoclonal antibodies are also commonly used for metastatic colorectal cancer (Price, Segelov et al. 2013) (Fig. 1-4). There are three targeted monoclonal antibodies approved by the FDA to treat metastatic colorectal cancer: bevacizumab (Avastin, anti-VEGFA), cetuximab (Erbix, anti-EGFR) and panitumumab (Vectibix, anti-EGFR). In addition, there are many small molecule inhibitors targeting oncogenic proteins or overexpressed molecule

(e.g. HDACs) being investigated, such as histone deacetylase inhibitors (HDACi) (Mariadason 2008).

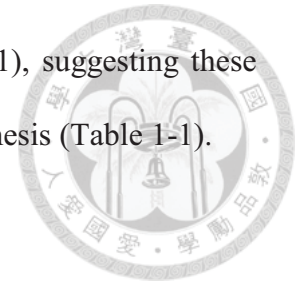


Non-Hodgkin's Lymphoma

According to the report published by American Cancer Society, non-Hodgkin's lymphomas (NHLs) make up approximately 3-4% of deaths in the United States and about 85 percent of the cases are B-cell lymphomas (Siegel, Ma et al. 2014) (Fig. 1-1). Recent advances in molecular genetics have significantly deepened the understanding of the biology of these diseases. B-cell lymphomas arise during different steps of B-lymphocyte development and represent their malignant counterpart. (Nogai, Dorken *et al.* 2011) (Fig. 1-5) Somatic hypermutation (SHM) and class switch recombination (CSR) have been suggested to play an important role in lymphogenesis. Both reactions are mediated by the B-cell specific enzyme activation-induced cytidine deaminase (AID), and AID can mutate genes such as *BCL2*, *BCL6*, *MYC* and *PIMI*. However, the significance of these mutations is currently unclear, since they have also been detected in normal germinal center B cells.

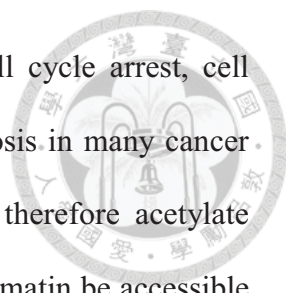
Current strategies for the treatment of NHLs, including B-cell lymphomas, are monoclonal antibodies (e.g. rituximab), either as single agent or in combination with chemotherapy or radiotherapy. However, monoclonal antibodies often result in relapse and resistance due to a variety of molecular mechanisms. Therefore, discovery and development of novel anticancer agents to improve overall survival in cancer patients becomes an essential and urgent medical need. Target therapy, such as proteasome inhibitors, mTOR inhibitors, tyrosine kinase inhibitors and histone deacetylase inhibitors (HDACi), plays an important role in clinical oncology (Johnston, Yuan *et al.*

2010; Mahadevan and Fisher 2011; Sawas, Diefenbach *et al.* 2011), suggesting these pathways represent key signal transductions in lymphoma tumorigenesis (Table 1-1).



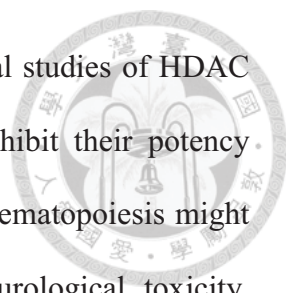
Histone Deacetylase (HDAC)

Histone deacetylases (HDACs) are a family of enzymes which remove acetyl group from histone lysine tails leading to chromatin condensation and transcriptional repression (Kazantsev and Thompson 2008) (Fig. 1-6). HDACs have already been found overexpressed in tumor cells, which make this target a potential target therapy option. At present, there are four classes of HDACs. Class I (HDAC1, 2, 3, and 8) mainly localizes in the nucleus; class II (IIa: HDAC4, 5, 7, and 9; IIb: HDAC6 and 10) may shuttle between cytoplasm and the nucleus. Class III HDACs also known as sirtuins (sirtuins 1-7) and requires NAD^+ as a cofactor for enzymatic activity, whereas HDAC11 has conserved residues in its catalytic center and is the sole member of Class IV. Class I, II and IV are classical HDACs which need Zn^{2+} for enzymatic activity and inhibited by HDAC inhibitors due to chelating Zn^{2+} ion in their catalytic sites (Fig. 1-7 and Fig. 1-8; Table 1-2) (Bolden, Peart *et al.* 2006) (Dokmanovic, Clarke *et al.* 2007; Kazantsev and Thompson 2008). In addition to acetylate histone proteins, HDACs can also target to non-histone substrate (e.g. p53, HSP90, YY1 *etc.*) (Spange, Wagner *et al.* 2009) (Table 1-3). Identified acetylated non-histone proteins demonstrate that reversible lysine acetylation affects mRNA stability, and the localization, interaction, degradation and function of proteins (Spange, Wagner *et al.* 2009) (Fig. 1-9). Most non-histone proteins targeted by acetylation are relevant for tumorigenesis, cancer cell proliferation and immune functions. For example, HDAC6-mediated Hsp90 deacetylation stabilizes Akt, c-Myc and other oncoproteins stability and enables of the glucocorticoid receptor by ligands.



HDAC inhibitors have multiple mechanisms of inducing cell cycle arrest, cell differentiation and cell death through apoptosis, autophagy or necrosis in many cancer cells. HDAC inhibitors may inhibit HDAC enzyme activity and therefore acetylate histone proteins to loose chromatin condensation, which makes chromatin be accessible for transcription factors to enhance downstream apoptosis gene transcription. In addition to acetylating histone proteins, HDAC inhibitors may also target to non-histone proteins to exert its antitumor activity. They have also shown to inhibit angiogenesis, migration and metastasis (Fig. 1-10) (Bolden, Peart *et al.* 2006; Marks and Breslow 2007; Xu, Parmigiani *et al.* 2007; Marks and Xu 2009). According to their broad effect on anticancer, HDAC inhibitors become promising anticancer agents and are effective especially in hematological malignancies undergoing many clinical trials (Prince, Bishton *et al.* 2009; Stimson, Wood *et al.* 2009). Vorinostat (SAHA) (Mann, Johnson *et al.* 2007) and romidepsin (Whittaker, Demierre *et al.* 2010) are now two HDAC inhibitors (vorinostat and romidepsin) approved by FDA for cutaneous T-cell lymphoma (CTCL) and belinostat for peripheral T-cell lymphoma (PTCL). Panobinostat has been recently approved for multiple myeloma (MM), which is to be used in combination with bortezomib and dexamethasone. There are also many HDAC inhibitors in clinical trials (Ma, Ezzeldin *et al.* 2009) (Table 1-4).

The structure of HDAC inhibitors can be divided into three main groups: hydroxamates, benzamides and thiols. Generally, these HDAC inhibitors are composed of three parts: cap, zinc-binding domain, and linker connects the two. Zinc-binding domain chelates the active site zinc ion (Zn^{2+}) of HDACs. Surface recognition cap moiety is well-tolerated for extraordinary variability, which occludes the entrance of the active site pocket (Fig. 1-11). Although many HDAC inhibitors are under investigated,



various toxicity profile and side effects arise in the available clinical studies of HDAC inhibition in the treatment of cancer. Since HDAC inhibitors exhibit their potency, especially in hematologic malignancy, the toxicity against normal hematopoiesis might be predictable. Gastrointestinal side effects, constitutive and neurological toxicity, metabolic toxicity, electrolyte disturbance, and cardiac effects are also described in clinical trials. On the other hand, HDAC inhibition may change gene expression due to epigenetic regulation; however, HDAC inhibitors usually affect less than 10% of genes in cancer cells. Divergent effects of HDAC inhibition on the global gene expression profiles have also been a problem, and this is further complicated by altered HDAC expression induced by HDAC inhibitors. Although initial studies of HDAC inhibitors are encouraging and promising in the treatment of cancer, additional pharmacological characterization and detailed mechanisms are still needed (Bruserud, Stapnes et al. 2007) (Table 1-5).

PI3K/Akt/mTOR Pathway

Upregulation of the PI3K/Akt/mTOR pathway occurs in many human cancers, including lymphoma, therefore, this pathway is considered as a target for anticancer therapy in several human cancer types (Vivanco and Sawyers 2002; Hennessy, Smith *et al.* 2005; Johnston, Yuan *et al.* 2010). Activation of phosphatidylinositol-3 kinase (PI3K) enables recruitment of the serine/threonine kinase Akt to the cell membrane and therefore phosphorylates and activates Akt. Akt then activates downstream protein mTOR which therefore phosphorylates translation initiation through ribosomal p70S6 kinase (p70S6k) or eukaryotic translation initiation factor 4E (eIF4E) binding proteins (4E-BPs) and this promotes its dissociation from the translation factor eIF4E which allows stimulating RNA translation (Engelman 2009). Akt could also activate GSK3 β to

manipulate cell cycle and glucose metabolism (Liu, Cheng *et al.* 2009). Akt is a key regulator of this pathway promoting cell growth and cell survival (Fig. 1-12) (Manning and Cantley 2007) and an important oncoprotein dysregulated in many cancers causing tumor progression. Many Akt inhibitors are being developed for clinical investigation (Table 1-6) (Pal, Reckamp *et al.* 2010) .

Apoptosis

Current cancer therapies, for example, chemotherapy, radiation therapy, immunotherapy or recently gained popularity small molecule inhibitors, primarily exert their antitumor effect by triggering apoptosis in cancer cells. Apoptosis is a process of programmed cell death (PCD), which is used by multicellular organisms to dispose of unwanted cells in a diversity of settings. Most cases of apoptosis may result in caspases activation. Caspases cleave a number of different substrates in the cytoplasm or nucleus leading to many of the morphologic features of apoptotic cell death, which include blebbing, cell shrinkage, nuclear fragmentation, chromatin condensation and chromosomal DNA fragmentation (Fulda and Debatin 2006).

To date, three main routes to apoptosis-associated caspase activation have been firmly established in mammals. The extrinsic pathway, which stimulator activates death receptors and then activates the initiator caspase 8, can propagate the apoptosis signal by direct cleavage of downstream effector caspases such as caspase 3. The intrinsic pathway is initiated by the release of apoptogenic factors such as cytochrome c from the mitochondrial intermembrane space. The release of cytochrome c into the cytosol triggers caspase 3 activation through formation of the cytochrome c/Apaf-1/caspase 9-containing apoptosome. When caspase 3 is activated, it may activate enzyme that

detect and signal DNA single-strand breaks, which is called poly(ADP-ribose) polymerase (PARP) (Taylor, Cullen et al. 2008) (Fig. 1-13).



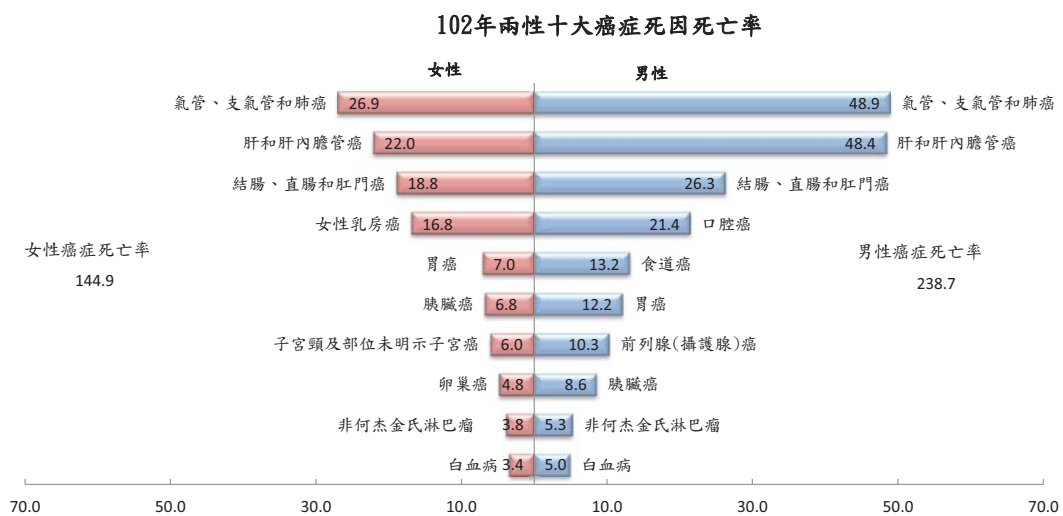




Figure 1-1. Ten Leading Cancer Types for Cancer Related Deaths by Sex in Taiwan, 2011. (Ministry of Health and Welfare, Taiwan, 2014)

Estimated New Cases*

		Males		Females			
Prostate	233,000	27%			Breast	232,670	29%
Lung & bronchus	116,000	14%			Lung & bronchus	108,210	13%
Colorectum	71,830	8%			Colorectum	65,000	8%
Urinary bladder	56,390	7%			Uterine corpus	52,630	6%
Melanoma of the skin	43,890	5%			Thyroid	47,790	6%
Kidney & renal pelvis	39,140	5%			Non-Hodgkin lymphoma	32,530	4%
Non-Hodgkin lymphoma	38,270	4%			Melanoma of the skin	32,210	4%
Oral cavity & pharynx	30,220	4%			Kidney & renal pelvis	24,780	3%
Leukemia	30,100	4%			Pancreas	22,890	3%
Liver & intrahepatic bile duct	24,600	3%			Leukemia	22,280	3%
All Sites	855,220	100%	All Sites	810,320	100%		

Estimated Deaths



		Males		Females			
Lung & bronchus	86,930	28%			Lung & bronchus	72,330	26%
Prostate	29,480	10%			Breast	40,000	15%
Colorectum	26,270	8%			Colorectum	24,040	9%
Pancreas	20,170	7%			Pancreas	19,420	7%
Liver & intrahepatic bile duct	15,870	5%			Ovary	14,270	5%
Leukemia	14,040	5%			Leukemia	10,050	4%
Esophagus	12,450	4%			Uterine corpus	8,590	3%
Urinary bladder	11,170	4%			Non-Hodgkin lymphoma	8,520	3%
Non-Hodgkin lymphoma	10,470	3%			Liver & intrahepatic bile duct	7,130	3%
Kidney & renal pelvis	8,900	3%			Brain & other nervous system	6,230	2%
All Sites	310,010	100%	All Sites	275,710	100%		

Figure 1-2. Ten Leading Cancer Types for the Estimated New Cancer Cases and Deaths by Sex, United States, 2014. (Siegel, Ma et al. 2014)

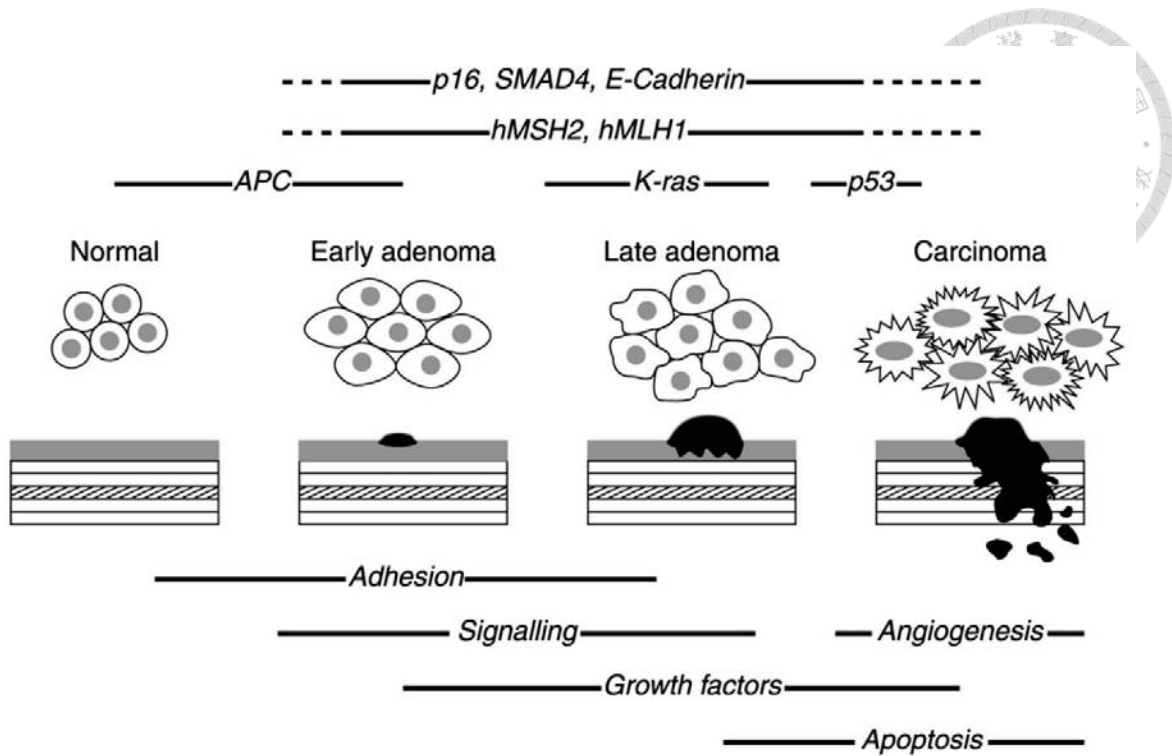


Figure 1-3. Basic outline of the adenoma to carcinoma sequence. The temporal order in which key genes may be affected is shown above the histological stages of disease during which they are thought to occur. Broken lines are used where the order of accumulation of genetic events is uncertain. Functional pathways affected are indicated at the bottom of the diagram. (Fearnhead, Wilding et al. 2002)

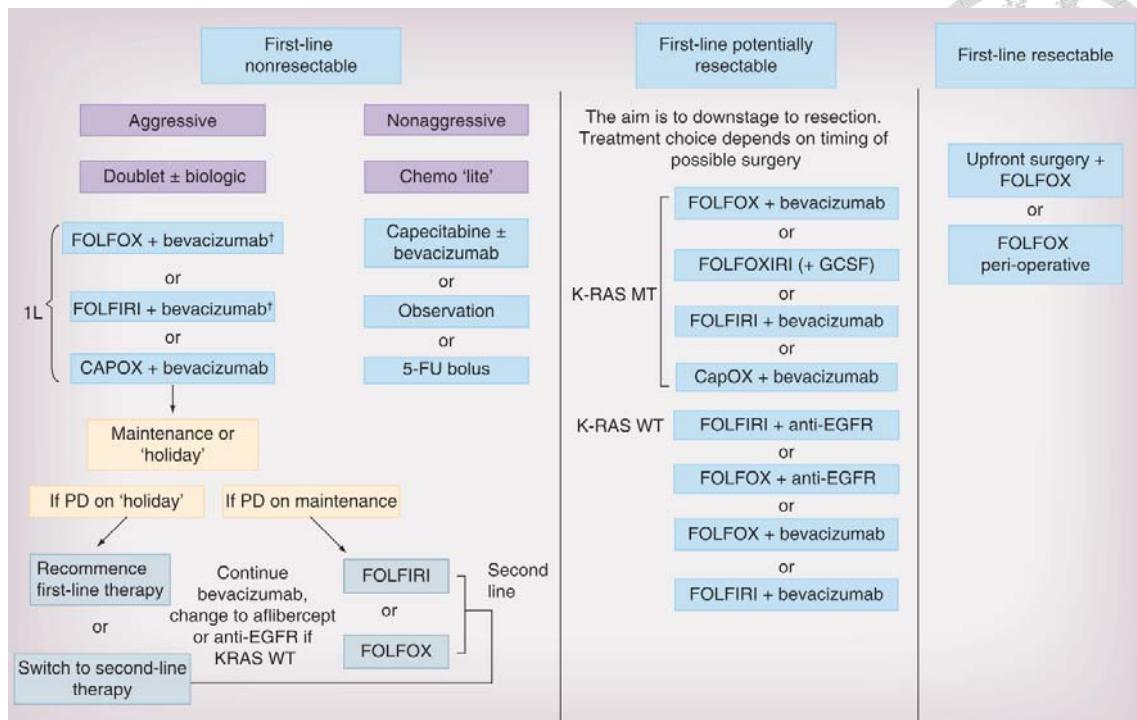


Figure 1-4. Proposed chemotherapy management algorithm for metastatic colorectal cancer. † If aim is downstaging or bulky and symptomatic disease is present in KRAS WT patients, anti-EGFR should also be considered. EGFR: EGF receptor; MT: Mutation; PD: Progressive disease; WT: Wild-type. (Price, Segelov et al. 2013)

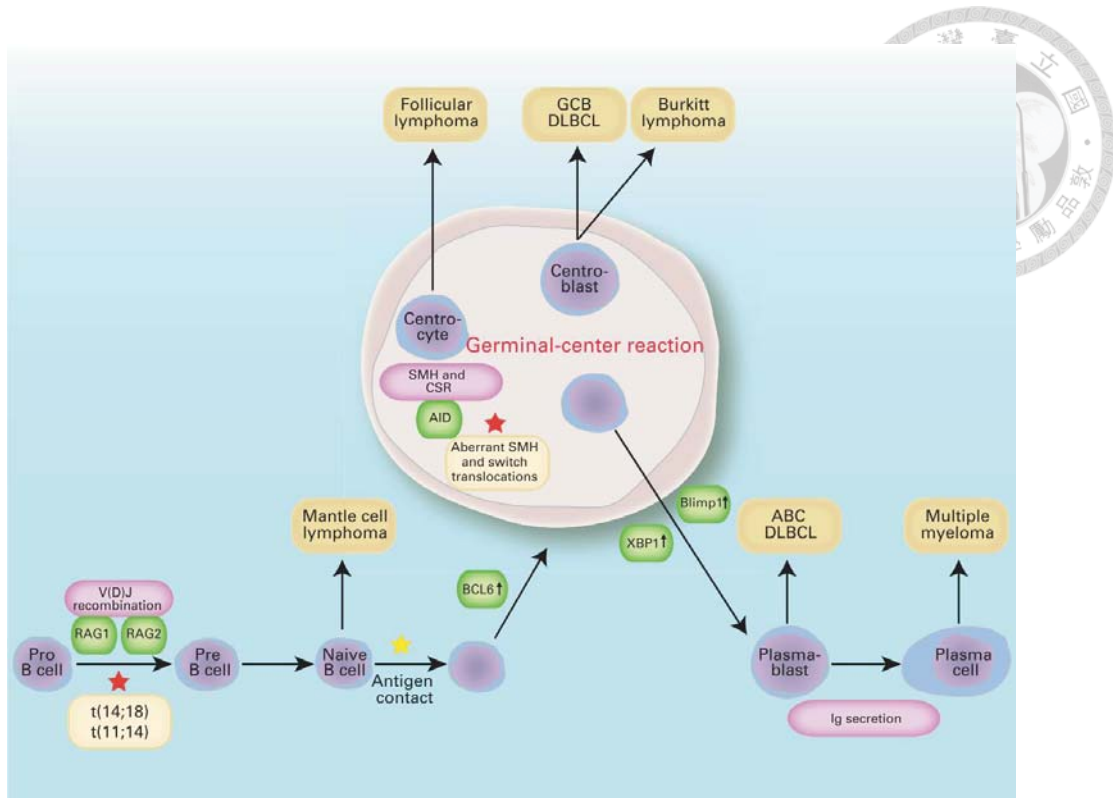


Figure 1-5. Lymphomas arise at different stages of B-cell differentiation. Specific recombination events are prone to the development of chromosomal aberrations. Recombination activating gene 1 (RAG1)-dependent and RAG2-dependent V(D)J recombination takes place in the bone marrow. The potentially resulting t(14;18) and t(11;14) represent critical first steps in lymphomagenesis of different lymphoma subtypes. After antigen contact, the stimulated B cells migrate to the lymph node and form the germinal center after upregulation of BCL6. The events during the germinal center reaction include activation-induced cytidine deaminase (AID)-mediated somatic hypermutation and class-switch recombination, which are critical events for lymphoma evolution. The germinal center reaction is terminated by the differentiation of B cells into plasma cells. XBP1 and Blimp-1 are key regulators for plasmacytic differentiation. GCB DLBCL, germinal center B-cell-like diffuse large B-cell lymphoma; SMH, somatic hypermutation; CSR, class-switch recombination; ABC DLBCL, activated B-cell-like diffuse large B-cell lymphoma; Ig, immunoglobulin. (Nogai, Dorken *et al.* 2011)

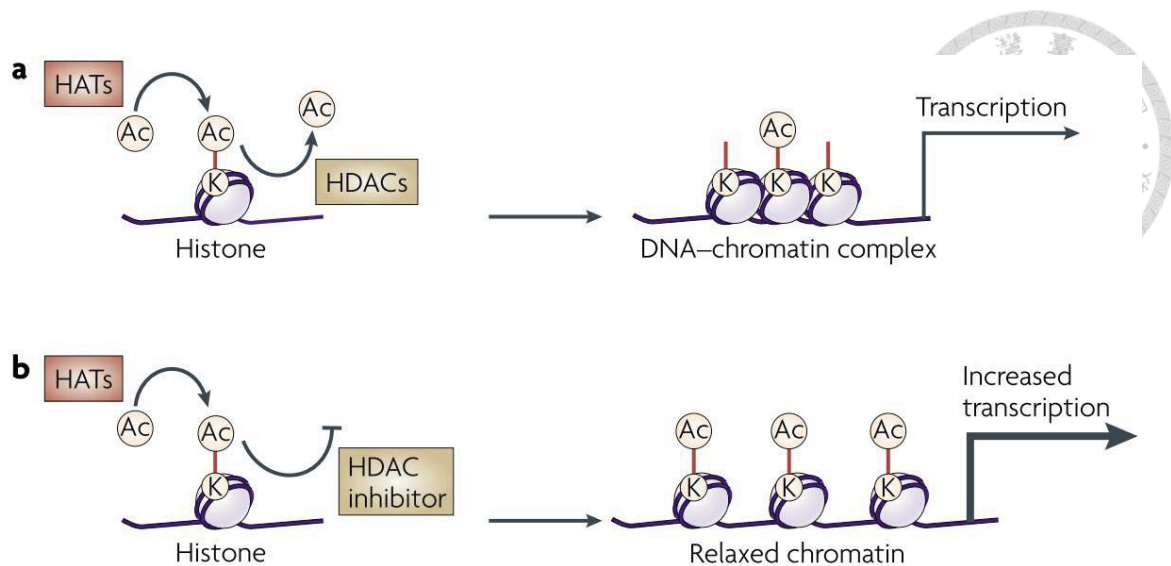
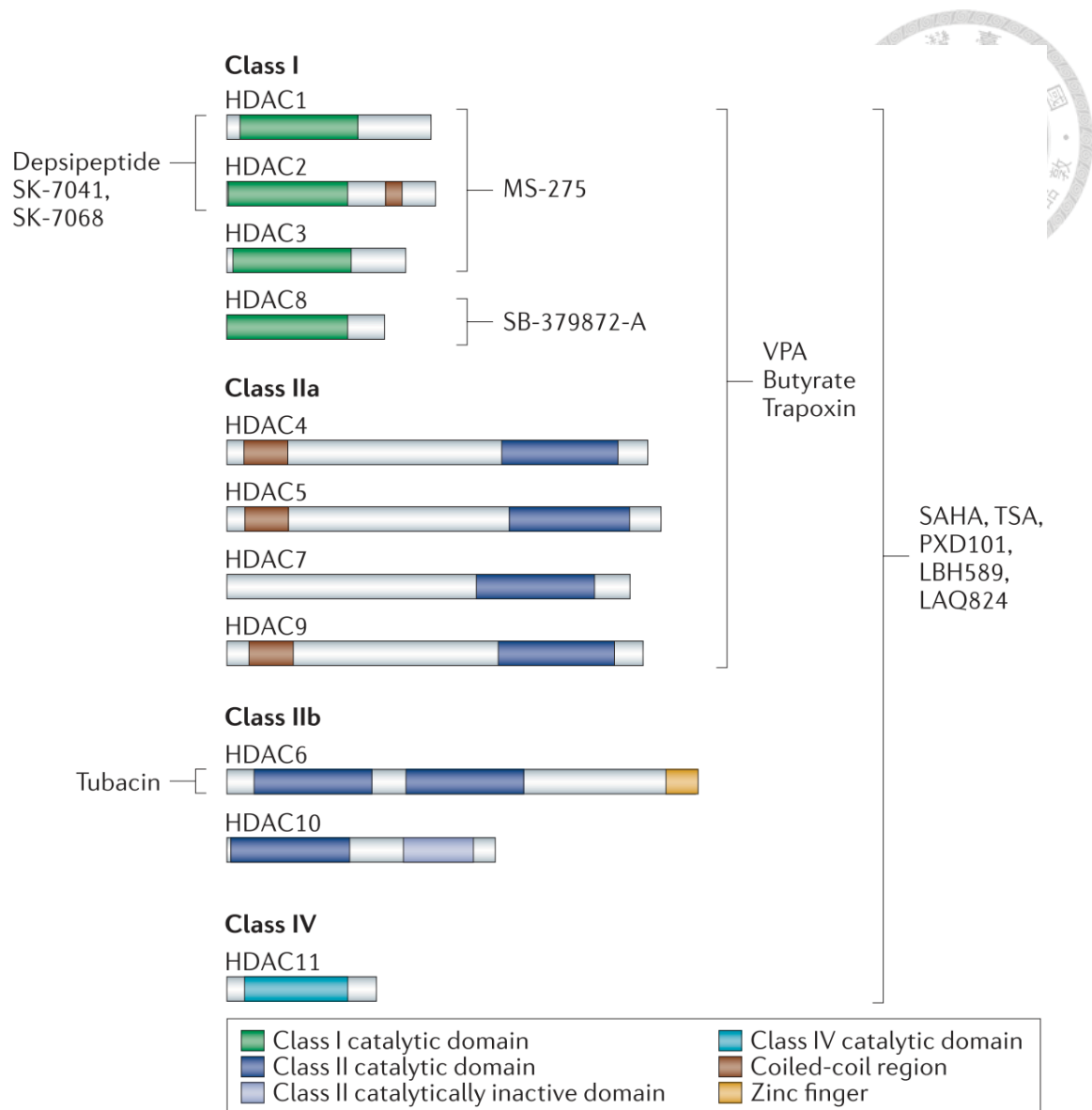


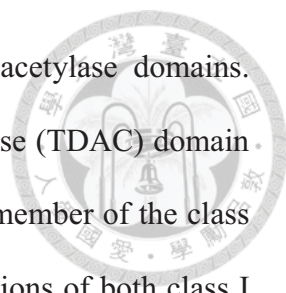
Figure 1-6. Effect of HDAC inhibitors on chromatin remodelling and transcription.

a. Levels of histone acetylation at specific lysine (K) residues are determined by concurrent reactions of acetylation (Ac) and deacetylation, which are mediated by histone acetylases (HATs) and histone deacetylases (HDACs). This histone acetylation is vital for establishing the conformational structure of DNA–chromatin complexes, and subsequently transcriptional gene expression. b. By blocking the deacetylation reaction, HDAC inhibitors change the equilibrium of histone acetylation levels, leading to increased acetylation, chromatin modification to relax conformation and transcription upregulation. (Kazantsev and Thompson 2008)



SAHA, suberoylanilide hydroxamic acid; SIRT, sirtuin; TSA; trichostatin A; VPA, valproic acid.

Figure 1-7. The histone deacetylase family. Histone deacetylases (HDACs) catalyse the removal of acetyl groups from lysine residues in histone amino termini, leading to chromatin condensation and transcriptional repression. Eighteen HDACs have been identified in humans, and they are subdivided into four classes based on their homology to yeast HDACs, their subcellular localization and their enzymatic activities. The class I HDACs (1, 2, 3 and 8) are homologous to the yeast RPD3 protein, can generally be detected in the nucleus and show ubiquitous expression in various human cell lines and tissues. Class II HDACs (4, 5, 6, 7, 9 and 10) share homologies with the yeast Hda1 protein and can shuttle between the nucleus and the cytoplasm. The class IIb HDACs,



HDAC6 and 10 are found in the cytoplasm and contain two deacetylase domains. HDAC6 has unique substrate specificity with an α -tubulin deacetylase (TDAC) domain specific for the cytoskeletal protein α -tubulin. HDAC11 is the sole member of the class IV HDACs. It shares sequence similarity with the catalytic core regions of both class I and II enzymes but does not have strong enough identity to be placed in either class. The figure shows the class I (HDAC1, 2, 3 and 8), class IIa (HDAC4, 5, 7 and 9), class IIb (HDAC6 and 10) and class IV (HDAC11) HDACs with the various structural/functional domains listed. The capacity of structurally diverse HDACi to inhibit the activity of different HDAC classes or specific HDACs is also shown. (Bolden, Peart *et al.* 2006)

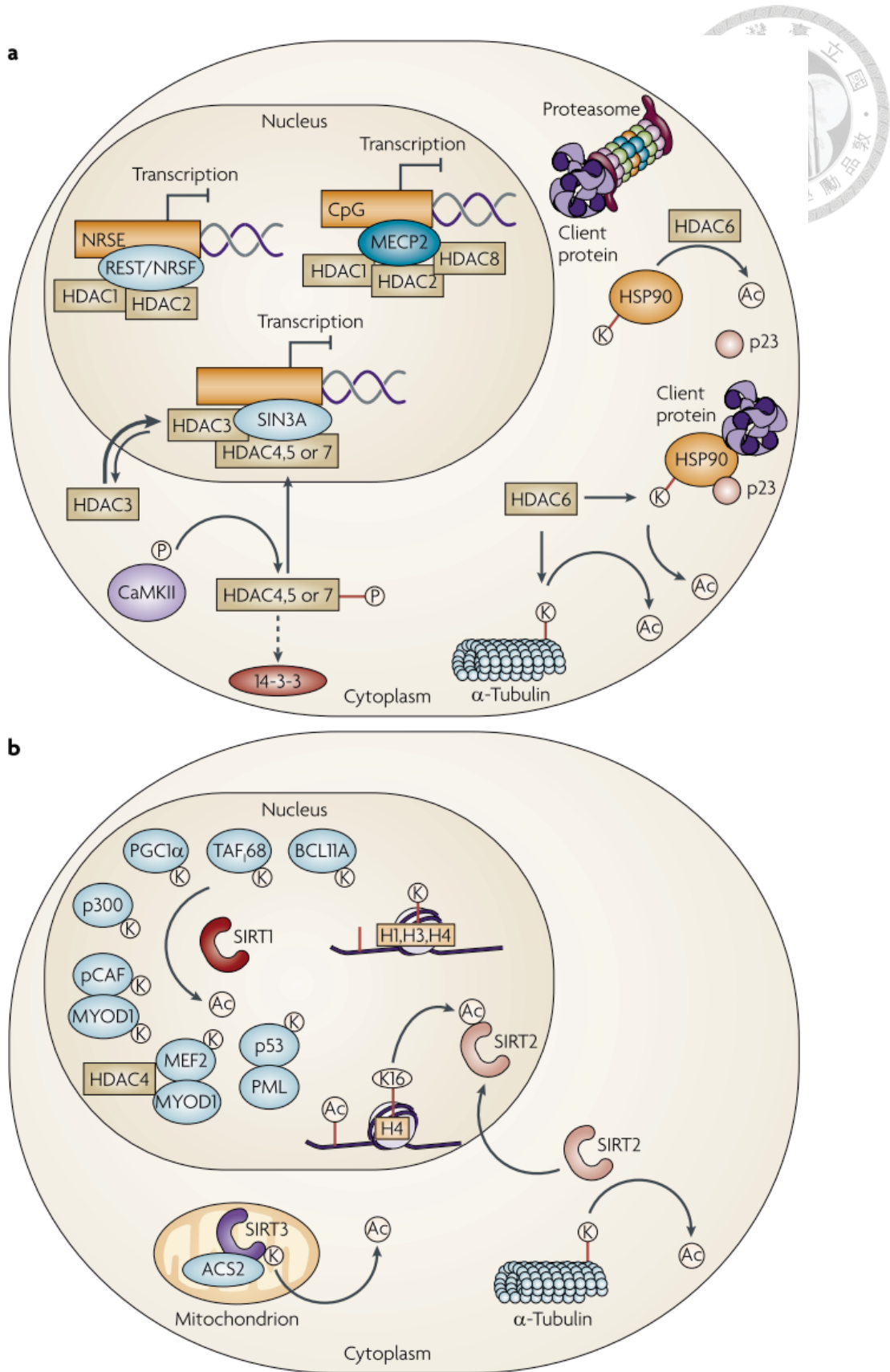
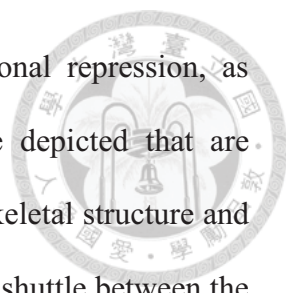


Figure 1-8. Schematic of representative HDAC effects in the nucleus and cytoplasm. a. Histone deacetylase (HDAC) complexes form in the nucleus to regulate



transcription, typically through mechanisms leading to transcriptional repression, as depicted by the blocked lines at promoters. Some examples are depicted that are relevant to CNS disorders. In addition, HDAC6 is involved in cytoskeletal structure and proteasomal degradation, whereas HDAC4, HDAC5 or HDAC7 can shuttle between the nucleus and cytosol and are phosphorylated in the cytosol. b | Schematic depiction of several protein targets of sirtuin 1 (SIRT1) deacetylation in the nucleus, as well as proposed roles for SIRT2 in histone deacetylation and cytoskeletal structure, and SIRT3 in mitochondrial function. ACS2, acetyl-CoA synthetase; BCL11A, B-cell CLL/lymphoma 11A (zinc finger protein); CaMKII, calcium/calmodulin-dependent protein kinase 2; HSP90, heat-shock protein 90; MECP2, methyl-CpG-binding protein 2; MEF2, myocyte enhancing factor 2; MYOD1, myogenic differentiation 1; NRSE, neuron restrictive silencer element; pCAF, p300/CBP-associated factor (also known as KAT2B); PGC1a, peroxisome proliferator-activated receptor-g, coactivator 1a; PML, promyelocytic leukaemia; REST/NRSF, RE1-silencing transcription factor. (Kazantsev and Thompson 2008)

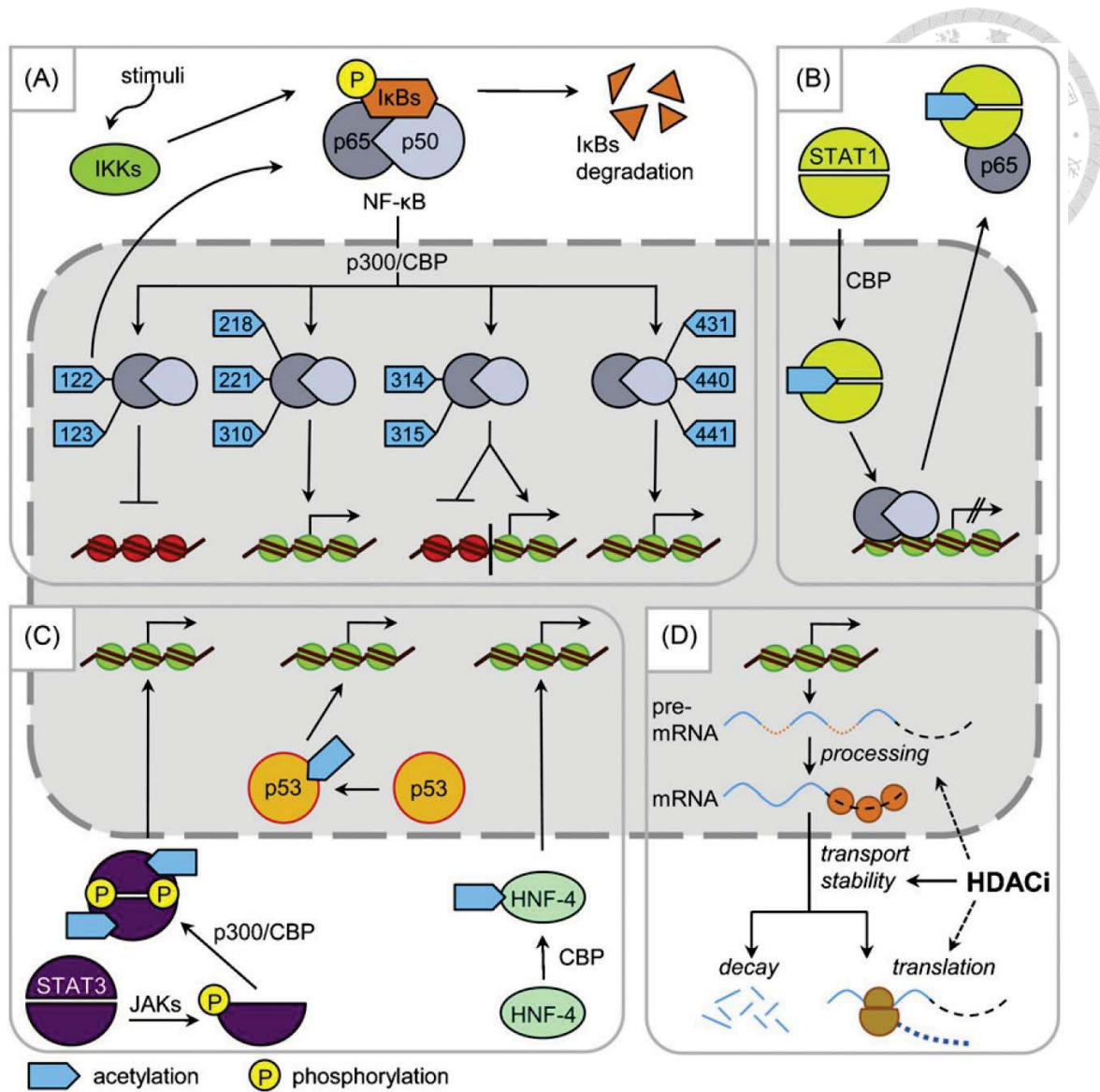


Figure 1-9. Effects of acetylation on signaling, transcription and posttranscriptional events. (A) p300/CBP-mediated site-specific acetylation of p65 or p50 has a major impact on the transcriptional activity of NF- κ B in vitro. Acetylation of p65 (K 218, K 221 and K 310) or p50 (K 431, K 440 and K 441) activates transcription. The acetylation of p65 on K 122 and K 123 inhibits its DNA binding, favours I κ B binding and results in the cytoplasmic accumulation of NF κ B. Acetylation of p65 on K 314 and K 315 regulates a specific set of NF κ B target genes. (B) Acetylation of STAT1 induces its interaction with p65. The resulting complex dissociates from DNA, translocates into the cytoplasm and inhibits the transcriptional activity of NF- κ B. (C)

Acetylation of transcription factors can affect dimerization (e.g., STAT3), DNA binding affinity (e.g., p53) or subcellular localization (e.g., HNF-4) and thereby transcriptional activity. (D) HDACi alters the cellular acetylation state of various proteins including factors needed for pre-mRNA processing or translation. Additionally HDACi have been shown to alter mRNA stability. (Spange, Wagner et al. 2009)

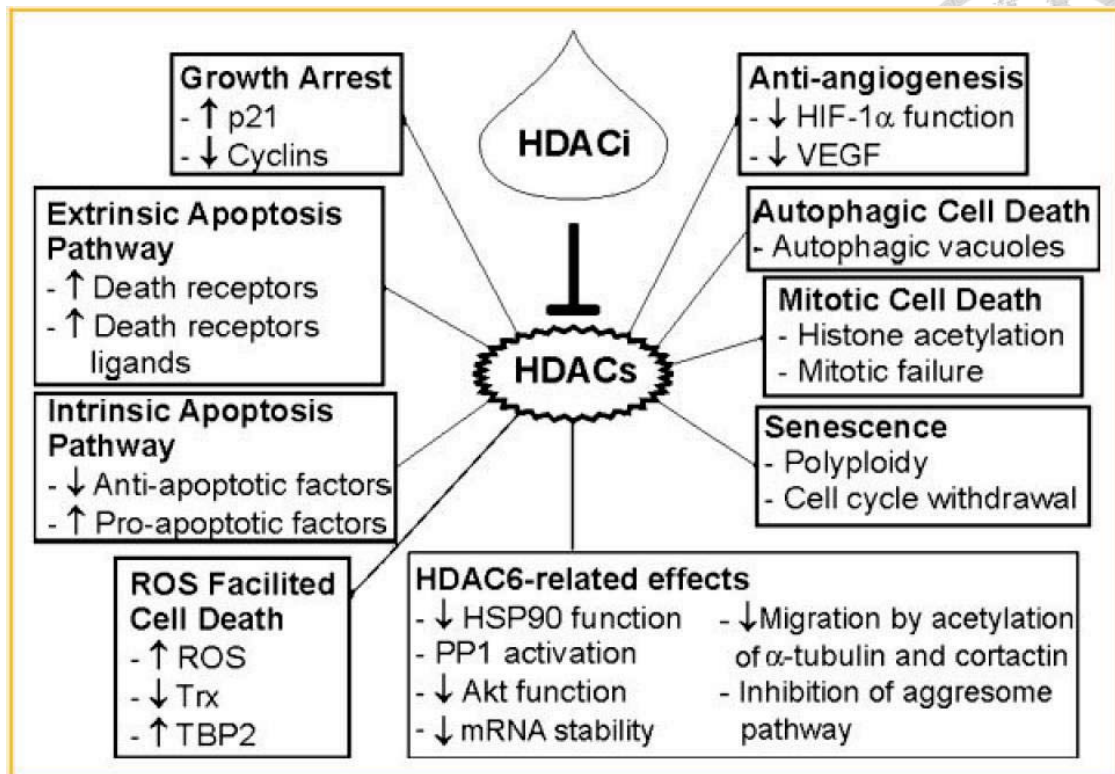


Figure 1-10. Zinc-dependent histone deacetylase inhibitors can induce transformed cell growth arrest and death by different pathways. HDAC6, histone deacetylase 6; HIF-1 α , hypoxia induced factor-1 α ; HSP90, heat shock protein 90; PP1, protein phosphatase 1; ROS, reactive oxygen species; TBP2, thioredoxin binding protein 2; Trx, thioredoxin; VEGF, vascular endothelial growth factor. (Marks and Xu 2009)

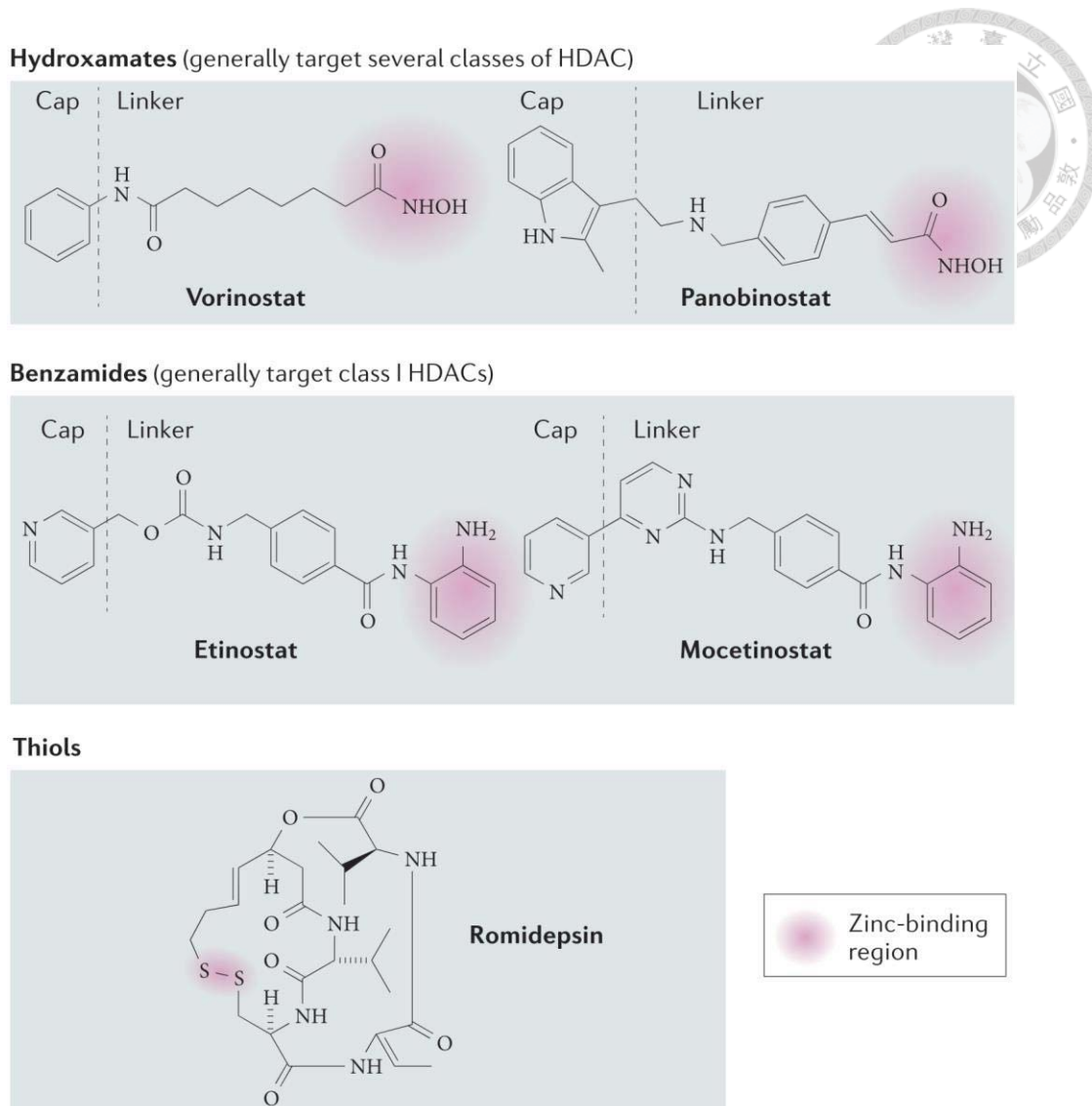


Figure 1-11. Structure of HDAC inhibitors. In general, the pharmacophore of histone deacetylase (HDAC) inhibitors is composed of three regions: a ‘cap’ region or ‘surface recognition domain’, which occludes the entrance of the active site pocket; a ‘zinc-binding group’, which chelates the zinc ion in the active site and is required for catalytic function; and a ‘linker’ region, which connects the two. Historically, most HDAC inhibitors have been hydroxamates; however, other zinc-binding groups are now being used to increase specificity and selectivity, including benzamide derivatives, thiols, sulphamides, ketones and trithiocarbonate. Hydroxamate derivatives generally inhibit HDACs from multiple classes (for example, vorinostat and panobinostat), whereas benzamide derivatives are generally restricted to inhibiting class I HDACs (for

example, etinostat, mocetinostat and the HDAC3-specific inhibitors RG2833 and RGFP966). The cap region is predominantly responsible for selectivity, and as the cap region can not only bind to the HDAC itself but also to other complex components near the active site, it could be used to design inhibitors that target HDACs residing in specific complexes. Finally, linker modifications may also serve to direct specificity, such as the addition of an aromatic ring that can fit into the enlarged catalytic pocket of HDAC7 that is not present in class I or class IIb HDACs. (Falkenberg and Johnstone 2014)

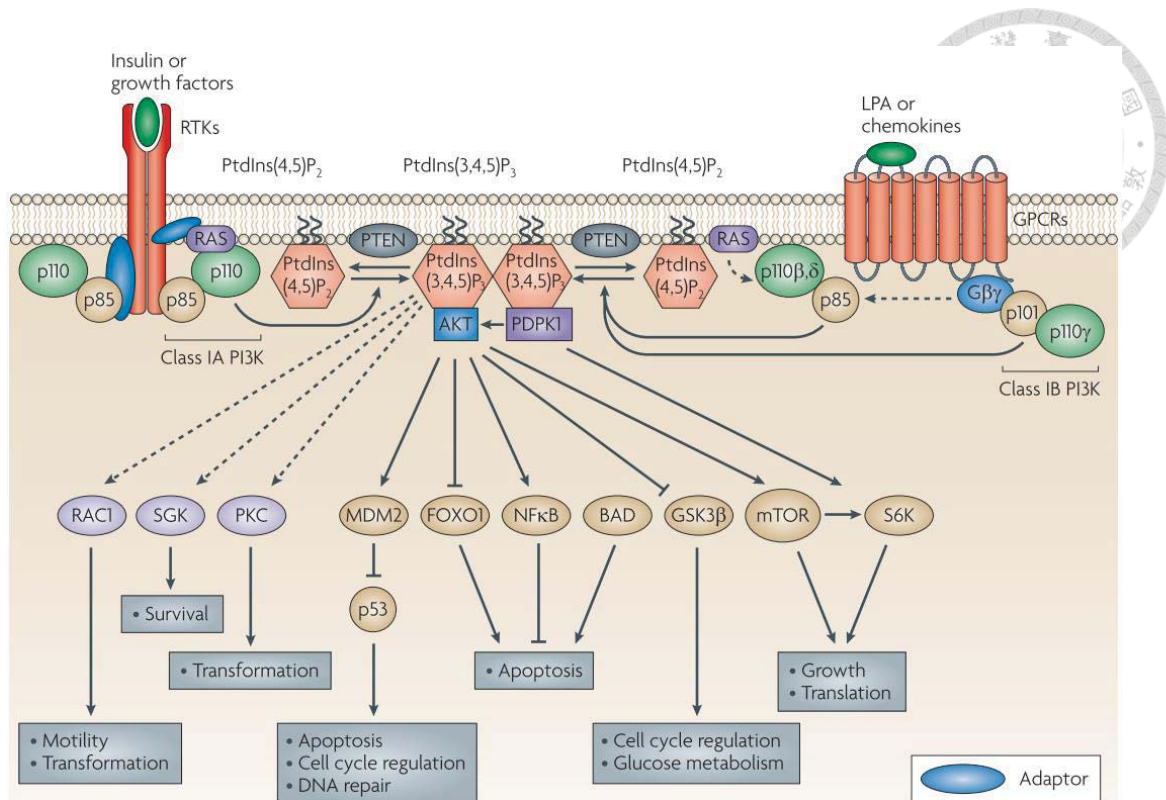
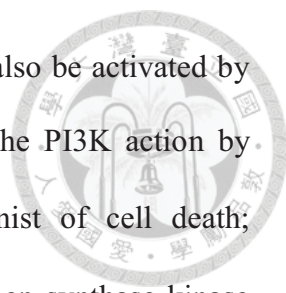


Figure 1-12. The class I PI3K signalling pathway. Following growth factor stimulation and subsequent activation of receptor tyrosine kinases (RTKs), class IA phosphoinositide 3-kinases (PI3Ks), consisting of p110 α -p85, p110 β -p85 and p110 δ -p85, are recruited to the membrane by direct interaction of the p85 subunit with the activated receptors (for example, platelet-derived growth factor receptor) or by interaction with adaptor proteins associated with the receptors (for example, insulin receptor substrate 1). The activated p110 catalytic subunit converts phosphatidylinositol-4,5-bisphosphate (PtdIns(4,5)P₂) to phosphatidylinositol-3,4,5-trisphosphate (PtdIns(3,4,5)P₃) at the membrane, providing docking sites for signalling proteins that have pleckstrin homology domains, including putative 3-phosphoinositide-dependent kinase 1 (PDK1) and serine-threonine protein kinase AKT (also known as protein kinase B). PDK1 phosphorylates and activates AKT, which elicits a broad range of downstream signalling events. The class IB PI3K (p110 γ -p101) can be activated directly by G protein-coupled receptors (GPCRs) through interaction with the G $\beta\gamma$



subunit of trimeric G proteins. The p110 β and p110 δ subunits can also be activated by GPCRs. PTEN (phosphatase and tensin homologue) antagonizes the PI3K action by dephosphorylating PtdIns(3,4,5)P3. BAD, BCL2-associated agonist of cell death; FOXO1, forkhead box O1 (also known as FKHR); GSK3 β , glycogen synthase kinase 3 β ; mTOR, mammalian target of rapamycin; NF- κ B, nuclear factor- κ B; PKC, protein kinase C; RAC1, RAS-related C3 botulinum toxin substrate 1; SGK, serum and glucocorticoid - regulated kinase; S6K, ribosomal protein S6 kinase; LPA, lysophosphatidic acid. (Liu, Cheng *et al.* 2009)

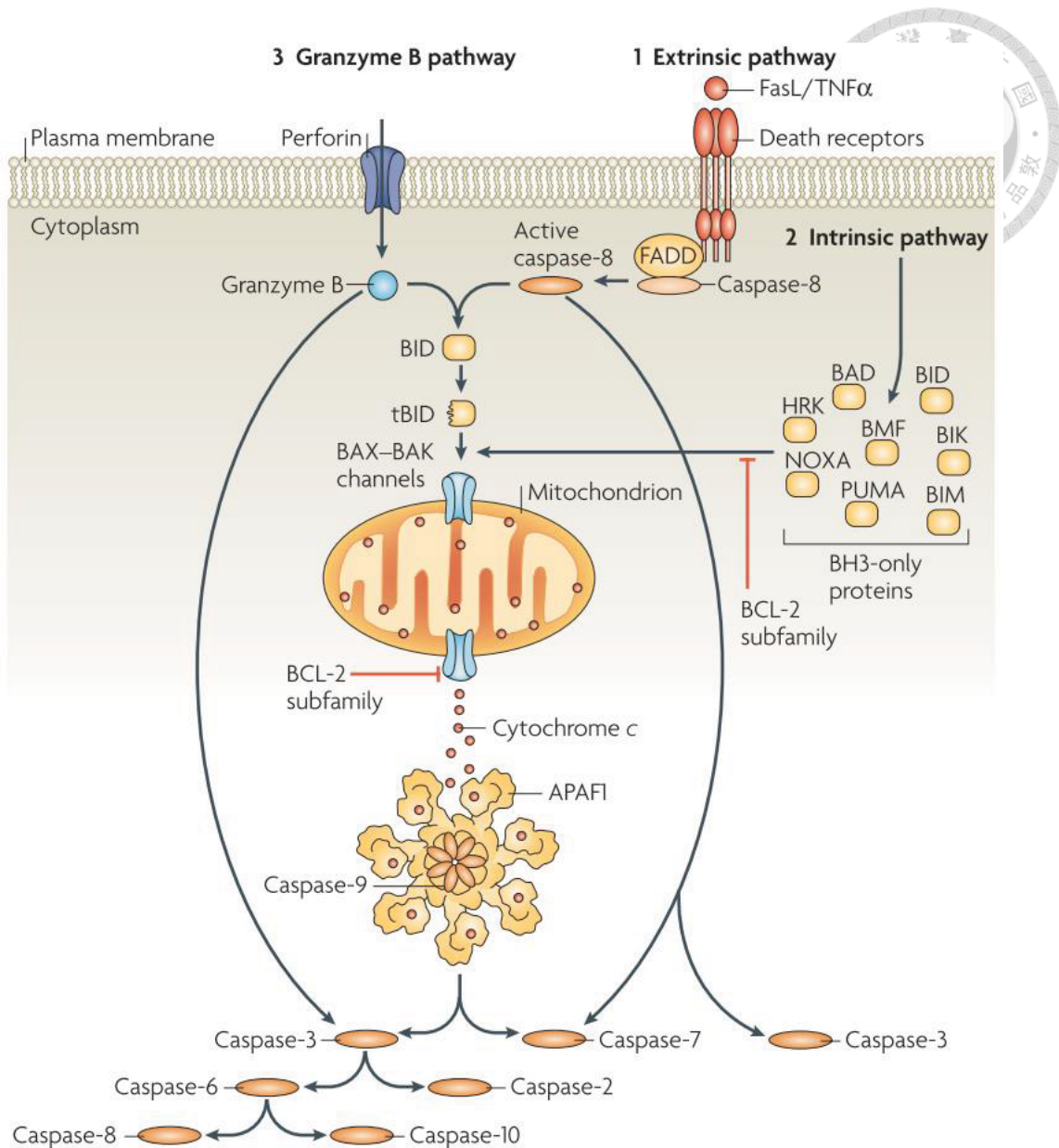
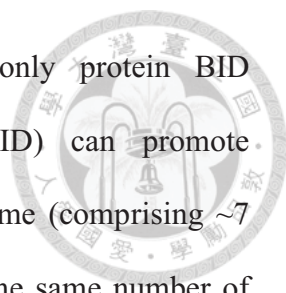


Figure 1-13. Caspase activation pathways. Caspase activation by the extrinsic pathway (route 1) involves the binding of extracellular death ligands (such as FasL or tumour necrosis factor- α (TNF α)) to transmembrane death receptors. Engagement of death receptors with their cognate ligands provokes the recruitment of adaptor proteins, such as the Fas-associated death domain protein (FADD), which in turn recruit and aggregate several molecules of caspase-8, thereby promoting its autoprocessing and activation. Active caspase-8 then proteolytically processes and activates caspase-3 and -7, provoking further caspase activation events that culminate in substrate proteolysis and cell death. In some situations, extrinsic death signals can crosstalk with the intrinsic



pathway through caspase-8-mediated proteolysis of the BH3-only protein BID (BH3-interacting domain death agonist). Truncated BID (tBID) can promote mitochondrial cytochrome c release and assembly of the apoptosome (comprising ~7 molecules of apoptotic protease-activating factor-1 (APAF1) and the same number of caspase-9 homodimers). In the intrinsic pathway (route 2), diverse stimuli that provoke cell stress or damage typically activate one or more members of the BH3-only protein family. BH3-only proteins act as pathway-specific sensors for various stimuli and are regulated in distinct ways (BOX 1). BH3-only protein activation above a crucial threshold overcomes the inhibitory effect of the anti-apoptotic B-cell lymphoma-2 (BCL-2) family members and promotes the assembly of BAK–BAX oligomers within mitochondrial outer membranes. These oligomers permit the efflux of intermembrane space proteins, such as cytochrome c, into the cytosol. On release from mitochondria, cytochrome c can seed apoptosome assembly. Active caspase-9 then propagates a proteolytic cascade of further caspase activation events. The granzyme B-dependent route to caspase activation (route 3) involves the delivery of this protease into the target cell through specialized granules that are released from cytotoxic T lymphocytes (CTL) or natural killer (NK) cells. CTL and NK granules contain numerous granzymes as well as a pore-forming protein, perforin, which oligomerizes in the membranes of target cells to permit entry of the granzymes. Granzyme B, similar to the caspases, also cleaves its substrates after Asp residues and can process BID as well as caspase-3 and -7 to initiate apoptosis. BAD, BCL-2 antagonist of cell death; BAK, BCL-2-antagonist/killer-1; BAX, BCL-2-associated X protein; BID, BH3-interacting domain death agonist; BIK, BCL-2-interacting killer; BIM, BCL-2-like-11; BMF, BCL-2 modifying factor; HRK, harakiri (also known as death protein-5); PUMA, BCL-2 binding component-3. (Taylor, Cullen et al. 2008)

Table 1-1. Investigational therapeutic targets in lymphoma treatment.

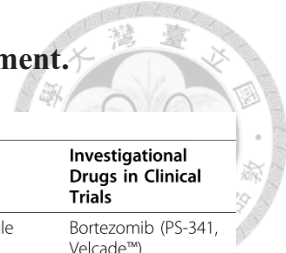


Table 1 Investigational therapeutic targets in lymphoma treatment

Pathway/Protein	Oncogenic Mechanism	Molecular Target(s)	Drug Class	Investigational Drugs in Clinical Trials
Ubiquitin-proteasome pathway [6,7]	Dysregulation of intracellular cell cycle proteins	NF- κ B inhibitory protein ($I\kappa$ B)	Small-molecule proteasome inhibitors	Bortezomib (PS-341, Velcade™)
Akt/mTOR pathway [8-10]	Aberrant activation of mTOR-mediated regulation of cell growth, proliferation, apoptosis, angiogenesis, nutrient uptake	mTORC1 (mTORC2?)	mTOR inhibitors	Temsirolimus (CCI-779, Torisel®) Everolimus (RAD001, Afinitor®) Ridaforolimus (formerly deforolimus, AP23573)
Cell-mediated immunity, cytokines [11]	Aberrant activation of prosurvival cytokines and cellular immune response	TNF- α , IL-6, IL-8, and VEGF; T cells and NK cells	Immunomodulatory drugs (IMiDs)	Lenalidomide (Revlimid®)
VEGF receptors, PDGF receptors [12,13]	Tumor proliferation, angiogenesis	Tyrosine kinase	Tyrosine kinase inhibitors	Sunitinib (SU11248, Sutent®) Sorafenib (Nexavar®)
Histone deacetylase [14]	Dysregulated histone deacetylation in promoters of growth regulatory genes (gene silencing)	Histone deacetylase	Histone deacetylase inhibitors (HDACIs)	Vorinostat (Zolinza®) Romidepsin (FK228) Valproic acid Panobinostat (LBH589) Others

Abbreviations: IL-6 = interleukin-6; IL-8 = interleukin-8; mTOR = mammalian target of rapamycin; PDGF = platelet-derived growth factor; PI3K = phosphoinositide 3-kinase; TNF- α = tumor necrosis factor-alpha; VEGF = vascular endothelial growth factor.

(Johnston, Yuan *et al.* 2010)

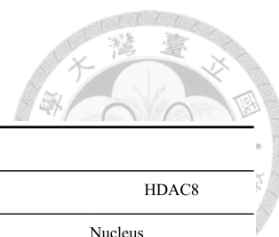


Table 1-2. HDAC characteristics

Class I						
	HDAC1	HDAC2	HDAC3	HDAC3	HDAC8	
Localization	Nucleus	Nucleus	Nucleus	Nucleus	Nucleus	
Size (amino acids)	483	488	428	428	377	
Chromosomal localization	1p34.1	6q21	5q31	5q31	Xq13	
Catalytic sites	1	1	1	1	1	
Tissue distribution	Ubiquitous	Ubiquitous	Ubiquitous	Ubiquitous	Ubiquitous? Smooth muscle differentiation	
Substrates (partial list)	Androgen receptor, SHP, p53, MyoD, E2F-1, Stat3	Glucocorticoid receptor, YY-1, Bcl-6, Stat3	SHP, YY-1 GATA-1, RelA, Stat3, MEF2D	SHP, YY-1 GATA-1, RelA, Stat3, MEF2D		
Binding partners (partial list)			CDK9, SP1, PP4c	CDK9, SP1, PP4c	EST1B	
Knockout phenotype	EL increased histone acetylation, increase in p21 and p27	Cardiac defect				

Class IIA				Class IIB		Class IV
HDAC4	HDAC5	HDAC7	HDAC9	HDAC6	HDAC10	HDAC11
Nucleus/cytoplasm 1,084 2q37.2	Nucleus/cytoplasm 1,122 17q21	Nucleus/cytoplasm 855 12q13	Nucleus/cytoplasm 1,011 7p21-p15	Mostly cytoplasm 1,215 Xp11.22-23	Mostly cytoplasm 669 22q13.31-q13.33	Nucleus/cytoplasm 347 3p25.2
1 H, SM, B	1 H, SM, B	1 H, PL, PA, SM	1 B, SM	2 H, L, K, PA	1 L, S, K	2 B, H, SM, K
GCMa, GATA-1, HP-1	GCMa, Smad7, HP-1	PLAG1, PLAG2		α -Tubulin, Hsp90, SHP, Smad7		
ANKRA, RFXANK	CAMPTA, REA, estrogen receptor	FOX3P, HIF-1 α , Bcl-6, endothelin receptor, α -actinin 1, α -actinin 4, androgen receptor, Tip60	FOX3P	Runx2		
Defects in chondrocyte differentiation	Cardiac defect	Maintenance of vascular integrity, increase in MMP10	Cardiac defect			

Abbreviations: H, heart; SM, skeletal muscle; B, brain; PL, placenta; PA, pancreas; L, liver; K, kidney; S, spleen. EL, embryonic lethal. Stat3, signal transducers and activators of transcription 3; CDK9, cyclin-dependent kinase 9; MMP10, matrix metalloproteinase 10; Hsp90, heat shock protein 90; HIF-1 α , hypoxia-inducible factor-1 α . (Dokmanovic, Clarke et al. 2007)



Table 1-3. Selected acetylated proteins.

Biological implication	Proteins affected by acetylation	
Protein stability	Acetylation increases stability p53, p73, Smad7, c-Myc, Runx3, AR, H2A.z, E2F1, NF-E4, ER81, SREBP1a, HNF6, BACE1	Acetylation decreases stability GATA1, HIF-1 α , pRb, SV40 T-Ag
DNA binding	Increased DNA binding p53, SRY, STAT3, GATA transcription factors, E2F1, p50 (NF κ B), E κ , p65 (NF κ B), c-Myb, MyoD, HNF-4, AML1, BETA2, NF-E2, KLF13, TAL1/SCL, TAF(1)68, AP endonuclease	Decreased DNA binding YY1, HMG-A1, HMG-N2, p65 (NF κ B), DEK, KLF13, Fen-1
Gene expression	Transcriptional activation p53, HMG-A1, STAT3, AR, ER α (basal), GATA transcription factors, EKLF, MyoD, E2F1, p65(NF κ B), GR, p73, PGC1 α , MEF2D, GCMA, PLAG1, PLAGL2, Bcl-6, β -Catenin, KLF5, Sp1, BETA2, Cart1, RIP140, TAF(1)68	Transcriptional inactivation E κ (ligand-bound), HIF-1 α , STAT1, FOXO1, FOXO4, RIP140
Protein interactions	Enhanced STAT3, AR, EKLF, Importin A, STAT1, TFIIIB, α -Tubulin, actin, cortactin	Decreased p65(RelA), Ku70, Hsp90
Localisation	Ac \rightarrow nucleus PCAF, SRY, CtBP2, POP-1, HNF-4, PCNA Sub-nuclear WRN, PCNA	Ac \rightarrow cytosol c-Abl, p300, PAP
mRNA stability	Increased p21, Brm	Decreased Tyrosinhydrolase (Th), eNOS
Enzymatic activity	Enhanced p300, ATM	Decreased PTEN, HDAC1, Mdm2, ACS, Neil2, Pol β
Mitochondrial proteins	ACS (Ac-CoA-Synthetase), Sod1/2, Profilin I, Thioredoxin; multiple components of metabolic and oxidative phosphorylation machinery	
Viral proteins	E1A, S-HDAg, L-HDAg, HIV Tat, SV40 T-Ag	

(Cheng, Park et al. 2008; Spange, Wagner et al. 2009)

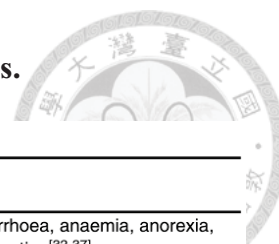


Table 1-4. Histone deacetylase (HDAC) inhibitors in clinical trials.

Table I. Histone deacetylase (HDAC) inhibitors in clinical trials

Class	Compound	Specificity	Dose range	Development phase	Adverse effects
Hydroxamate	Vorinostat (SAHA) ^[24]	Class I/II	μmol/L	US FDA approved	Fatigue, nausea, vomiting, diarrhoea, anaemia, anorexia, thrombocytopenia, QTc prolongation ^[32-37]
	Belinostat (PXD 101) ^[25,31]	Class I/II	μmol/L	II	Fatigue, nausea, vomiting, diarrhoea, constipation, flushing, QTc prolongation ^[38]
	LAQ 824 ^[27]	Class I/II	nmol/L	I	Fatigue, nausea, vomiting, diarrhoea, anorexia, constipation, thrombocytopenia, neutropenia, lymphopenia, anaemia, QTc prolongation, ST segment/T-wave changes, headache ^[39]
	Panobinostat (LBH 589) ^[24,31]	Class I/II	nmol/L	I/II	Nausea, vomiting, diarrhoea, anorexia, thrombocytopenia, hypokalaemia, QTc prolongation, ST segment/T-wave changes, pericardial effusion ^[40]
	Pyroxamide ^[27]	Class I	μmol/L	I	NA
	Givinostat (ITF 2357) ^[24,26]	Class I/II	nmol/L	I	Fatigue, diarrhoea, thrombocytopenia, leukopenia, neutropenia, QTc prolongation ^[41,42]
	PCI 24781 ^[24]	Class I/II	nmol/L	I	NA
Cyclic peptide	Romidepsin (depsipeptide, FK 228) ^[24]	HDAC1, 2	nmol/L	II	Fatigue, nausea, vomiting, anorexia, thrombocytopenia, lymphopenia, leukopenia, neutropenia, anaemia, QTc prolongation, ST segment/T-wave changes, sinus or ventricular tachycardia ^[43-45]
Aliphatic acid	AN 9 (pivaloyloxymethyl butyrate) ^[24,25]	NA	μmol/L	II	Fatigue, nausea, vomiting, diarrhoea, anorexia, dysgeusia, fever, hyperglycaemia, hypokalaemia, hepatic transaminase elevation, anaemia ^[46,47]
	Sodium Phenylbutyrate ^[24]	Class I/IIα	mmol/L	II	Fatigue, nausea, vomiting, dyspepsia, neutropenia, anaemia, somnolence, confusion, light-headedness ^[48-51]
	Valproic acid ^[26]	Class I/IIα	mmol/L	II	Fatigue, nausea, vomiting, leukopenia, thrombocytopenia, neurological toxicities: neurosensory, neurocortical, vertigo, somnolence ^[52]
	Valproic acid, topical (Baceca [®]) ^[24]	Class I	NA	II	NA
	Valproic acid, oral (Savicol [™]) ^[24]	Class I	NA	II	NA
Benzamide	Entinostat (MS 275) ^[24,26]	HDAC1, 2, 3	μmol/L	II	Fatigue, nausea, asthenia, anorexia, anaemia, thrombocytopenia, hypoalbuminaemia, hypophosphataemia, hyponatraemia, headache ^[53,54]
	Tacedinaline (CI 994) ^[27]	NA	μmol/L	I/II	Fatigue, nausea, vomiting, diarrhoea, constipation, mucositis, thrombocytopenia ^[55]
	MGCD 0103 ^[24,25]	Class I	μmol/L	II	Fatigue, nausea, vomiting, anorexia, diarrhoea, dehydration, constipation, abdominal pain, dyspnoea ^[56,57]

NA = not available; QTc = corrected QT interval; SAHA = suberoylanilide hydroxamic acid.

(Ma, Ezzeldin *et al.* 2009)

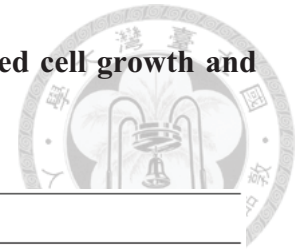
Table 1-5. Clinical Toxicity of HDAC Inhibitors: A Summary of the Results from Available Phase I Studies.



	Valproic acid (small molecular weight carbohydrate)	Sodium diphenyl- butyrate (small molecu- lar weight carbohydrate)	Depsiptide (FK228) (cyclic peptide)	Suberoylanilide hydroxamic acid (hydroxamine)	MS-275 (benzamide)
Hematological					
Thrombocytopenia		+	+++	+++	+++
Neutropenia		+	+++	+++	+++
Anemia			+++	+	+++
Lymphopenia					+++
Neurological-constitutive					
Fatigue	+		+++	++	+++
Anorexia	+		++	++	+++
Headache	+		+		+++
Confusion	+				
Tinnitus/hearing impairment	+				
Metabolic					
Tumor lysis syndrome		+	+		
Hypophosphatemia			+		+
Hypocalcemia	+	+	++		++
Hyperglycemia				++	+
Hypoalbuminemia					++
Hypercalcemia					+
Hyponatremia	+	+			+
Hypokalemia		+			
Gastrointestinal					
Nausea, vomiting	++	+	++		+++
Constipation				++	+
Diarrhoea			+	++	+
Taste change			+		+++
Cardiovascular					
Hypotension			++		
ST/T abnormalities			+++	++	
Arrhythmia			+		(+?)
Additional side effects					
Fever			++		
Tumor/bone pain	+	+		+	
Increased creatinin				+	+

(Bruserud, Stapnes et al. 2007)

Table 1-6. Signal transduction cascades relevant to Akt-mediated cell growth and proliferation.



Drug	Manufacturer	Description
Perifosine	AEterna Zentaris	Phase II trials show activity in hematologic malignancies (Waldenstrom's macroglobulinemia and multiple myeloma) and solid tumors (RCC, NSCLC, colorectal cancer). Phase III trials underway in metastatic colorectal cancer and multiple myeloma
MK-2206	Merck & Co	Single agent MTD defined in a Phase I study in advanced solid tumors. Ongoing Phase I studies are assessing the combination of MK-2206 with cytotoxic therapy, and disease specific studies in HER2-overexpressing breast cancer are assessing MK-2206 with trastuzumab and trastuzumab/lapatinib
RX-0201	Rexahn	Phase II studies ongoing in RCC and pancreatic cancer
PBI-05204	Phoenix Biotechnology	Phase I trial in advanced solid tumors ongoing
GSK2141795	GlaxoSmithKline	Phase I trial in advanced solid tumors ongoing
Erucylphosphocholine (ErPC)	AEterna Zentaris	In preclinical development
GSK690693	GlaxoSmithKline	Clinical development suspended
XL-418	Exelixis	Clinical development suspended

(Pal, Reckamp *et al.* 2010)

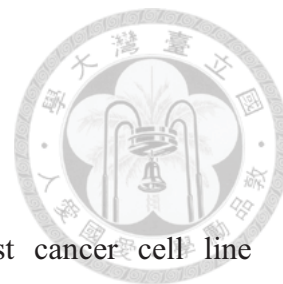
Chapter 2 Materials and Methods



2.1 Materials

MPT0E028 and SAHA were synthesized and provided by Professor Jing-Ping Liou (Taipei Medical University, Taipei, Taiwan). RPMI-1640 medium and Trizol were purchased from Invitrogen (Carlsbad, CA, USA). Fetal bovine serum (FBS), penicillin-streptomycin solution and sodium pyruvate were obtained from GIBCO/BRL Life Technologies (Grand Island, NY, USA). 3-(4,5-Dimethyl-thiazol-2-yl)-2,5-diphenyl-tetrazolium bromide (MTT), propidium iodide (PI), sulforhodamine B (SRB), LY294002 and all of the other chemical reagents were purchased from Sigma Chemical (St. Louis, MO, USA). The following antibodies were used: caspase 8, caspase 9, p-Akt(T308), Akt, p-mTOR, mTOR, p-GSK3 β , p-eIF4E, p-p70S6K(T421/S424), p-p70S6K(T389), HDAC1, HDAC2, HDAC4, acetyl- α -tubulin, BID, STAT2, STAT4, STAT5A, STAT6, histone 3, c-myc (Cell Signaling Technologies, Boston, MA, USA); PARP, HDAC6, HRP-conjugated anti-mouse and anti-rabbit IgG (Santa Cruz Biotechnology, Santa Cruz, CA, USA); p-Akt (s473) (Epitomics, Burlingame, CA, USA); caspase 6, caspase 7, p53, STAT1 (BD Biosciences PharMingen, San Jose, CA, USA); caspase 3 (Imgenex, San diego, CA, USA); acetyl-histone H3, STAT5B (Upstate Biotechnology, Lake Placid, NY, USA); actin (Chemicon, Billerica, MA, USA). Random primer and M-MLRT were purchased from Promega (Madison, WI, USA). Pro-Teq was purchased from Protech (Taipei, Taiwan). Primers were purchased from Purigo Biotech Inc (Taipei, Taiwan).

2.2 Methods



Cell Culture

Human colorectal cancer cell line HCT116, human breast cancer cell line MDAMB231, human B cell lymphoma cell line Ramos and human umbilical vein endothelial (HUVEC) cells were purchased from American Type Culture Collection (Manassas, VA, USA). BJAB cells were a kind gift from Professor Ping-Ning Hsu (National Taiwan University Hospital and National Taiwan University, College of Medicine, Taipei, Taiwan). NCI-ADR was obtained from the DTP Human Tumor Cell Line Screen (Developmental Therapeutics Program, NCI). HCT116, MDAMB231, NCI-ADR and BJAB cells were cultured in RPMI-1640 with 10% heat-inactivated fetal bovine serum and penicillin (100 units/ml)/streptomycin (100 $\mu\text{g/ml}$); Ramos cells were cultured in RPMI-1640 with 10% heat-inactivated fetal bovine serum and penicillin (100 units/ml)/streptomycin (100 $\mu\text{g/ml}$) and sodium pyruvate (1 mM/ml); HUVEC cells were cultured in M199 with 20% heat-inactivated fetal bovine serum (v/v) and penicillin (100 units/mL)/streptomycin (100 $\mu\text{g/mL}$). All cells were maintained in humidified air containing 5% CO_2 at 37°C. Cell density was maintained between 1×10^5 and 1×10^6 cell/ml and passaged every 2 to 3 days.

NCI-60 cancer cell lines screening

The NCI-60 cancer cell lines screening was conducted by the NCI's Developmental Therapeutics Program (DTP; <http://www.dtp.nci.nih.gov/branches/btb/ivclsp.html>).

MTT assay

Cell viability was assessed by MTT assay. Ramos and BJAB cells were plated in 24-well plate (4×10^5 cells/well) while HUVEC cells were plated in 96-well plate (5000 cells/well) and treated with different doses of MPT0E028 and SAHA for 24 h. After the treatment, 100 μ l of 0.5 mg/ml 3-(4,5-Dimethylthiazol-2-yl)-2,5-diphenyltetrazolium bromide (MTT) were added to each well and incubated at 37°C to stained cells forming an insoluble blue formazan product. After 1 h incubation, 100 μ l of extraction reagent (0.1M sodium acetate buffer or DMSO) were added to each well and mix thoroughly to lyse cells. The plates were then measured at 550 nm using an enzyme-linked immunosorbent assay (ELISA) reader (Packard, Meriden, CT, USA).

Sulforhodamine B (SRB assay)

HCT116, MDAMB231 and NCI-ADR cells were seeded in 96-well plates in medium with 5% fetal bovine serum overnight. Cells were fixed with 10% trichloroacetic (TCA) representing cell population at the time of drug treatment (T_0). After incubation with vehicle (0.1% DMSO), MPT0E028 or SAHA for 48 h, cells were fixed with 10% TCA at 37°C for 10 min and then stained with SRB at 0.4% (w/v) in 1% acetic acid at room temperature for 10 min. Excess SRB was washed away twice by 1% acetic acid and dye-containing cells were lysed with 10 mmol/L Trizma base. The absorbance was read under wavelength of 515 nm. By measuring time zero (T_0), control group (C) and treatment group (T_x), cell proliferation percentage was calculated using the equation as following: $100 - [(T_x - T_0) / (C - T_0)] \times 100\%$. The concentration caused 50% growth inhibition is called GI_{50} (growth inhibition).

Crystal violet assay

HUVEC cells were seeded into 96-well culture plates (5000 cells/well) in quadruplicate. After 24 h incubation, cells were fixed with 0.1% crystal violet/20% methanol, representing cell population at the time of drug treatment (T_0). Other cells were treated with MPT0E028 or SAHA for 48 h. After 48 h incubation at 37°C, cells were stained with 0.1% crystal violet/20% methanol for 10 minutes and washed for 3 times. Then the dye was eluted by 0.1 M sodium citrate/75% ethanol, and the absorbance is measured at 550 nm.

Protein extraction and Western blot

After treatment of cells for the indicated agents and time course, cells were washed with ice-cold PBS, lysed with ice-cold lysis buffer (1 mM EGTA, 1 mM EDTA, 150 mM NaCl, 1% Triton X-100, 2.5 mM sodium pyrophosphate, 1 mM PMSF, 1 mM Na_3VO_4 , 1 $\mu\text{g}/\text{ml}$ leupeptin, 1 $\mu\text{g}/\text{ml}$ aprotinin, 5 mM NaF in 20 mM Tris-HCl buffer, pH 7.5), incubated on ice for 30 min and then centrifuge at 4°C for 30 min to extract protein. Protein concentration was evaluated by BiorRad protein assay kit. Proteins were added 5X sample buffer (312.5 mM Tris pH 6.8, 10% SDS, 50% glycerol, 0.05% bromophenol blue, 10% 2-mercaptoethanol) and then denatured at 100°C for 10 min. Equivalent aliquots of protein were electrophoresized on 8 to 15% sodium dodecyl sulfate-polyacrylamide gel electrophoresis (SDS-PAGE) and transferred to poly(vinylidene difluoride) (PVDF) membranes. The membranes were incubated with specific antibodies overnight at 4°C and then applied to appropriate horseradish peroxidase-conjugated anti-mouse or anti-rabbit immunoglobulin G secondary antibodies for 1 h at room temperature. Signal detection was performed with chemiluminescence reagents (Amersham, Buckinghamshire, UK).

Flow cytometry analysis

Following drug treatment, cells were harvested and washed with PBS, and then the pellets were resuspended and fixed in ethanol (75%, v/v) overnight at -20°C. After centrifugation, the fixed cells were washed with ice-cold PBS once and incubated in 0.1M of phosphate–citric acid buffer (0.2 M NaHPO₄, 0.1 M citric acid, pH 7.8) for 30 min at room temperature. The cells were centrifuged and stained with propidium iodide staining buffer containing Triton X-100 (0.1%, v/v), RNase A (100 mg/ml) and propidium iodide (80 mg/ml) for 30 min. Cell cycle distribution was performed using a FACScan flow cytometry with CellQuest software (Becton Dickinson, Mountain View, CA,USA).

ELISA for Akt detection

BJAB cells were plated in 6-cm dish (1×10^6 cells/ml) and treated with different concentrations of MPT0E028 and SAHA for 24 h. After the treatment, cells were lysed with ice-cold lysis buffer mentioned above and equivalent aliquots of protein were subjected to a PathScan phospho-Akt1 (Ser473) sandwich ELISA kit (Cell Signaling Technology) following manufacture's instruction. In briefly, whole cell lysate was first half-diluted with sample diluent and added 100 μ l into the well incubating overnight at 4°C. After the reaction, wells were washed 4 times with 200 μ l wash buffer and then added 100 μ l of Akt1 mouse detection antibody incubating 1 h at 37°C. Washed 4 times again and then added 100 μ l of anti-mouse IgG HRP-linked antibody incubating 30 min at 37°C. After incubation, washed the well once again and then added 100 μ l TMB (3, 3', 5, 5''-tetramethylbenzidine) substrate for color production and finally added 100 μ l STOP solution. The results were measured by spectrophotometer at wavelength 450 nm.

Akt kinase activity

MPT0E028 was submitted to Ricerca Pharma Services (Taiwan Pharmacol. Lab.) for Kinome Diversity Screening using enzyme-based kinase activity assay. In briefly, Akt activity was assayed using human recombinant insect Sf21 cells for Akt kinase source and crosstide peptide (GRPRTSSFAEG, 15 $\mu\text{g}/\text{mL}$) as a substrate (Cross, Alessi *et al.* 1995). Cell lysate was incubated with kinase assay buffer (50 mM HEPES pH 7.4, 10 mM MgCl_2 , 0.2 mM Na_3VO_4 , and 1 mM DTT) for 60 min at 25°C, and analyzed by ELISA quantitation of Crosstide-P.

Enzyme-based HDAC biochemical assays

The HDACs *in vitro* activities of recombinant human HDAC 1, 2, 4, 6 and 8 (BPS Biosciences) were detected by fluorogenic release of 7-amino-4-methylcoumarin from substrate upon deacetylase enzymatic activity. Half maximal inhibitory concentration (IC_{50}) is determined at the drug concentration that results in 50% reduction of HDAC activity increase in control wells during the compound incubation.

HeLa nuclear extract HDAC activity Assay

The HeLa nuclear extract HDAC activity was measured by using the HDAC Fluorescent Activity Assay Kit (BioVision, CA, USA) according to manufacturer's instructions (Hassig, Symons *et al.* 2008). Briefly, the HDAC fluorometric substrate and assay buffer were added to HeLa nuclear extracts in a 96-well format and incubated at 37°C for 30 min. The reaction was stopped by adding lysine developer, and the mixture was incubated for another 30 min at 37°C. Additional negative controls included incubation without the nuclear extract, without the substrate, or without both. TSA at 1

μM served as the positive control. A fluorescence plate reader with excitation at 355 nm and emission at 460 nm was used to quantify HDAC activity. Half maximal inhibitory concentration (IC_{50}) is determined at the drug concentration that results in 50% reduction of HeLa HDAC activity increase in control group during the compound incubation.

Cell-based HDAC fluorescence activity assay

Cells were plated in 10-cm dish (1×10^6 cells/ml) and treated with different concentrations of MPT0E028 and SAHA for 24 h, and then cell lysate was subjected to a HDAC Fluorometric Activity Assay Kit (K330-100, Biovision Inc.) to determine the HDAC activity. 50 μg of cell lysate was added to react with fluorometric substrate t-butoxycarbonyl-Lys (AC)-amido-4-methylcoumarin (Boc-Lys (AC) AMC) and incubated at 37°C for 30 minutes. After the incubation, the lysine developer in this kit was added and the mixture was incubated for another 30 min at 37°C . Fluorescence was detected by plate reader paradigm detection platform (Beckman coulter) with $\text{Ex}=360$ (excitation) and $\text{Em}=465$ nm (emission).

Transient transfection

Myr-Akt plasmids were kindly provided by Professor Chien-Huang Lin (Taipei Medical University, Taipei, Taiwan). PcDNA-FLAG-HDAC1 (plasmid 13820), pcDNA-FLAG-HDAC4 (plasmid 13821), pcDNA-FLAG-HDAC6 (plasmid 13823) were purchased from Addgene (Cambridge, MA, <http://www.addgene.org>). Transfections for BJAB cells were done by nucleofection using nucleofector solution L, program T-016, according to the manufacturer's instructions (Amaxa, Inc.). A total of 4×10^6 cells were used per transfection and mixed with 0.5 or 1 μg of myr-Akt,

pcHDAC1, pcHDAC4 and pcHDAC6. After transfection, BJAB cells were recovered for 24 h incubating at 37°C.



RT-PCR

For RT-PCR analysis, total cellular RNA was extracted from BJAB cells using Trizol reagent (Invitrogen Corp., Carlsbad, CA, USA) following the manufacturer's instruction. First strand cDNA was synthesized using 5 µg of mRNA incubating with random primer at 65°C for 5 min and then reacting with moloney murine leukemia virus reverse transcriptase (M-MLVRT) at 37°C for 1 h. PCR was then performed with primers for STAT1(5'-AAGGTGGCAGGATGTCTCGT-3'/ 5'-TGGTCTCGTGTTCT TCTGTTCTG-3'), STAT2 (5'-AAGCACTGCTAGGCCGATTA-3'/ 5'-GGCTGGGTT TCTACCACAAA-3'), STAT3 (5'-TGGAAGAGGCGGCAGCAGATAGC-3'/ 5'-CAC GGCCCCATTCCCACAT-3'), STAT4 (5'-TCAAGTCCAACAGTTAGAAATCA-3'/ 5'-TAAACAGTTTGAATAACCACAG-3'), STAT5A (5'-CACAGATCAAGCAAG TGGTC-3'/ 5'-CTGTCCATTGGTCGGCGTAA-3'), STAT5B (5'-GTAAACCATGGC TGTGTGGA-3'/ 5'-AAATAATGCCGCACCTCAAT-3'), STAT6 (5'-CCAAGACAA CAACGCCAAAGC-3'/ 5'-AGGACACCATCAAACCACTGCC-3'), p53 (5'-CAGCC AAGTCTGTGACTTGCACGTAC-3'/5'-CTATGTCGAAAGTGTTTCTGTCATC-3'), c-myc (5'-TACCCTCTCAACGACAGCAG TCTTGACATTCTCCTCGGTG-3') and done with following the procedure: after a "hot-start" for 5-10 min at 94°C, 25-35 cycles were used for amplification, with a melting temperature of 94°C, an annealing temperature of 53-68°C, and an extending temperature of 72°C, each for 1 min, followed by a final extension at 72°C for 7 min. PCR products were separated on 1.5% agarose gel and visualized by ethidium bromide staining.

Microarray analysis

Ramos and BJAB cells were treated with 3 μM and 10 μM MPT0E028 for 12 h respectively, and then total cellular RNA was extracted using Trizol reagent (Invitrogen Corp., Carlsbad, CA, USA) following the manufacturer's instruction. Total cellular RNA was purified using the Purelink™ HiPure Plasmid Midiprep kit (Invitrogen, Carlsbad, CA). Purified RNA samples were submitted to Phalanx Biotech (Hsinchu, Taiwan) for microarray analysis. We used Phalanx Human OneArray to measure MPT0E028-induced gene expression and detailed description of Phalanx Biotech company microarray procedure can be found at <http://www.phalanxbiotech.com/>. Each microarray contains 30,275 oligonucleotides: 29,187 human genome probes, and 1,088 experimental control probes. Each array was performed in duplicate. The genes with a threshold of 1.2 times fold-change were selected and BioCarta Pathway and KEGG (Kyoto Encyclopedia of Genes and Genomes) pathway databases were used to identify functionally related gene pathways.

In vivo HCT116 xenograft model

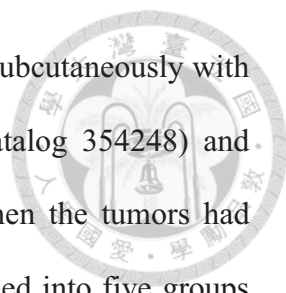
Female nude-athymic mice were 8 weeks old, and had a body weight (BW) range of 17.2-22.0 g, on D1 of the study. The animals were fed ad libitum water (reverse osmosis, 1 ppm Cl) and PicoLab Rodent Diet 20 Modified and Irradiated Lab Diet® consisting of 20.0% crude protein, 9.9% crude fat, and 4.7% crude fiber. The mice were housed on National Taiwan University Laboratory Animal Center, NTUMC, on a 12-hour light cycle at 21–23 °C and 60–85% humidity. The human HCT116 colorectal adenocarcinoma cells used for implantation were harvested during log phase growth and resuspended in phosphate-buffered saline at 5×10^7 cells/mL. Each mouse was injected s.c. in the right flank with 1.0×10^7 cells (0.2 mL cell suspension). Tumors were

monitored twice weekly and then daily as their volumes approached 1,200 mm³. Tumor size, in mm³, was calculated from: where w = width and l = length in mm of the tumor. Tumor volume = $(w^2 \times l)/2$. All animal experiments followed ethical standards, and protocols have been reviewed and approved by Animal Use and Management Committee of National Taiwan University (IACUC Approval No: 20100225).

***In vivo* Ramos engraftment model and BJAB xenograft model**

Male NOD/SCID mice and nude mice (NTUH Animal Facility) were 5 weeks old and had a body weight (BW) range of 20-24 g on day one of the study. The mice were carefully maintained and all animal procedures were in accordance with the Institutional Animal Care and Use Committee procedures and guidelines. All animal experiments followed ethical standards, and protocols has been reviewed and approved by Animal Use and Management Committee of National Taiwan University (IACUC Approval No: 20100225).

In Ramos engraftment model, human B-cell lymphoma Ramos cells were resuspended at 10^7 cells/ml in culture medium at room temperature, and 2×10^6 cells were inoculated into male NOD/SCID mice via tail vein. Treatment began 1 week after engraftment. Both MPT0E028 and SAHA were dissolved in vehicle (0.5% carboxymethyl cellulose + 0.1 % Tween 80 in 5% dextrose). After engraftment, mice were randomly placed into three groups and received the following treatment by oral gavage during the study: (a) vehicle alone, (b) MPT0E028 at 100 mg/kg daily, and (c) SAHA at 200 mg/kg daily. Survival rate was used as end point for this study.

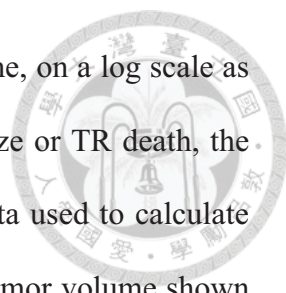


In BJAB xenograft model, the male nude mice were injected subcutaneously with the same volume of BD Matrigel Matrix HC (BD bioscience, catalog 354248) and BJAB cells (2×10^7 cell/mouse) into the flank of each animal. When the tumors had grown to the size of around 80 to 100 mm³, the animals were divided into five groups (n=7) and receive the following treatment by oral gavage for 31 days during the study: (a) vehicle alone, (b) MPT0E028 at 50 mg/kg daily, (c) MPT0E028 at 100 mg/kg daily, (d) MPT0E028 at 200 mg/kg daily, and (e) SAHA at 200 mg/kg daily. Both MPT0E028 and SAHA were dissolved in vehicle (0.5% carboxymethyl cellulose + 0.1 % Tween 80 in 5% dextrose). Tumor size was measured twice weekly and calculated from $V = 0.5lw^2$, where w = width (w) and l = length (l). At the end of study, tumors were carefully removed and frozen in liquid nitrogen for subsequent western analysis.

Statistical analysis

Each experiment was performed at least three times and the data are presented as mean \pm SEM for the indicated number of separate experiments. Student's *t*-test was used to compare the mean of each group with that of the control group in experiments and one-way ANOVA was used in animal study. *P*-values less than 0.05 were considered significant (**P* < 0.05, ***P* < 0.01, ****P* < 0.001).

The logrank test was used to determine the statistical significance of the difference between the TTE values of two groups, except any NTR deaths. Statistical and graphical analyses were performed with Prism 3.03 (GraphPad) for Windows. The two-tailed statistical analyses were conducted at *P* = 0.05. Kaplan-Meier plots show the percentage of animals remaining in the study versus time. The Kaplan-Meier plots use the same data set as the logrank test.



The tumor growth curves show the group median tumor volume, on a log scale as a function of time. When an animal exits the study due to tumor size or TR death, the final tumor volume recorded for the animal is included with the data used to calculate the median at subsequent time points. Therefore, the final median tumor volume shown by the curve may differ from the MTV, which is the median tumor volume for mice remaining in the study on the last day (excluding all with tumors that have attained the endpoint). If more than one TR death occurs in a group, the tumor growth curves are truncated at the time of the last measurement that precedes the second TR death. Tumor growth curves are also truncated when the tumors in more than 50% of the assessable animals in a group have grown to the endpoint volume. (* $P < 0.05$; ** $P < 0.01$; *** $P < 0.001$; compared with the respective control group)

Chapter 3




新型組蛋白去乙酰酶抑制劑, MPT0E028, 在人類大腸
直腸癌於體內體外引起細胞凋亡之機轉探討

**Anticancer Activity of MPT0E028, a Novel Potent
Histone Deacetylase Inhibitors, in Human Colorectal
Cancer HCT116 Cells *in vitro* and *in vivo***

PLoS One. 2012;7(8):e43645

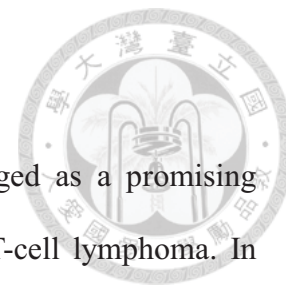
中文摘要



組蛋白去乙醯酶 (histone deacetylase, HDAC) 抑制劑在近年來成為具有潛力的癌症治療藥物，尤其針對於表皮性 T 細胞淋巴瘤(cutaneous T-cell lymphoma, CTCL)。此篇研究中，我們發現 MPT0E028，一個具有 *N*-hydroxyacrylamide 官能基的新穎組蛋白去乙醯酶抑制劑，可以抑制人類大腸癌細胞 HCT116 於體內體外的生長。藉由 NCI-60 screening assay 發現 MPT0E028 在微莫耳濃度即可抑制固態腫瘤與血液腫瘤細胞株的生長，並且於人類大腸直腸癌細胞 HCT116 細胞株中最具有活性。實驗中也發現，MPT0E028 能有效引發細胞凋亡反應且有效抑制組蛋白去乙醯酶(HDAC)的活性，並且比第一個被美國食品藥物管理局所核准的組蛋白去乙醯酶抑制劑 SAHA 更為有效。在 HCT116 異體移植腫瘤實驗中發現，腫瘤生長可被 MPT0E028 有效延緩並且隨濃度增加抑制效果漸增。根據動物體內實驗結果顯示，MPT0E028 具有比 SAHA 更強效的抑制腫瘤能力，並且兩者給藥組均不會使動物體重下降，也未發現明顯的副作用產生。綜合所有實驗結果顯示，MPT0E028 具有某些特性而有潛力成為一個新穎的抗癌治療藥物。

關鍵字: MPT0E028，組蛋白去乙醯酶 (HDAC)，大腸直腸癌，細胞凋亡

Abstract



Recently, histone deacetylase (HDAC) inhibitors have emerged as a promising class of drugs for treatment of cancers, especially subcutaneous T-cell lymphoma. In this study, we demonstrated that MPT0E028, a novel *N*-hydroxyacrylamide-derived HDAC inhibitor, inhibited human colorectal cancer HCT116 cell growth *in vitro* and *in vivo*. The results of NCI-60 screening showed that MPT0E028 inhibited proliferation in both solid and hematological tumor cell lines at micromolar concentrations, and was especially potent in HCT116 cells. MPT0E028 had a stronger apoptotic activity and inhibited HDACs activity more potently than SAHA, the first therapeutic HDAC inhibitor proved by FDA. The growth of HCT116 tumor xenograft was delayed and inhibited after treatment with MPT0E028 in a dose-dependent manner. Based on *in vivo* study, MPT0E028 showed stronger anti-cancer efficacy than SAHA. Neither significant body weight loss nor other adverse effects were observed in both MPT0E028- and SAHA-treated groups. Taken together, our results demonstrate that MPT0E028 has several properties and is potential as a promising anti-cancer therapeutic drug.

Key words: MPT0E028, histone deacetylase (HDAC), colorectal cancer, apoptosis

3.1 Results



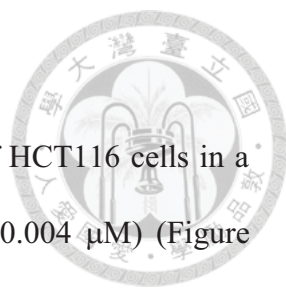
The synthesis of MPT0E028

The synthesis of MPT0E028 (**1**) is depicted in Figure 3-1. Commercially available methyl indole-5-carboxylate (**2**) was reacted with sodium cyanoborohydride in the presence of acetic acid afforded the methyl indoline-5-carboxylate (**3**) in 93% yield. The N1-sulfonylation of indoline (**3**) with benzenesulfonyl chloride in pyridine and then LiAlH₄-mediated C5-ester reduction, followed by the PDC oxidation produced the desired 1-benzenesulfonylindoline-5-carbaldehyde (**4**) in 42% yield (3 steps). Wittig reaction of methyl(triphenylphosphoranyli-dene)acetate with the indoline-5-carboxyaldehyde **4** and treatment of lithium hydroxide (LiOH) in MeOH gave cinnamic acid (**5**) in 73% yield. The conversion of carboxylic acid (**5**) to the hydroxamic acid (**1**) was accomplished in 72% yield by the treatment of NH₂OTHP in the presence of PYBOP and Et₃N, followed by trifluoroacetic acid-mediated deprotection.

The effect of MPT0E028 on proliferation of cancer cell lines

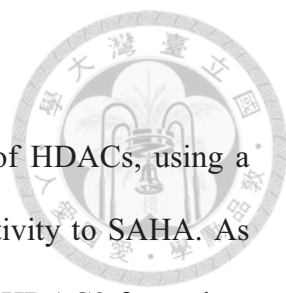
To determine whether MPT0E028 exhibits anti-cancer activity in human cancer cells, we tested the anti-proliferative activity of MTP0E028 using the NCI-60 cancer cell lines screening panel (Paull, Hamel *et al.* 1995). As shown in Table 3-1, MPT0E028 significantly inhibited cell proliferation in all human cancer cell lines examined at micromolar concentrations, but was especially potent in HCT116 cell line. Therefore, we chose HCT116 cells for further studies of the anti-cancer activity of MPT0E028 *in vitro* and *in vivo*.

MPT0E028 significantly induced HCT116 cell apoptosis



First, we demonstrated that MPT0E028 inhibits the growth of HCT116 cells in a concentration-dependent manner using SRB assay ($GI_{50} = 0.09 \pm 0.004 \mu\text{M}$) (Figure 3-2A). Two other cell lines, MDA-MB-231 and NCI-ADR from the NCI-60 screening panel, were also chosen to analyze the sensitivity of MPT0E028 (MDAMB231, $GI_{50} = 0.19 \pm 0.04 \mu\text{M}$; NCI-ADR, $GI_{50} = 0.14 \pm 0.02 \mu\text{M}$). MPT0E028 also inhibited cell proliferation significantly in these two cell lines (Figure 3-S1A, 3-S1B) but showed less potent compared to HCT116. We also determined the safety margin of MPT0E028 in human normal cells (e.g. HUVEC) and found that MPT0E028 show 20-40 folds less sensitive against normal cells ($GI_{50} = 3.57 \pm 0.45 \mu\text{M}$), suggesting MPT0E028 specifically targets malignant tumor cells (Figure 3-S1C). To investigate the effect of MPT0E028 on cell cycle progression, cellular DNA content was measured by flow cytometry. We showed that treatment with MPT0E028 increased the number of cells in the sub-G1 phase of the cell cycle (Figure 3-2B and 3-2C). The reference compound was an HDACi, suberoylanilide hydroxamic acid (SAHA; vorinostat), with a GI_{50} of $0.82 \pm 0.07 \mu\text{M}$, which exhibited antiproliferative activity (Figure 3-2A) and induced apoptosis in HCT116 cells (Figure 3-2B and 3-2D) in a concentration-dependent manner but showed less effective compared to MPT0E028. In Figure 3-2E, MPT0E028 also induced sub-G1 population in a time-dependent manner, while SAHA showed weaker effect and delayed cytotoxicity. MPT0E028 also induced caspase 3 and PARP activation in a concentration-dependent manner (Figure 3-2F). MPT0E028-induced apoptosis was abolished when cotreatment with caspase-inhibitor z-VAD-fmk, suggesting that MPT0E028 induced apoptosis through caspase-dependent pathway. These results suggest that MPT0E028 induced HCT116 cells cytotoxicity through the apoptosis pathway.

MPT0E028 is an inhibitor of HDACs activity



We next examined the effect of MPT0E028 on the activity of HDACs, using a panel of human recombinant HDAC proteins, and compared its activity to SAHA. As shown in Table 3-2, MPT0E028 significantly inhibited HDAC1 and HDAC2 from class I as well as HDAC6 from class IIb at low nanomolar concentrations. While MPT0E028 was more potent than SAHA against recombinant HDAC1 and 2, it has little activity against recombinant HDAC4 and HDAC8, which is similar to the inhibitory pattern of SAHA. We confirmed that MPT0E028 inhibited nuclear HDAC activity in the cervical adenocarcinoma cell line HeLa ($IC_{50} = 11.1 \pm 2.8$ nM) and in HCT116 cells ($IC_{50} = 4.43 \pm 0.5$ μ M), which were approximately 9–30 times more potent than SAHA ($IC_{50} = 118.8 \pm 13.2$ nM and 129.4 ± 13.9 μ M, respectively) (Figure 3-3A and 3-3B). The potent HDACs inhibitory effect of MPT0E028 could also be observed in MDAMB231 and NCI-ADR cells (Figure 3-S2.) These results suggested that MPT0E028 is a novel and potent HDAC inhibitor.

Effects of MPT0E028 on α -tubulin and histone H3 acetylation in HCT116 cells

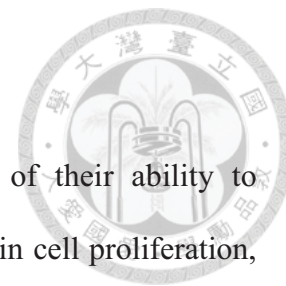
Because α -tubulin and histone H3 are common downstream targets of HDACs, we examined the effects of MPT0E028 on α -tubulin and histone H3 acetylation in HCT116 cells using western blot analysis. As shown in Figure 1-4, MPT0E028 induced stronger hyperacetylation of histone H3 than that of SAHA (Figure 3-4A and 3-4B), which is consistent with its potent inhibitory effect on class I HDAC1 and 2. In contrast, SAHA exhibited more potent α -tubulin acetylation than MPT0E028 (Figure 3-4A and 3-4C), suggesting that SAHA is more potent against class IIb HDAC6, which is consistent with our finding in Table 3-2.

MPT0E028 inhibits growth of human colon cancer xenografts *in vivo*

Finally, we evaluated the efficiency of MPT0E028 and SAHA using *in vivo* tumor HCT116 xenografts in a nude mice model (Figure 3-5A and 3-5B) (Table 3-3). Once a tumor was palpable with the size of approximately 55 mm³, mice were randomized into vehicle control and treatment groups (8 mice per group). Control mice received the vehicle (0.5% carboxymethyl cellulose + 0.1% Tween 80). Tumors in all 3 groups were allowed to reach an endpoint volume of 1,200 mm³. The median time to endpoint (TTE) for control mice was 16.6 days. In mice that were orally treated with SAHA (200 mg/kg, daily), the TTE increased to 27.0 days, which corresponds to a T-C of 10.0 days and a percent tumor growth delay (TGD) of 63%. According to the logrank analysis, SAHA produced significant antitumor activity ($P = 0.0251$). Oral treatment with MPT0E028 (200, 100, and 50 mg/kg, daily) increased the median TTE to 36.9, 19.2, and 15.5 days, respectively, corresponding to a T-C of 20, 2.6, and 0 days and a percent TGD of 122%, 16%, and 0%, respectively. Based on the logrank analysis, MPT0E028 exhibits significant antitumor activity at 200 mg/kg ($P = 0.0031$). Notably, 3 mice in a group that were treated with 200 mg/kg MPT0E028 and 1 mouse in another group that was treated with 100 mg/kg MPT0E028 showed complete tumor regression after treatment (Table 3-3). In addition, we also determined that the growth of HCT116 cancer cells xenografts was suppressed by 73.5%, 32.0%, and 21.9% (percent tumor growth inhibition [TGI] values) after treatment with MPT0E028 at 200, 100, and 50 mg/kg, respectively, whereas SAHA at 200 mg/kg suppressed tumor growth by 47.7% (%TGI) (Figure 3-5C). No significant difference in body weight or other adverse effects were observed upon treatment with MPT0E028 (Figure 3-5D). We also determined the effect of MPT0E028 on the expression of caspase3, PARP, acetyl-histone H3 and acetyl- α -tubulin *in vivo* in HCT116 xenograft tumor tissues. Mice were treated with 200

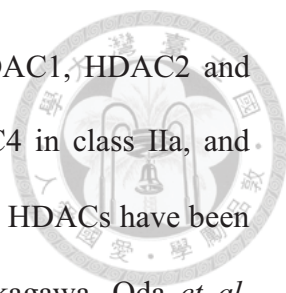
mg/kg MPT0E028 or SAHA for 7 days (oral, daily) and then tumors were carefully removed and subjected to western blot analysis. As shown in figure 3-5E, caspase 3, PARP and acetyl-histone H3 were substantially induced in MPT0E028-treated group while acetyl- α -tubulin were found more profoundly in SAHA-treated group, which is consistent with our finding *in vitro*. Taken together, MPT0E028 induced a dose-dependent delay and inhibition of tumor growth and displayed stronger anti-tumor activity *in vivo* than SAHA.

3.2 Discussion



HDACs are important targets for cancer therapy because of their ability to transcriptionally regulate the expression of genes that are involved in cell proliferation, differentiation, and apoptosis (Khosravi-Far, White *et al.* 2007; Takai and Narahara 2007). HDACi are currently in clinical trials for the treatment of solid tumors and in leukemia patients. Two HDACi, SAHA and FK228, have received the US FDA approval for the treatment of patients with cutaneous T-cell lymphoma. In this study, we report the synthesis of a new chemical compound 3-(1-benzenesulfonyl-2,3-dihydro-1H-indol-5-yl)-N-hydroxyacrylamide (MPT0E028), that has a potent HDACi activity. MPT0E028 was designed based on our prior research with microtubule destabilizing agents using indoline-1-arylsulfonamides as a core structure (Chang, Hsieh *et al.* 2006; Chang, Lai *et al.* 2010). After coupling an *N*-hydroxyacrylamide functional group at the 5-position of indoline ring, we afforded the desired MPT0E028.

Furthermore, we evaluated the anti-cancer activity of MPT0E028 *in vitro* and *in vivo*. We found that MPT0E028 induced cytotoxicity in numerous human cancer cell lines from the NCI-60 panels and performed mechanistic studies in HCT116 cells, which showed high sensitivity to MPT0E028. When compared to SAHA, treatment with MPT0E028 induced stronger inhibition of cancer cell ($GI_{50} = 0.82 \pm 0.07 \mu\text{M}$ and $0.09 \pm 0.004 \mu\text{M}$, respectively) but not normal cell growth ($GI_{50} = 3.57 \pm 0.45 \mu\text{M}$) and produced a significantly higher number of sub-G1 (apoptotic) cells as determined by flow cytometry. Also, MPT0E028 induced more profound caspase 3 and PARP activation. Taken together, MPT0E028 inhibits cancer cells growth and induces apoptotic cell-death.

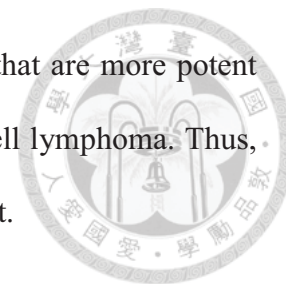


We demonstrated that MPT0E028 inhibits the activity of HDAC1, HDAC2 and HDAC8 in class I as well as HDAC6 in class IIb, but not HDAC4 in class IIa, and consistently induces acetylation of histone H3 and α -tubulin. Class I HDACs have been shown to be overexpressed in human colorectal cancer cells (Nakagawa, Oda *et al.* 2007), which may contribute to perturbed cancer cell proliferation, differentiation, and apoptosis by both epigenetic or non-epigenetic modification (Zhu, Martin *et al.* 2004; Wilson, Byun *et al.* 2006). Inhibition of HDAC activity induced the intrinsic and extrinsic apoptotic pathway, leading to cancer cell death (Tsapis, Lieb *et al.* 2007; Darvas, Rosenberger *et al.* 2010). In addition, HDACi could induce expression of p21 by stabilizing and inducing transcriptional activity of RUNX3, leading to induction of cancer cell apoptosis (Chi, Yang *et al.* 2005; Zopf, Neureiter *et al.* 2007). The inhibition of HDAC activity by MPT0E028 was 10–30 times stronger than that by SAHA in HeLa and HCT116 cells.

Finally, we examined the efficiency of MPT0E028 against the human HCT116 colorectal adenocarcinoma cell growth in mice. Median tumor growth and Kaplan-Meier curve analysis demonstrated strong antitumor activity of MPT0E028. Daily administration of MPT0E028 resulted in significant antitumor activity. Moreover, compared to SAHA, MPT0E028 displayed stronger anti-tumor activity. Based on these results, MPT0E028 is a novel synthetic HDACi with unique pharmacologic properties that should be tested in human colorectal cancer therapy.

In summary, we have identified a novel inhibitor of HDAC activity, MPT0E028, with antitumor activity *in vitro* and *in vivo*. The results presented here show that

MPT0E028 inhibits HDACs activity and has antitumor properties that are more potent than SAHA, which is currently in clinical use in subcutaneous T-cell lymphoma. Thus, MPT0E028 is suitable for further testing as a novel anti-cancer agent.



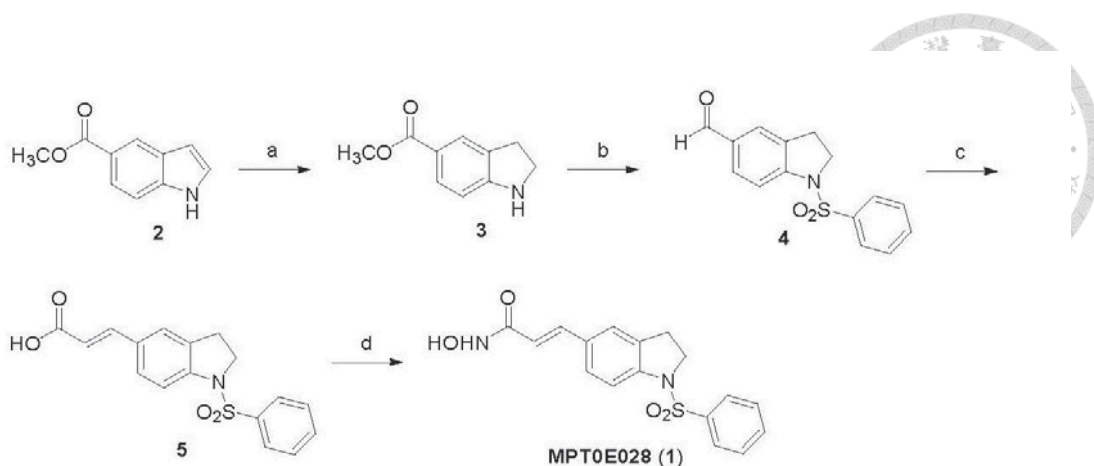


Figure 3-1^a. The synthesis of MPT0E028. ^aReagents and conditions: (a) NaBH₃CN, AcOH, 0°C–r.t.; (b) (i) benzenesulfonyl chloride, pyridine, reflux; (ii) LiAlH₄, THF, 0°C–r.t.; (iii) pyridinium dichromate (PDC), molecular sieves, CH₂Cl₂, r.t.; (c) (i) methyl(triphenylphosphorylidene)-acetate, CH₂Cl₂, r.t.; (ii) 1 M LiOH_(aq), dioxane, 40°C; (d) (i) NH₂OTHP, PYBOP, Et₃N, DMF, r.t.; (iii) trifluoroacetic acid, CH₃OH, r.t. Abbreviations: NaBH₃CN, sodium cyanoborohydride; AcOH, acetyl acid; LiAlH₄ (LAH), lithium aluminium hydride; THF, tetrahydrofuran; PDC, pyridinium dichromate; NH₂OTHP, *O*-(tetrahydro-2H-pyran-2-yl)hydroxylamine; PYBOP, benzotriazol-1-yl-oxytripyrrolidinophosphonium hexafluorophosphate; Et₃N, triethylamine; DMF, dimethylformamide; TFA, trifluoroacetic acid.

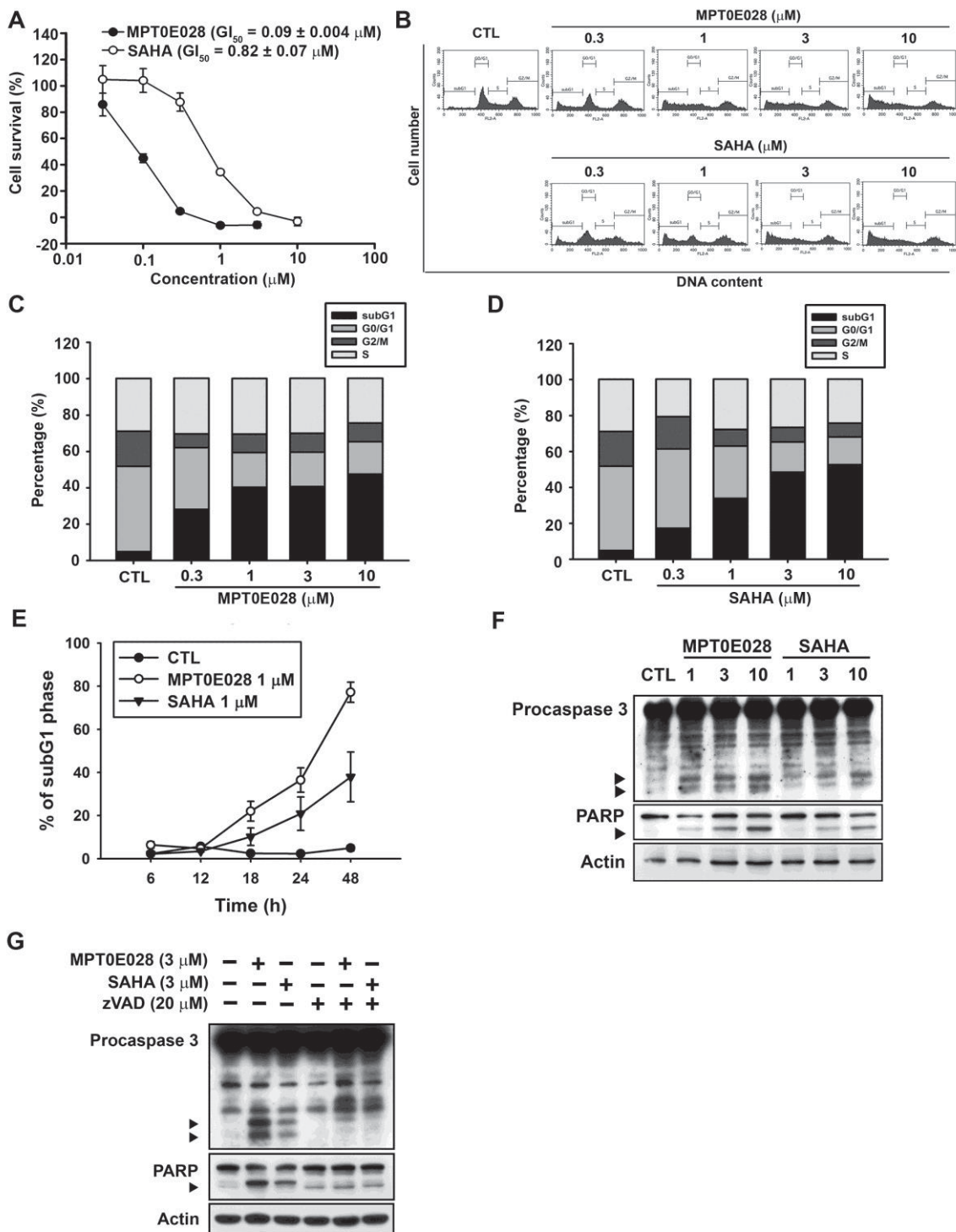
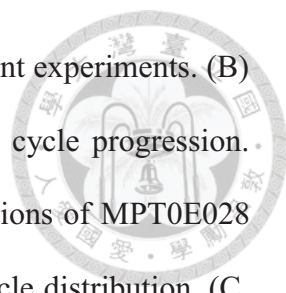


Figure 3-2. The effects of MPT0E028 on cell growth and cell cycle progression in human HCT116 cells. (A) Concentration-dependent effect of MPT0E028 and SAHA on cell growth. HCT116 cells were incubated without or with the indicated concentrations of MPT0E028 or SAHA for 48 h. Cell growth was evaluated by SRB



assay. Data were expressed as mean \pm S.E.M. of at least 3 independent experiments. (B) Concentration-dependent effects of MPT0E028 and SAHA on cell cycle progression. HCT116 cells were treated without or with the indicated concentrations of MPT0E028 or SAHA for 24 h and were analyzed by flow cytometry for cell cycle distribution. (C, D) Data shown are the means of at least 3 independent experiments. (E) Time-dependent effects of MPT0E028 and SAHA on subG1 population. HCT116 cells were treated without or with 1 μ M MPT0E028 or SAHA for the indicated time interval and were analyzed by flow cytometry for subG1 population. (F) MPT0E028 induced-caspase 3 and PARP activation. HCT116 cells were treated without or with the indicated concentration of MPT0E028 or SAHA for 24 h subject to western blot for caspase 3 and PARP analysis. (G) MPT0E028 induced caspase-dependent cell apoptosis. HCT116 cells were treated without or with 3 μ M MPTE028, SAHA or 20 μ M z-VAD-fmk for 24 h and subjected to western blot for caspase 3 and PARP analysis.

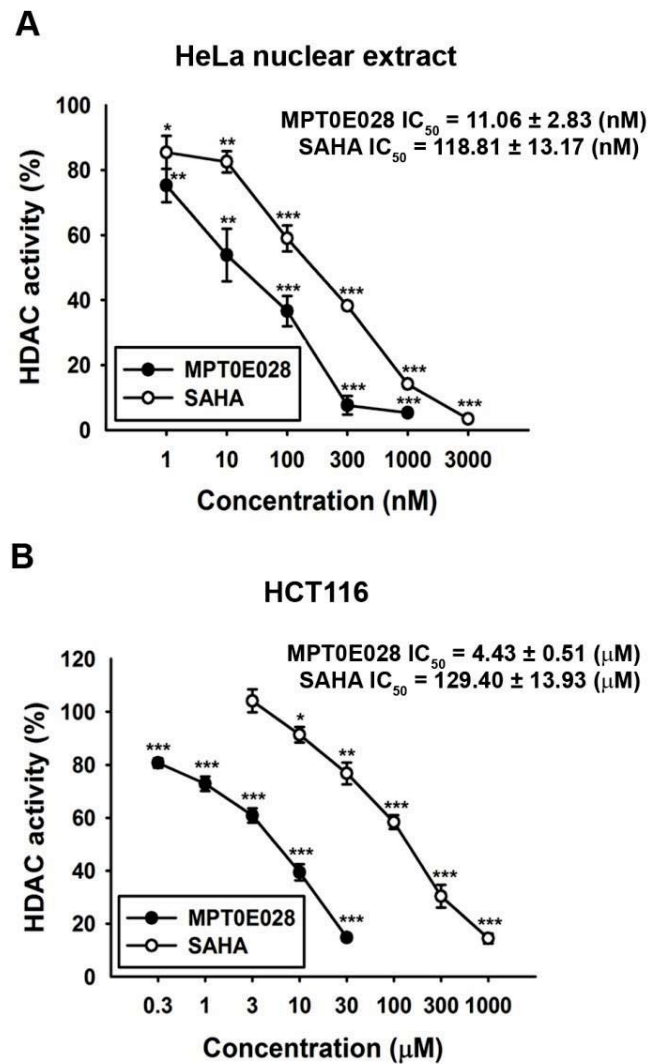


Figure 3-3. Inhibition of HDACs activity by MPT0E028 and SAHA. (A) Inhibition of HDACs activity in HeLa nuclear extracts. Data were expressed as the mean of at least 3 independent experiments. (B) Inhibition of total HDAC activity by MPT0E028 and SAHA. HCT116 cells were treated with the indicated concentrations of MPT0E028 and SAHA for 24 h, and proteins were isolated to determine the inhibition of total HDAC enzyme activity. Data are expressed as the mean \pm S.E.M. of at least 3 independent experiments.

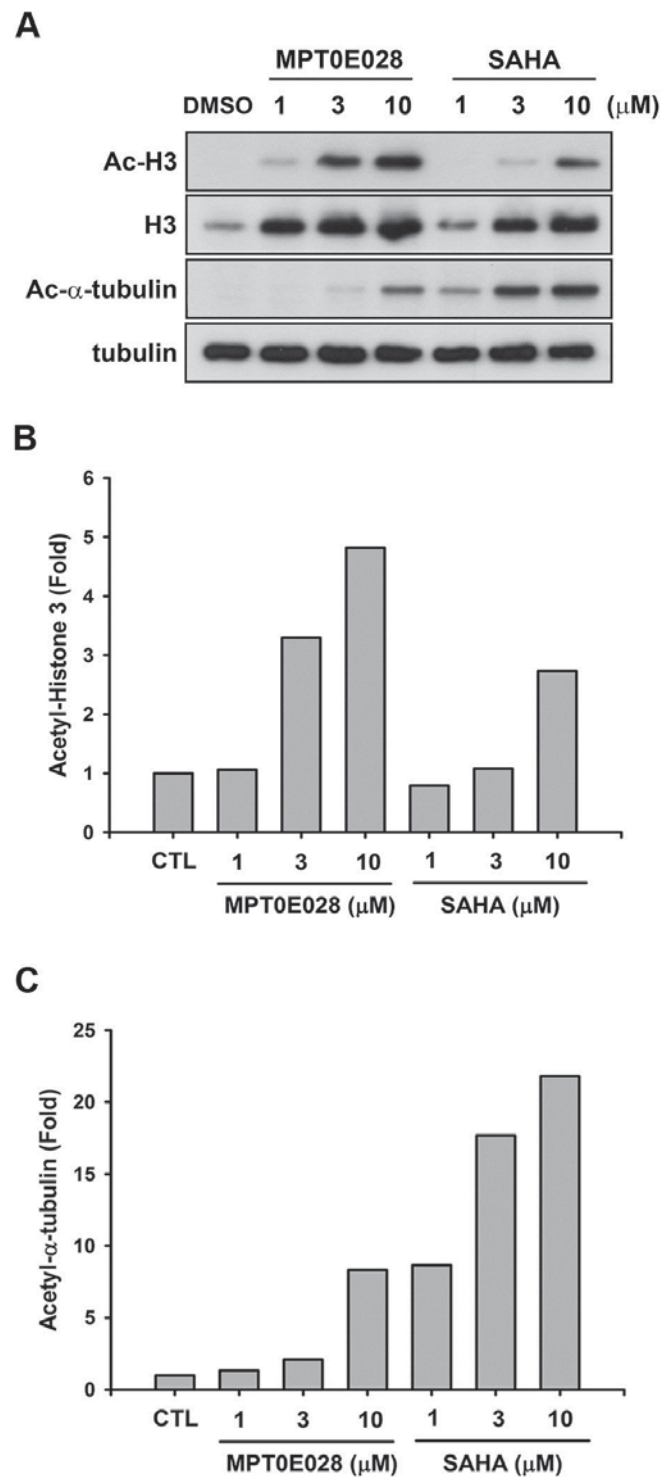
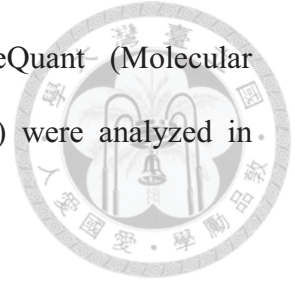


Figure 3-4. Effect of MPT0E028 and SAHA on α -tubulin and histone H3 acetylation. (A) HCT116 cells were treated with MPT0E028 and SAHA for 24 h at the indicated concentrations. Cell lysates were prepared and subjected to SDS-PAGE and immunoblotting using acetyl-histone H3, histone H3, acetyl- α -tubulin, and α -tubulin

antibodies. Quantitative analysis of western blot with ImageQuant (Molecular Dynamics, USA); acetyl-histone H3 (B) and acetyl α -tubulin (C) were analyzed in HCT116 cells.



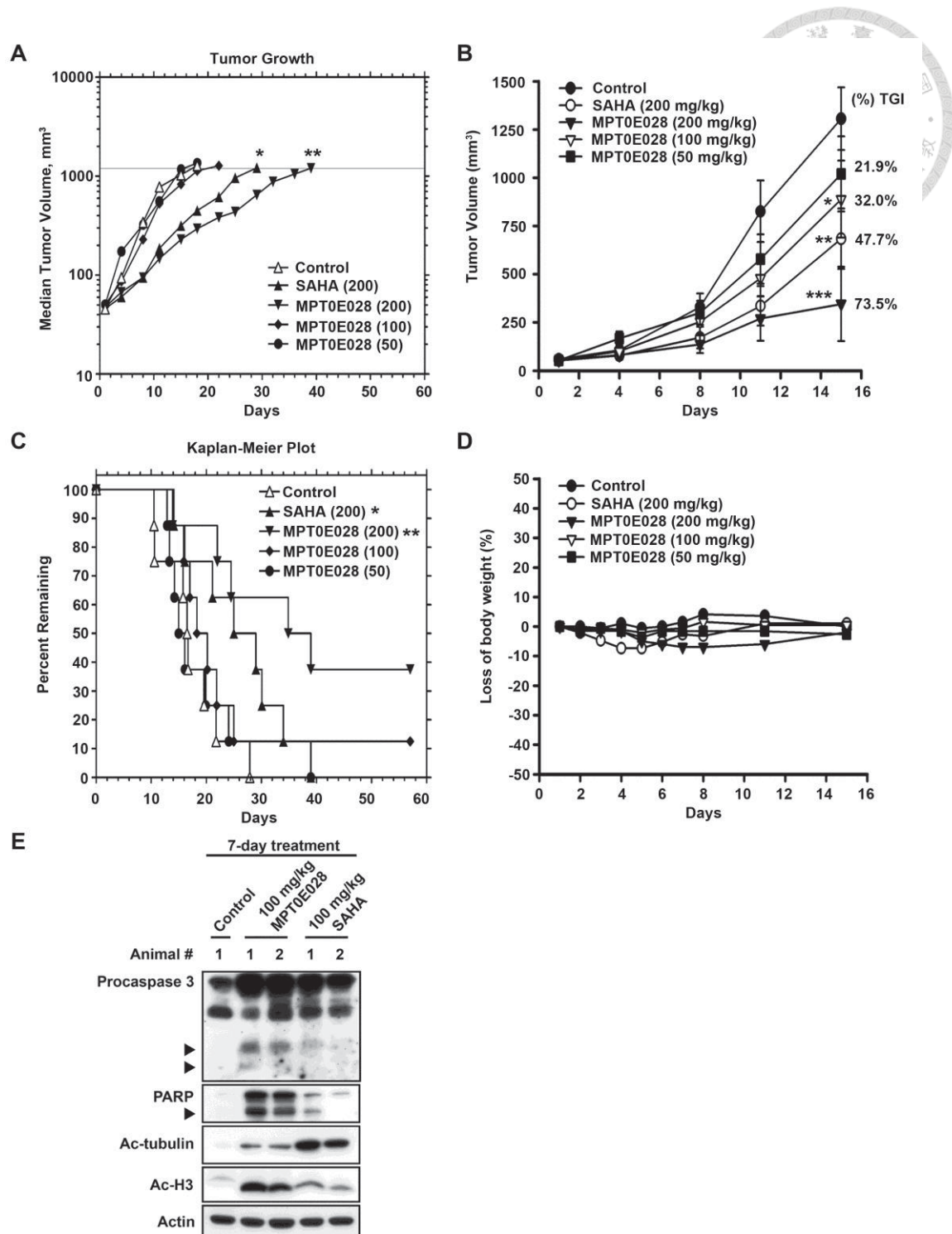


Figure 3-5. The effect of MPT0E028 on the growth of HCT116 cells *in vivo*. All tumors grew to the 1,200-mm³ endpoint volume. (A) Tumors were measured regularly and growth delay was calculated for treatment groups relative to control tumors (TGD). (B) Kaplan-Meier survival analysis was based on the tumor growth endpoint. (C)

Inhibition of tumor growth curves represented a mean \pm SEM and percentage change in mean tumor volume (percent TGI). (D) Body weights were measured daily during the first week and then 2 times per week. The body weight ratio was calculated relative to the baseline measurement. (E) *In vivo* effect of MPT0E028 on the expression of caspase 3, PARP, acetyl-histone H3 and acetyl- α -tubulin in HCT116 xenograft tumors as determined by western blotting.

Table 3-1. Anti-proliferative effects of MPT0E028 in the NCI-60 cell line panels.

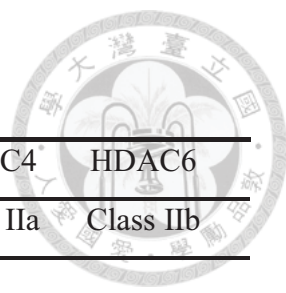
Panels	Cell Line	GI ₅₀ (M)	TGI (M)	LC ₅₀ (M)	Panel	Cell Line	GI ₅₀ (M)	TGI (M)	LC ₅₀ (M)	
Leukemia	CCRF-CEM	1.65E-7	>1.00E-4	>1.00E-4	Melanoma	LOX IMVE	2.22E-7	7.18E-7	2.88E-6	
	HL-60 (TB)	4.39E-7	>1.00E-4	>1.00E-4		MALME-3M	3.75E-8	9.07E-7	>1.00E-4	
	K-562	1.15E-7	>1.00E-4	>1.00E-4		M14	1.79E-7	1.11E-6	6.45E-6	
	MOLT-4	3.17E-7	>1.00E-4	>1.00E-4		MDA-MB-435	1.46E-7	7.06E-7	1.13E-5	
	RPMI-8226	8.11E-8	>1.00E-4	>1.00E-4		SK-MEL-2	4.33E-7	3.89E-6	3.49E-5	
	SR	6.01E-8	>1.00E-4	>1.00E-4		SK-MEL-28	4.06E-7	2.74E-6	>1.00E-4	
Non-Small Cell Lung Cancer	A549/ATCC	2.30E-7	1.09E-6	9.03E-6	SK-MEL-5	1.36E-7	3.10E-7	7.05E-7		
	EKVX	5.34E-7	>1.00E-4	>1.00E-4	UACC-257	1.27E-7	1.65E-6	>1.00E-4		
	HOP-62	1.87E-7	1.06E-6	1.92E-5	UACC-62	7.16E-8	3.39E-7	1.66E-6		
	HOP-92	2.10E-7	8.14E-7	1.80E-5	Ovarian Cancer	IGROV1	1.83E-7	5.33E-7	2.39E-6	
	NCI-H226	1.24E-6	3.88E-6	1.90E-5		OVCAR-3	2.33E-7	9.33E-7	7.30E-6	
	NCI-H23	1.88E-7	9.22E-7	3.84E-6		OVCAR-4	5.09E-7	3.18E-5	>1.00E-4	
	NCI-H322M	1.86E-7	1.14E-5	>1.00E-4		OVCAR-5	6.02E-8	3.16E-7	2.58E-6	
	NCI-H460	1.44E-7	1.66E-6	2.16E-5		OVCAR-8	1.21E-7	1.75E-6	>1.00E-4	
NCI-H522	1.67E-7	8.45E-7	1.30E-5	NCI/ADR-RES		3.85E-8	2.39E-7	>1.00E-4		
Colon Cancer	COLO 205	1.28E-7	2.64E-7	5.46E-7		SK-OV-3	1.90E-7	6.01E-7	4.26E-6	
	HCC-2998	1.94E-7	5.22E-7	2.06E-6		Renal Cancer	786-0	3.00E-7	1.33E-6	4.02E-6
	HCT-116	5.63E-8	2.04E-7	5.66E-7	A498		2.43E-7	1.13E-6	5.13E-6	
	HCT-15	4.30E-7	1.31E-5	9.02E-5	ACHN		1.67E-7	5.76E-7	4.08E-6	
	HT29	1.18E-7	7.16E-7	6.81E-5	CAKI-1		2.18E-7	9.59E-7	>1.00E-4	
	KM12	2.86E-7	1.49E-6	5.78E-6	RXF 393		1.12E-7	3.34E-7	9.98E-7	
	SW-620	1.47E-7	1.12E-5	>1.00E-4	SN12C		4.58E-7	1.02E-5	>1.00E-4	
	CNS Cancer	SF-268	4.64E-7	3.40E-6	7.04E-5		TK-10	1.03E-7	6.60E-7	3.36E-5
SF-295		6.03E-8	3.40E-7	2.43E-6	UO-31		1.69E-7	1.46E-6	5.63E-6	
SF-539		2.41E-7	1.15E-6	3.39E-6	Prostate Cancer	PC-3	2.40E-7	2.10E-5	>1.00E-4	
SNB-19		4.34E-7	1.64E-6	5.65E-6		DU-145	1.79E-7	1.92E-6	>1.00E-4	
SNB-75		5.91E-8	6.27E-6	3.28E-5		Breast Cancer	MCF-7	2.30E-7	1.05E-5	6.27E-5
U251		1.99E-7	8.20E-7	3.76E-6			MAD-MB-231/ATCC	2.41E-7	8.22E-7	2.04E-5
							HS 578T	2.53E-7	1.79E-5	>1.00E-4
							BT-549	6.80E-7	5.84E-6	>1.00E-4
				T-47D			1.21E-7	4.45E-7	>1.00E-4	
				MDA-MB-468			1.96E-7	1.15E-6	6.31E-6	

GI₅₀ : 50% of growth inhibition;

TGI: total growth inhibition;

LC₅₀ : 50% of lethal concentration.

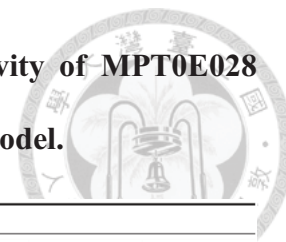
M: Concentration in molar (M).

Table 3-2. Activity of MPT0E028 and SAHA against HDACs

Compound	HDAC1	HDAC2	HDAC8	HDAC4	HDAC6
	Class I			Class IIa	Class IIb
IC ₅₀ (nM ± SE)					
MPT0E028	53.0 ± 12.0	106.2 ± 23.0	2532.6 ± 314.7	>10000	29.5 ± 6.4
SAHA	102.2 ± 22.1	336.2 ± 91.2	2898.9 ± 128.7	>10000	19.5 ± 3.1

HDAC activity was determined indirectly by measuring the fluorescence generated by a deacetylated fluorogenic peptide product (**Materials and Methods**). Data represent triplicate determinations from three independent experiments (mean ± SE). HDAC Class I isoforms: HDAC1, HDAC2, and HDAC8, HDAC Class II isoforms: HDAC4 and HDAC6.

Table 3-3. Treatment response summary for anti-cancer activity of MPT0E028 and SAHA in the human HCT116 colorectal cancer xenograft model.



Compound (n)	Dose (mg/kg)	Route	Schedule	Median TTE	T-C	%TGD	No. of CR	Logrank Significance	P value
Control (8)	-	po	qd to endpoint	16.6	-	-	0		
SAHA (8)	200	po	qd to endpoint	27.0	10	63%	0	*	0.0251
MPT0E028 (8)	200	po	qd to endpoint	36.9	20	122%	3	**	0.0031
MPT0E028 (8)	100	po	qd to endpoint	19.2	2.6	16%	1	ns	0.3084
MPT0E028 (8)	50	po	qd to endpoint	15.5	-	-	0	ns	0.7890

n = number of animals; Study Endpoint = 1200 mm³, Days in Progress = 60; TTE = time to endpoint; T-C = difference between median TTE (days) of treated versus control group; %TGD (tumor growth delay) = [(T-C)/C] × 100; CR = complete regression; Statistical Significance = Logrank test; ns = not significant; * = $P < 0.05$ compare with control. qd = once daily; po = oral administration.

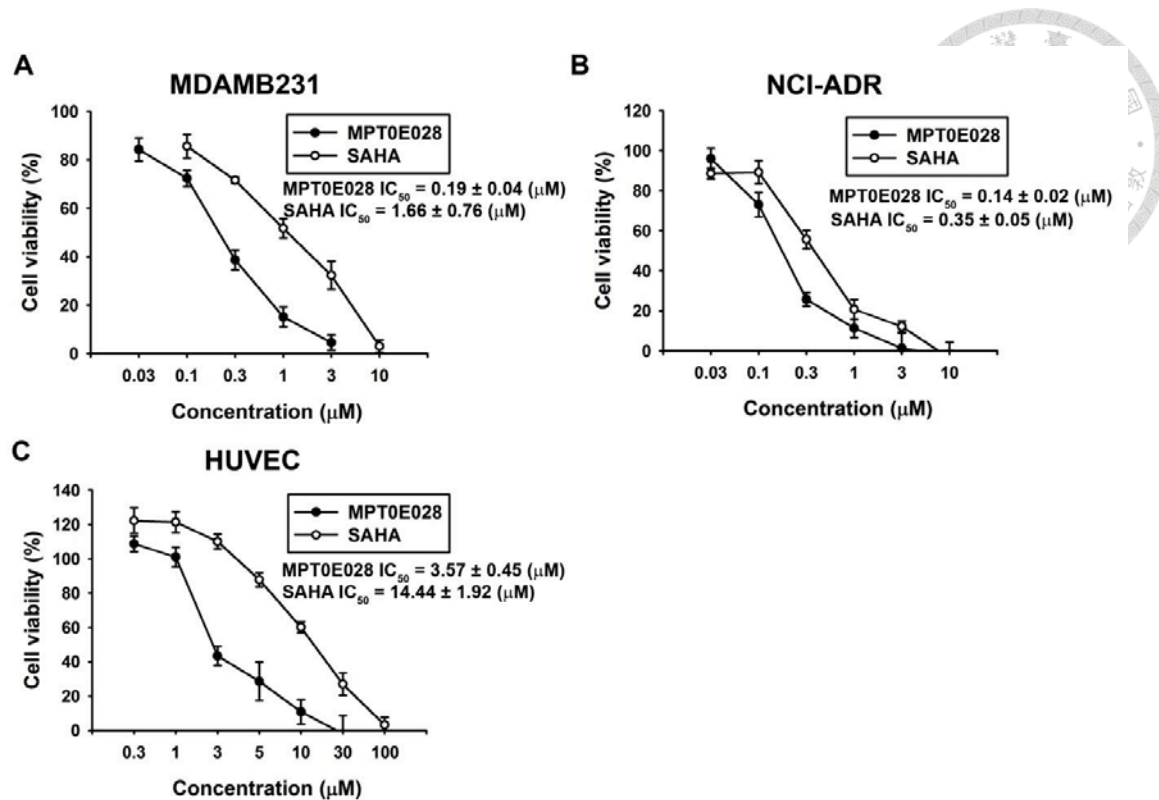


Figure 3-S1. The effects of MPT0E028 on cell growth in human MDAMB231, NCI-ADR and HUVEC cells. Concentration-dependent effect of MPT0E028 and SAHA on cell growth in (A) MDAMB231, (B) NCI-ADR and (C) HUVEC cells. Cells were incubated without or with the indicated concentrations of MPT0E028 or SAHA for 48 h. Cell growth was evaluated by SRB and crystal violet assay. Data were expressed as mean \pm S.E.M. of at least 3 independent experiments.

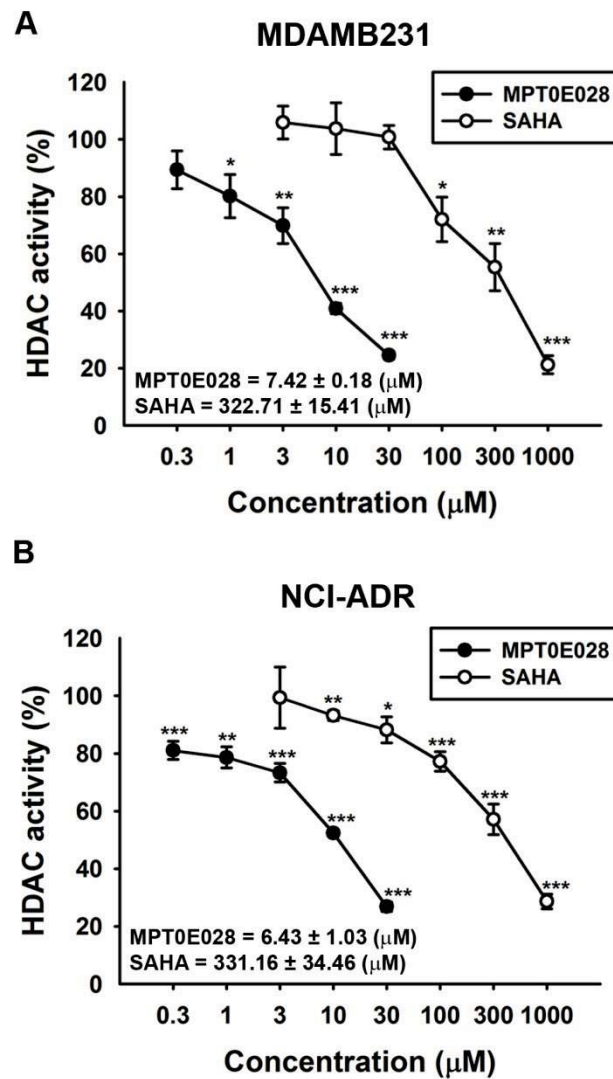


Figure 3-S2. Inhibition of total HDAC activity by MPT0E028 and SAHA in MDAMB231 and NCI-ADR cells. (A) MDAMB231 and (B) NCI-ADR cells were treated with the indicated concentrations of MPT0E028 and SAHA for 24 h, and the total lysate were subjected to total HDAC enzyme activity detection. Data are expressed as the mean \pm S.E.M. of at least 3 independent experiments.

Chapter 4




新型組蛋白去乙酰酶抑制劑, MPT0E028, 在人類 B 細胞
淋巴瘤體內體外引起細胞凋亡之機轉探討

**Novel Histone Deacetylase Inhibitor, MPT0E028,
Displays Potent Growth-Inhibitory Activity against
Human B-cell Lymphoma *in vitro* and *in vivo***

Oncotarget. 2014 Dec 31.

[Epub ahead of print]

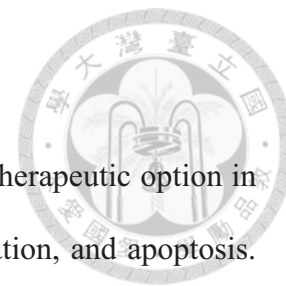
中文摘要



組蛋白去乙酰酶(HDAC)抑制劑因具有使癌細胞產生生長停滯、抑制分化及促使細胞凋亡的能力，近年來已成為具有前景的癌症治療選擇。在本篇論文中，我們發現 MPT0E028，一個新穎的 HDAC 抑制劑，可藉由產生細胞凋亡而抑制 B 細胞淋巴瘤存活率，並具有比 SAHA (第一個被美國食品藥物管理局核可的組蛋白去乙酰酶抑制劑)更強的抑制癌症生長能力。MPT0E028 除了可抑制 HDAC 外，藉由 kinome diversity screening assay 也發現 MPT0E028 可以直接接合並作用在 Akt 上。並且，MPT0E028 在 B 細胞淋巴瘤中具有比 SAHA 更強的抑制 Akt 磷酸化能力。藉由瞬時轉染實驗也發現 MPT0E028 可同時藉由獨立抑制 HDAC 及 Akt 而造成細胞凋亡進而抑制癌症生長。以微陣列實驗分析基因表現，發現 MPT0E028 可以調控許多致癌基因，例如 TP53, MYC, STAT family 等。並且，在動物實驗中發現，MPT0E028 (50–200 mg/kg, po, qd)可以使帶有人類 B 細胞淋巴瘤 Ramos 細胞的老鼠延長存活率，而在異種移植 BJAB 細胞的老鼠上可以抑制腫瘤生長。簡言之，MPT0E028 在體內體外均能有效抑制恶性細胞，而有潛力成為癌症治療的新藥物。

關鍵字： MPT0E028，B 細胞淋巴瘤，組蛋白去乙酰酶(HDAC)，Akt，細胞凋亡

Abstract



Histone deacetylase (HDAC) inhibitor has been a promising therapeutic option in cancer therapy due to its ability to induce growth arrest, differentiation, and apoptosis. In this study, we demonstrated that MPT0E028, a HDAC inhibitor, reduces the viability of B-cell lymphomas by inducing apoptosis and shows a more potent HDAC inhibitory effect compared to SAHA, the first HDAC inhibitor approved by the FDA. In addition to HDACs inhibition, MPT0E028 also possesses potent direct Akt targeting ability as measured by the kinome diversity screening assay. Also, MPT0E028 reduces Akt phosphorylation in B-cell lymphoma with an IC_{50} value lower than SAHA. Transient transfection assay revealed that both targeting HDACs and Akt contribute to the apoptosis induced by MPT0E028, with both mechanisms functioning independently. Microarray analysis also shows that MPT0E028 may regulate many oncogenes expression (e.g., *TP53*, *MYC*, *STAT* family). Furthermore, *in vivo* animal model experiments demonstrated that MPT0E028 (50–200 mg/kg, po, qd) prolongs the survival rate of mice bearing human B-cell lymphoma Ramos cells and inhibits tumor growth in BJAB xenograft model. In summary, MPT0E028 possesses strong *in vitro* and *in vivo* activity against malignant cells, representing a potential therapeutic approach for cancer therapy.

Keywords: MPT0E028, B-cell lymphoma, Histone deacetylase (HDAC), Akt, apoptosis

4.1 Results

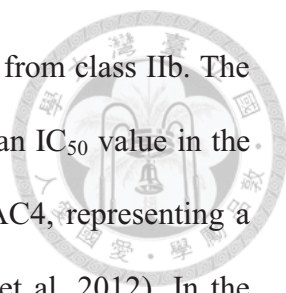


MPT0E028 induces apoptosis in B-cell lymphoma cells

First, we assayed two human B-cell lymphoma cells, Ramos and BJAB, for viability and human normal HUVEC cells for toxicity in the presence of various concentrations of MPT0E028 and SAHA for comparison. MPT0E028 (Fig. 4-1A) showed no toxic effect on human normal HUVEC cells ($IC_{50} > 30 \mu\text{M}$) (Fig. 4-1B), but induced significant concentration-dependent growth inhibition both in Ramos ($IC_{50} = 0.65 \pm 0.1 \mu\text{M}$) and BJAB lymphoma cells ($IC_{50} = 1.45 \pm 0.5 \mu\text{M}$) compared with SAHA ($IC_{50} = 2.61 \pm 0.4$ and $44.22 \pm 10.0 \mu\text{M}$ in Ramos and BJAB cells, respectively) (Fig. 4-1C). We also used FACS cytometry to analyze cell cycle progression and found that MPT0E028 substantially increased the subG1 phase population in a time- and concentration-dependent manner (Fig. 4-1D). Further, we used western blot analysis to characterize several caspases and PARP activation following the treatment of MPT0E028 at the indicated time. The results show that MPT0E028 induced caspase-3 and PARP cleavages, as well as caspase-6, -7, -8, and -9 activation in both cells (Fig. 4-1E). The data are consistent with that of flow cytometry, suggesting that MPT0E028 may induce apoptotic cell death. Taken together, MPT0E028 substantially induces growth inhibition and apoptosis more efficaciously than SAHA in a concentration- and time-dependent manner in human B- cell lymphoma cells.

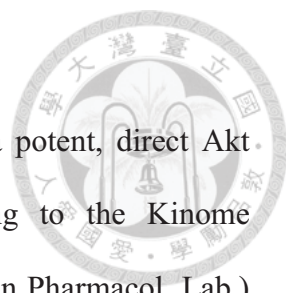
MPT0E028 inhibits histone deacetylase (HDAC) enzyme activity and induces apoptosis through HDAC inhibition

We have previously determined that MPT0E028 is a pan-HDAC inhibitor through direct HDAC targeting (Huang, Lee et al. 2012). In our previous study, we used an enzyme-based HDAC fluorescence activity assay to detect five isoforms of HDACs:



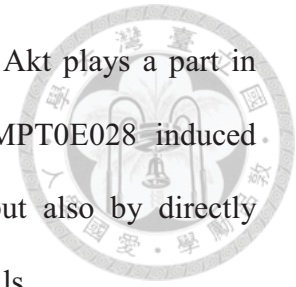
HDAC1, 2, and 8 from class I; HDAC4 from class IIa; and HDAC6 from class IIb. The results showed that MPT0E028 inhibited HDAC1, 2, 6, and 8 with an IC_{50} value in the nanomolar range (29.48–2532.57 nM) but had no effect upon HDAC4, representing a more potent HDAC inhibitory spectrum than SAHA (Huang, Lee et al. 2012). In the present study, we assessed HDAC enzyme activity under treatment of MPT0E028 and SAHA in human B-cell lymphoma by using cell-based HDAC fluorescence activity assay. As shown in Fig. 4-2A, MPT0E028 effectively inhibited HDAC enzyme activity in a concentration-dependent manner ($IC_{50} = 2.88 \pm 1.9 \mu\text{M}$ in Ramos, $4.54 \pm 1.2 \mu\text{M}$ in BJAB), whereas the inhibitory activity of SAHA was much weaker ($IC_{50} = 143.48 \pm 67.4 \mu\text{M}$ in Ramos, $149.66 \pm 40.3 \mu\text{M}$ in BJAB). Protein expression of HDAC1, 2, and 4 was also slightly downregulated after 24 h treatment of MPT0E028 in both cell lines, whereas HDAC6 was downregulated in Ramos cells but only slightly cleaved in BJAB cells, as determined by western blotting (Fig. 4-2B). Biomarkers of HDAC inhibition, which include hyperacetylation of histone 3, α -tubulin, and upregulation of p21 expression (Richon, Sandhoff et al. 2000), were all detected under treatment of MPT0E028 in a time-dependent manner in both Ramos and BJAB cells (Fig. 4-2B). To determine whether inhibition of HDACs is involved in the apoptosis induced by MPT0E028, transient transfection was performed using flag-tagged pcHDAC1, 4, and 6 for HDAC coexpression and pcDNA3.1 vector as control. As shown in Fig. 4-2C, HDAC1, 4, and 6 were all transfected successfully, and the acetylation level of histone 3 and α -tubulin were reversed when HDACs were coexpressed (Fig. 4-2D). MPT0E028-induced caspase 3 and PARP activation were also abolished by coexpressing HDACs (Fig. 4-2E), suggesting that MPT0E028 induces human B-cell lymphoma cells apoptosis through inhibition of HDACs.

MPT0E028 inhibits Akt/mTOR pathway activation



In addition to HDAC inhibition, MPT0E028 also possesses a potent, direct Akt targeting ability in a concentration-dependent manner according to the Kinome Diversity Screen Data Report from Ricerca Pharma Services (Taiwan Pharmacol. Lab.) using the enzyme-based ELISA quantitation method ($IC_{50} = 5.78 \mu\text{M}$) (Fig. 4-3A). Western blot analysis revealed that MPT0E028 caused a reduction of p-Akt (T308) in Ramos and p-Akt (S473) in BJAB cells, as well as the downstream protein deactivation of p-mTOR and p-GSK3 β in a time-dependent manner (Fig. 4-3B). Total Akt and downstream proteins expressions were also downregulated by MPT0E028 in Ramos cells (Fig. 4-3B, left panel), whereas these remained unchanged in BJAB cells (Fig. 4-3B, right panel), suggesting a different modulation of MPT0E028 in different cells. LY294002, a PI3K inhibitor, was used as a positive control to check the basal expression of Akt in both cells. As shown in Fig. 4-S1, p-Akt (S473) and p-Akt (T308) dephosphorylation could only be detected in BJAB cells and in Ramos cells, respectively, indicating that Akt phosphorylation is different among cell lines. To exploit the detailed mechanisms of p-Akt (S473) dephosphorylated by MPT0E028, we focused on BJAB cells. As shown in Fig. 4-3C, the effect of MPT0E028 on Akt dephosphorylation is about 6 times more potent than SAHA using the cell-based ELISA assay (MPT0E028, $IC_{50} = 5.90 \pm 1.6 \mu\text{M}$; SAHA, $IC_{50} = 32.89 \pm 11.3 \mu\text{M}$). To assess the role of Akt in MPT0E028-induced cell apoptosis, we examined the effect of overexpressing Akt on rescuing MPT0E028-induced apoptotic death by transiently transfect BJAB cells with constitutively active myr-Akt. Transfection of myr-Akt effectively reversed the inhibition effect of MPT0E028 on Akt phosphorylation and its downstream protein activation of p-mTOR and p-GSK3 β (Fig. 4-3D). Moreover, caspase 3 and PARP activation were also abolished when overexpressing Akt in

MPT0E028- and SAHA-treated cells (Fig. 4-3E), confirming that Akt plays a part in MPT0E028-induced cell apoptosis. These results suggest that MPT0E028 induced apoptotic cell death not only by inhibition of HDAC activity but also by directly targeting the Akt-dependent pathway in human B-cell lymphoma cells.



Correlation between HDAC and Akt inhibition of MPT0E028 on cell apoptosis

It has been reported that HDAC inhibitors may cause Akt depletion through modulation of gene expression (Chen, Ghazawi et al. 2006) and inhibit Akt phosphorylation through disruption of HDAC-PP1 (protein-phosphatase 1) complex (Chen, Weng et al. 2005). In this study, we aimed to determine the relationship between HDAC and Akt under the inhibitory effect of MPT0E028. First, we transfected BJAB cells with pcHDAC1, pcHDAC4, and pcHDAC6 (Fig. 4-4A), respectively, to further examine the individual role of HDACs in MPT0E028-inhibited Akt and downstream proteins activation. As shown in Fig. 4-4B, even though MPT0E028-inhibited p-Akt (S473) was slightly reversed when overexpressing HDAC1 and 6 in BJAB cells, the downstream protein p-mTOR did not reverse in any obvious fashion. The results indicated that MPT0E028 did not inhibit Akt phosphorylation through HDAC inhibition. We then transfected BJAB cells with myr-Akt to examine the role of Akt in rescuing MPT0E028-inhibited HDAC protein expression and enzyme activity. Overexpressing Akt neither influenced the HDAC protein expression inhibited by MPT0E028 nor the HDAC inhibition markers acetyl-histone 3, acetyl- α -tubulin, or p21 induced by MPT0E028 (Fig. 4-4C). MPT0E028-inhibited HDAC enzyme activity was similarly unaffected by Akt overexpression (Fig. 4-4D). These data indicated that MPT0E028 does not reduce HDAC enzyme activity or protein expression through Akt inhibition. Based on these results, it appears that MPT0E028 targets both HDACs and Akt

independently.



MPT0E028 affects many genes and protein expressions

Because HDAC inhibitors affect many gene expressions at the transcriptional level, we determined which genes were up- or downregulated by MPT0E028. We extracted RNA from MPT0E028-treated Ramos and BJAB cells and submitted to Phalanx Biotech (Hsinchu, Taiwan). Standard selection criteria to identify differentially expressed genes are established at $|\text{Fold change}| \geq 1$ and $P < 0.05$. According to the report, around 2,000 genes are upregulated and 1,600 genes downregulated under treatment of MPT0E028. Results showed that MPT0E028 may affect the entire *STAT* family (*STAT1*, *STAT2*, *STAT3*, *STAT4*, *STAT5A*, *STAT5B*, *STAT6*) as well as some oncoproteins such as *MYC*, *TP53*, and *BID* (Table. 4-1), which are key regulators participating in many pathways. We also performed RT-PCR and western blotting of these genes for mRNA (Fig. 4-5A) and protein (Fig. 4-5B) detection. However, analysis of these genes altered in expression revealed cell-line-specific response to MPT0E028. In these genes of interest, we found that *STAT6*, *TP53*, and *MYC* are inhibited consistently at gene, mRNA, and protein expression in both cell lines (Table. 4-1) (Fig. 4-5A and 4-5B). Evidence has shown that some HDACs correlate with *STAT6* (Mehrotra, Riley et al. 2011), p53 (Juan, Shia et al. 2000), and c-myc (Zhang, Chen et al. 14 June 2012). However, our data show that inhibition of *STAT6* and c-myc expression by MPT0E028 may not be mediated by HDACs (HDAC1, 4, and 6) inhibition in B-cell lymphoma cell lines (Fig. 4-5C). Other genes, however, revealed inconsistent expression of mRNA and protein levels, indicating that complicated regulations may exist at transcriptional and translational levels in the presence of MPT0E028.

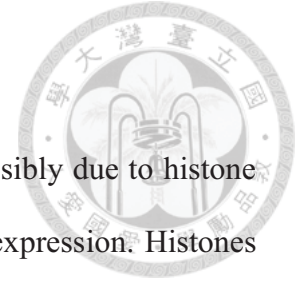
MPT0E028 prolongs survival rate and inhibits tumor growth *in vivo*

On the basis of MPT0E028-induced apoptotic effect *in vitro*, we further examined the *in vivo* antitumor effect of MPT0E028 in two animal models. We produced a Ramos engraftment in NOD/SCID mice and a BJAB xenograft in nude mice. In the Ramos engraftment model, mice were randomly divided into three groups receiving the following daily treatment by oral gavage: (a) vehicle, (b) MPT0E028 100 mg/kg, and (c) SAHA 200 mg/kg. The end point used for this study was survival rate. Survival rate in the MPT0E028-treated group was significantly prolonged compared with the control group, whereas the SAHA-treated group showed no significant efficacy (Fig. 4-6A). In the BJAB xenograft model, mice were randomly divided into five groups receiving the following daily treatment, also by oral gavage: (a) vehicle, (b) MPT0E028 50 mg/kg, (c) MPT0E028 100 mg/kg, (d) MPT0E028 200 mg/kg, and (e) SAHA 200 mg/kg. MPT0E028 showed an effective tumor reduction effect in a dose-dependent manner (40.4% of TGI, total growth inhibition) (Fig. 4-6B). The 200 mg/kg SAHA-treated group showed an effect similar to the 100 mg/kg MPT0E028-treated group (17.9% and 20.8% of TGI, respectively), representing more potent tumor reduction than MPT0E028. We also observed no significant difference in body weight between these groups, indicating that MPT0E028 exhibits little apparent toxicity *in vivo* (Fig. 4-6C). After 31 days of treatment, the mice were sacrificed, and tumors were carefully removed for western blot analysis. As shown in Fig. 4-6D, caspase 3 and PARP were activated in MPT0E028-treated and SAHA-treated groups, with MPT0E028 inducing a more profound effect. The acetylation levels of histone 3 and α -tubulin were also increased in MPT0E028- and SAHA-treated groups, and MPT0E028-inhibited Akt phosphorylation was also detected. As our data showed, the effect of MPT0E028 *in vivo* is consistent with that *in vitro*. Taken together, the antitumor activity of MPT0E028 against human

B-cell lymphoma tumor, as demonstrated by both engraftment and xenograft, was superior to that of SAHA, proving MPT0E028's potent antitumor effect *in vivo*.

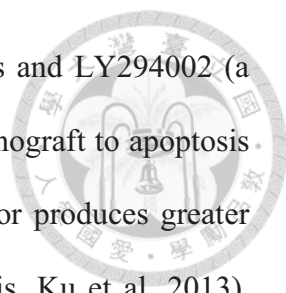


4.2 Discussion



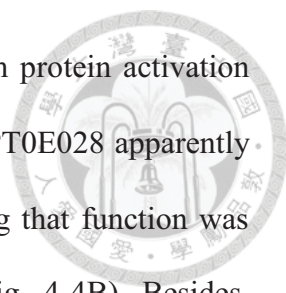
Epigenetic dysregulation occurs in many malignant cells, possibly due to histone modification leading to chromatin remodeling and abnormal gene expression. Histones can be modified in many different ways, including acetylation, methylation, phosphorylation, sumoylation and ubiquitination (Shelley L 2002). Modifying epigenetic changes is a recognized therapeutic strategy, and histone acetylation is one of these approaches. HDAC inhibitors relax the condensed chromatin, allowing the re-expression of genes that control cell proliferation and survival. On the other hand, HDAC inhibitors may cause non-histone substrates acetylation, which have been implicated in the anticancer activity of HDAC inhibitors (Blagosklonny, Robey et al. 2002; Glozak, Sengupta et al. 2005). Many HDAC inhibitors are in clinical trials and have become promising agents in recent years. We previously demonstrated that MPT0E028, a novel HDAC inhibitor, exhibited potent anticancer ability toward various cell lines, including hematological malignancies and solid tumors. This revealed a forceful apoptosis-inducing and HDAC inhibitory effect on colorectal carcinoma *in vitro* and *in vivo* (Huang, Lee et al. 2012). Since current HDAC inhibitors are more effective against certain hematological malignancies such as cutaneous T-cell lymphoma (CTCL) (Mercurio, Minucci et al. 2010), but not B-cell lymphoma, we further investigated the antitumor effect and detail mechanisms of MPT0E028 in B-cell lymphomas *in vitro* and *in vivo*. Our results demonstrate that MPT0E028 targeted both Akt and HDACs while inducing B-cell lymphoma cell apoptosis, suggesting MPT0E028 as a novel antitumor agent with dual functionality.

Combining HDAC inhibitors and PI3K/Akt pathway inhibition has been shown to further induce apoptosis in human cancer cells *in vitro* and *in vivo* (LoPiccolo,



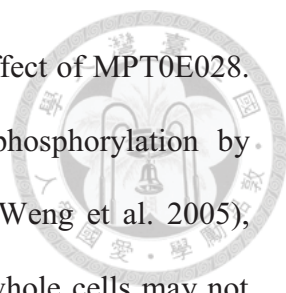
Blumenthal et al. 2008). For example, combining HDAC inhibitors and LY294002 (a PI3K inhibitor) sensitizes a non-small cell lung cancer (NSCLC) xenograft to apoptosis (Denlinger, Rundall et al. 2005); in prostate cancer, HDAC inhibitor produces greater antitumor activity when combines with PI3K/mTOR inhibitor (Ellis, Ku et al. 2013). Co-administration of HDAC inhibitors with perifosine (an Akt inhibitor) and rapamycin (an mTOR inhibitor) in human leukemia cells also promotes mitochondria injury and apoptosis (Rahmani, Reese et al. 2005; Nishioka, Ikezoe et al. 2008). Because MPT0E028 targets both HDACs and the Akt pathway, the benefit of omission from combination treatment and efficacious outcomes are predictable. Combination treatment with HDAC inhibitors plus PI3K/Akt pathway inhibition also potentiates the targeting effect of tumor angiogenesis (Verheul, Salumbides et al. 2008), invasion, and migration (Wedel, Hudak et al. 2011), indicating MPT0E028's wide-ranging usefulness. However, detailed function and mechanisms need to be further investigated.

Many studies have demonstrated that HDAC inhibitors also influence Akt phosphorylation (Fuino, Bali et al. 2003; Bali, George et al. 2004), but few studies have identified the relationship between HDAC and Akt under the effect of a HDAC inhibitor. Evidence show that HDAC inhibitors, such as valproic acid and butyrate, impede Akt1 and Akt2 expression, which leads to Akt deactivation and apoptotic cell death (Chen, Ghazawi et al. 2006). In another study, Chen *et al.* demonstrated that HDAC inhibitors cause Akt dephosphorylation by disrupting HDAC-protein phosphatase 1 (PP1) complexes, with HDAC1 and 6 contributing to this effect much more (Chen, Weng et al. 2005). Consistent with our data, we show that overexpression of HDAC1 potentiates the Akt-phopshorylation level at the baseline (Fig. 4-4B), and the MPT0E028-inhibited Akt phosphorylation could be partially rescued when HDAC1 and



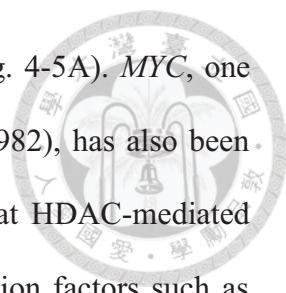
6 were overexpressed. However, in this study, the Akt downstream protein activation (e.g., p-mTOR, p-GSK3 β , p-p70S6K and p-eIF4E) inhibited by MPT0E028 apparently could not be rescued when HDACs were overexpressed, suggesting that function was not fully recovered under the inhibition effect of MPT0E028 (Fig. 4-4B). Besides, overexpressing Akt did not affect HDAC expression (Fig. 4-4C) or enzyme activity (Fig. 4-4D), demonstrating that MPT0E028 inhibits HDAC activity parallel to Akt deactivation. In Ramos cells, total Akt protein expression was depleted under the effect of MPT0E028 (Fig. 4-3B, left panel). One possible mechanism may involve transcription inhibition (Chen, Ghazawi et al. 2006), another possible explanation may relate to Hsp90 and proteasome degradation. Evidence has shown that HDAC6 directly regulates Hsp90 acetylation, and Akt is a client protein of Hsp90; therefore, inhibition of HDAC6 may disrupt the chaperone function of Hsp90, leading to Akt depletion (Sato, Fujita et al. 2000; Bali, Pranpat et al. 2005). We also performed microarray analysis in Ramos cells and observed that *Akt1* was downregulated (Log₂ ratio = -1.082, ****P* value < 0.001) under treatment of MPT0E028 (data not shown), suggesting MPT0E028 may influence Akt protein expression through transcription inhibition. Thus, MPT0E028 may inhibit Akt activation through different mechanisms due to characteristics of different cell types.

The values of IC₅₀ obtained from our enzyme-based HDAC activity assay (Huang, Lee et al. 2012) were around 100 times lower than that obtained from our cell-based assay (Fig. 4-2A). This phenomenon may be explained by the existence of a much more complicated environment in whole cells that prevents MPT0E028 from achieving its targets. However, enzyme-based (Fig. 4-3A) and cell-based Akt activity assay (Fig. 4-3C) show controversially similar values of IC₅₀, both around 5 μ M, illustrating other



indirect mechanisms may exist that facilitate the Akt-deactivation effect of MPT0E028. Chen *et al.* demonstrated that HDAC inhibitors cause Akt dephosphorylation by disrupting HDAC-protein phosphatase 1 (PP1) complexes (Chen, Weng et al. 2005), thereby releasing PP1 to deactivate Akt. MPT0E028 treatment in whole cells may not only target Akt directly but also inhibit phosphorylation through HDAC inhibition indirectly, therefore facilitating MPT0E028-inhibited Akt phosphorylation.

Since HDAC inhibitors modify histone acetylation, many genes may turn up or down due to epigenetic modulation under treatment (Peart, Smyth et al. 2005; Sikandar, Dizon et al. 2010). Microarray analysis showed that MPT0E028 may influence many genes, including the *STATs* family and some oncoproteins, in B-cell lymphoma cells (Table. 4-1). We found that STAT6, p53, and c-myc are consistent in gene, mRNA, and protein expression in both cells (Fig. 4-5A and 4-5B). STAT6 has been found to be constitutively active in some leukemia and lymphoma types, associated with cell proliferation and transformation (Buglio, Georgakis et al. 2008). SAHA may inhibit STAT6 mRNA and protein expression therefore decrease cell proliferation (Buglio, Georgakis et al. 2008). In our study, STAT6 was profoundly inhibited at transcriptional and translational levels under treatment of MPT0E028 (Fig. 4-5A and 4-5B). However, we found that HDAC1, 4, and 6 contributed little to MPT0E028-inhibited STAT6 expression (Fig. 4-5C), indicating that MPT0E028 may regulate STAT6 expression in a HDACs-independent manner. HDAC inhibitors that cause mutant p53 degradation by either restoring or mimicking p53 trans-functions (Blagosklonny, Trostel et al. 2005) or through HDAC6-Hsp90 chaperone axis have been reported (Li, Marchenko et al. 2011). Because Ramos (p53^{mutant} 1254D) and BJAB (p53^{mutant} H193R) cells both harbor mutant p53, MPT0E028-caused p53 degradation may be expected. However, p53 mRNA could



also be inhibited by MPT0E028 through unknown mechanisms (Fig. 4-5A). *MYC*, one of the major oncogenes in B-cell lymphoma (Taub, Kirsch et al. 1982), has also been affected by MPT0E028 (Fig. 4-5A and 4-5B). Evidence shows that HDAC-mediated deacetylation alters the transcriptional activity of nuclear transcription factors such as c-myc (Patel, Du et al. 2004). In our study, we found that HDAC1, 4, and 6 are barely evident in MPT0E028-inhibited c-myc expression (Fig. 4-5C). Recent findings show that HDAC3 may cooperate with c-myc to regulate microRNA expression and therefore malignant transformation in aggressive B-cell malignancies (Zhang, Chen et al. 14 June 2012). MPT0E028 may probably inhibit these cellular proteins through unknown mechanisms that need to be further elucidated. However, MPT0E028 at concentrations causing apoptosis decreases the expression of STAT6 and c-myc. Thus, downregulation of STAT6 and c-myc may play a part in MPT0E028-induced apoptosis in B-cell lymphoma.

Clinical trials using HDAC inhibitors alone have shown limited efficacy against solid tumors. Therefore, combinations with classical chemotherapeutic agents (Gatti, Sevko et al. 2014; Gueugnon, Cartron et al. 2014) or new small molecule inhibitors (Ha, Fiskus et al. 2014) are being investigated. According to our previous study, MPT0E028 also showed synergism in combination with tyrosine kinase inhibitors, such as erlotinib and sorafenib, in non-small cell lung cancer (NSCLC) and liver cancer, respectively (Chen, Chen et al. 2013; Chen, Chen et al. 2014). Therefore, combination treatment with different therapeutic agents in solid tumors may broaden the potential usage of MPT0E028. In the case of B-cell lymphoma, HDAC inhibitor has shown synergistic effect with anti-CD20 antibody rituximab (Shimizu, Kikuchi et al. 2010). However, emerging evidence has demonstrated that rationale should be followed to combine

HDAC inhibitors with immunotherapy to obtain synergistic effect due to complexity of HDAC inhibitors on immune system and tumor microenvironment (Kroesen, Gielen et al. 2014). Although MPT0E028 shows significant antitumor effect in B-cell lymphoma, detailed mechanisms still need to be further investigated.

In conclusion, our data suggest that MPT0E028 is a promising and effective anti-cancer HDAC inhibitor. We demonstrated that MPT0E028 exhibits a potent dual function of HDAC and Akt inhibition, leading to B-cell lymphoma apoptosis *in vitro* and *in vivo*. Its antitumor activities include inducing apoptosis, HDAC activity inhibition, Akt pathway deactivation, and regulation of many genes *in vitro*; and prolongation of survival rate and reduction of tumor volume *in vivo*. Our previous work (Huang, Lee et al. 2012; Chen, Chen et al. 2013; Chen, Chen et al. 2014) and current studies suggest that MPT0E028 has better efficacy *in vivo* and *in vitro* compared to SAHA. In totality, our results provide compelling evidence that MPT0E028 can be an effective antitumor agent in the treatment of B-cell lymphoma.

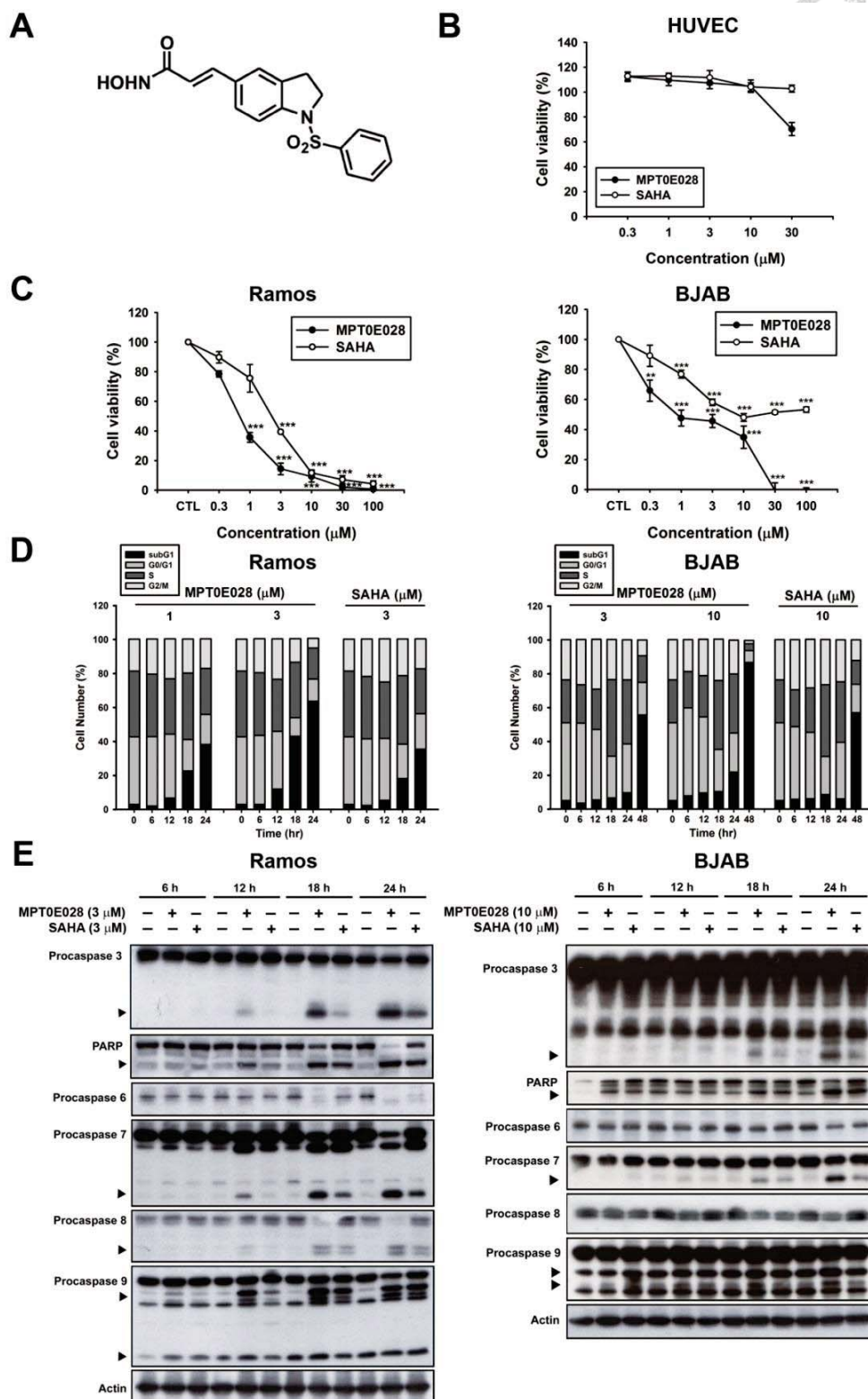


Figure 4-1. MPT0E028-induced apoptosis in human lymphoma cell lines. A. Structure of MPT0E028. B. Non-cytotoxic effect of MPT0E028 against normal cell line. C. Concentration-dependent effect of MPT0E028 or SAHA on the inhibition of cell

growth in B-cell lymphoma cell lines. In B and C, HUVEC, Ramos, and BJAB cells were treated with different concentrations of MPT0E028 or SAHA for 24 h, and then cell viability was determined by MTT assay. Data represent mean \pm SEM from at least three independent experiments ($*P < 0.05$; $**P < 0.01$; $***P < 0.001$; compared with the respective control group). D. Time- and concentration-dependent effect of MPT0E028 and SAHA on the progression of subG1 population. Ramos and BJAB cells were treated with different concentrations of MPT0E028 or SAHA for the indicated times and then cell cycles were determined by flow cytometry. E. Effect of MPT0E028 and SAHA on caspases and PARP activation. Ramos and BJAB cells were treated with indicated concentration of MPT0E028 or SAHA for the indicated time, and then whole-cell lysates were subjected to western analysis detecting caspase 3, 6, 7, 8, 9, and PARP.

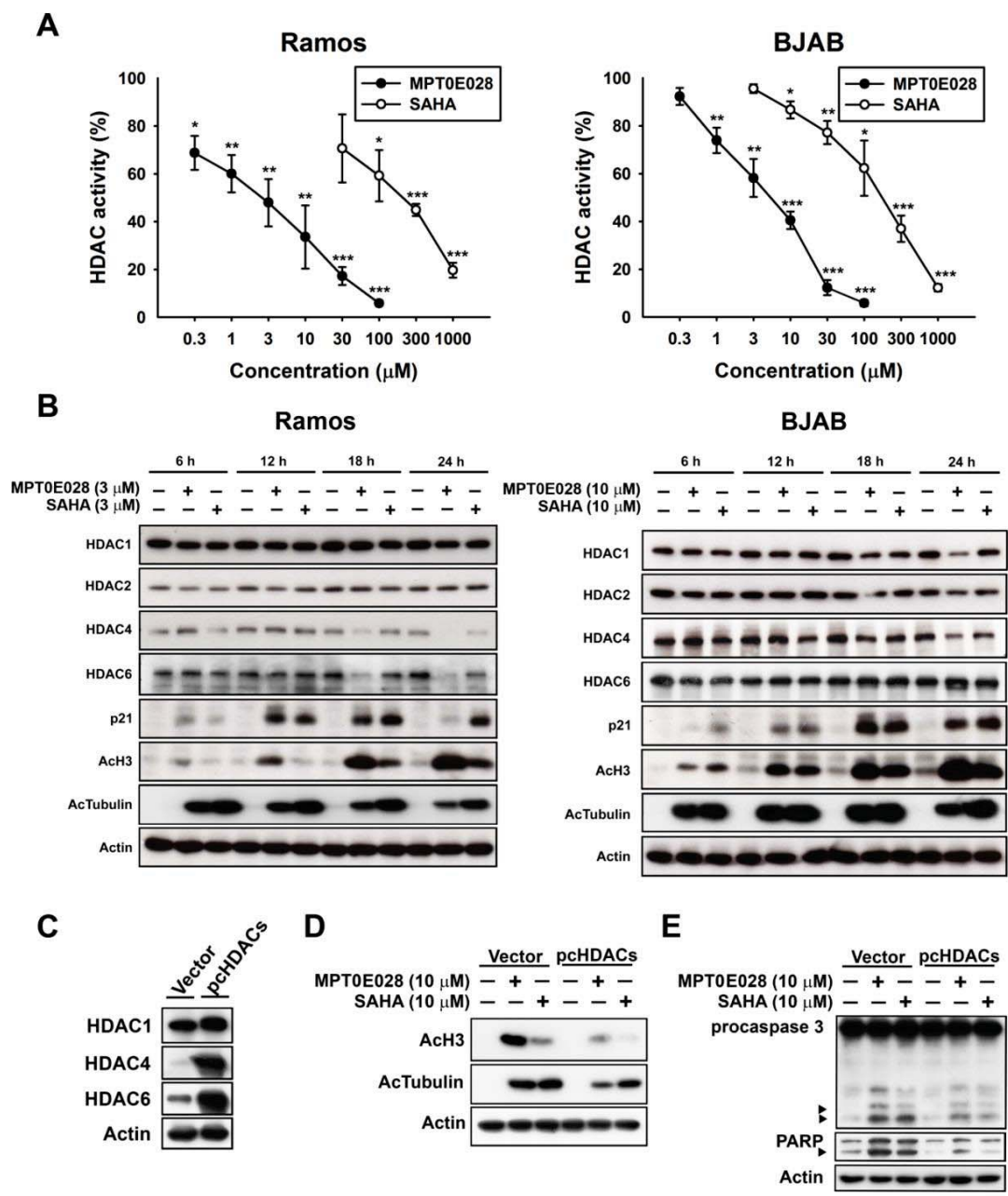


Figure 4-2. Effect of MPT0E028 on HDAC enzyme activity and protein expression in human B-cell lymphoma cells. A. Effect of MPT0E028 on HDAC enzyme activity. Ramos and BJAB cells were treated with different concentrations of MPT0E028 or SAHA for 24 h and then HDAC activities were detected as described in Materials and Methods. Data represent mean \pm SEM from at least three independent experiments. (* P < 0.05; ** P < 0.01; *** P < 0.001; compared with the respective control group) B. Effect of MPT0E028 on HDAC protein expression and HDAC inhibition markers. Cells

were treated with MPT0E028 or SAHA for the indicated time interval and then harvested for HDAC1, 2, 4, 6, and HDAC inhibition marker (acetyl-histone 3, acetyl- α -tubulin, and p21) detection using western blotting. C. Confirmation of the transfection effect of HDACs coexpression. D. Effect of HDACs coexpression on MPT0E028-induced HDAC inhibition markers upregulation. E. Contribution of HDACs to MPT0E028-induced cell apoptosis. BJAB cells were transiently transfected with plasmids encoding vector or flag-tagged human HDAC1, 4, and 6 by using nucleofection described in Materials and Methods. Whole cell lysates were subjected to western blotting for C. HDACs detection and then treated with 10 μ M MPT0E028 or SAHA for 24 h. Whole cell lysates were subjected to western blotting for D. acetyl-histone 3, acetyl- α -tubulin. E. caspase 3, and PARP detection.

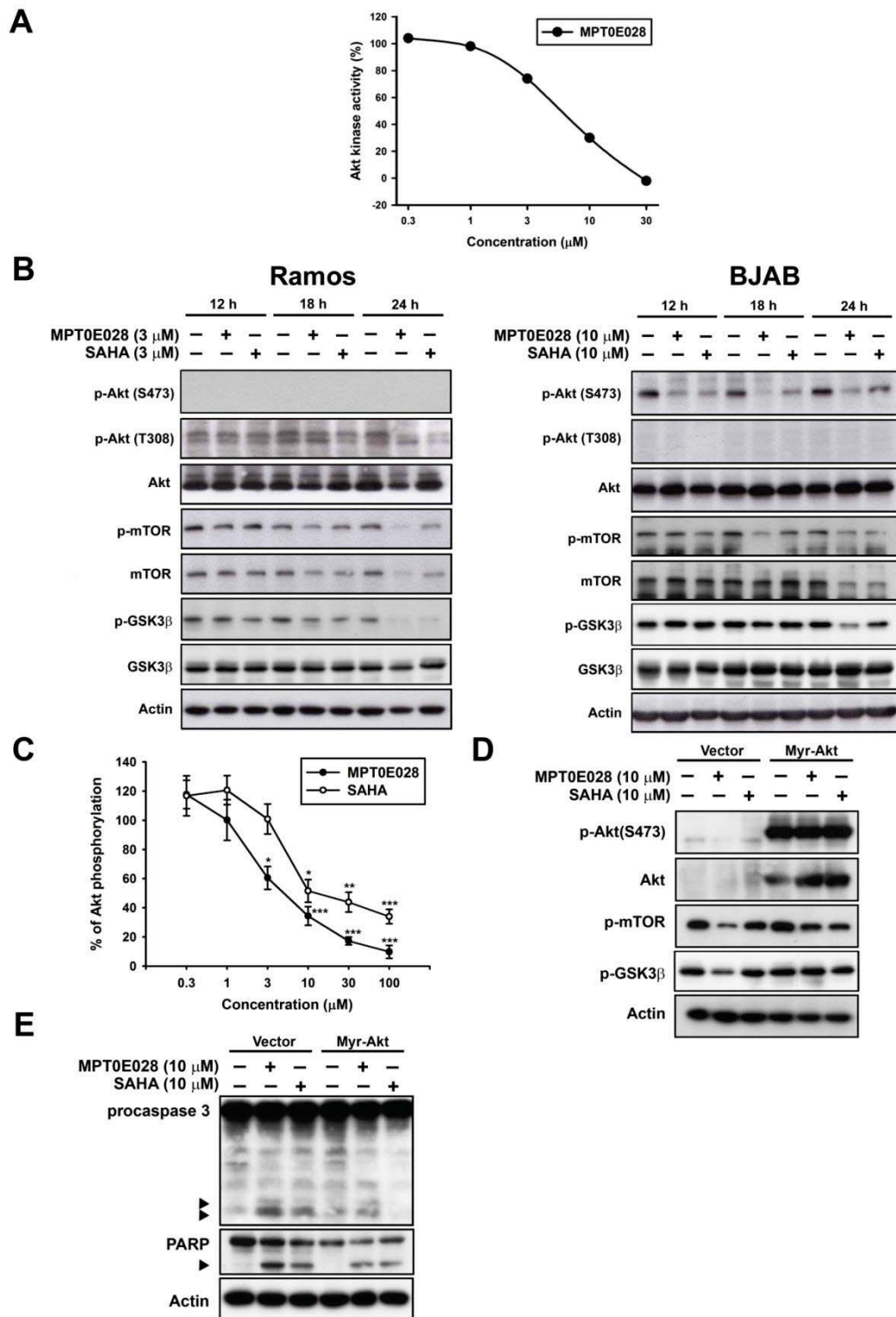
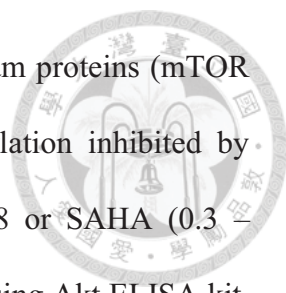


Figure 4-3. Effect of MPT0E028 on Akt and downstream proteins. A. Effect of Akt kinase activity inhibited by MPT0E028. Detailed procedure is described in Materials and Methods. B. Effect of MPT0E028 on Akt and downstream proteins phosphorylation. Cells were treated with MPT0E028 or SAHA for the indicated time interval and then



harvested for p-Akt (S473), p-Akt (T308), Akt, and Akt downstream proteins (mTOR and GSK3 β) detection using western blotting. C. Akt phosphorylation inhibited by MPT0E028. BJAB cells were treated with or without MPT0E028 or SAHA (0.3–100 μ M) for 24 h and then harvested for p-Akt (S473) detection using Akt ELISA kit. Data represent mean \pm SEM from at least three independent experiments. (* P < 0.05; ** P < 0.01; *** P < 0.001; compared with the respective control group) D. Confirmation of the transfection effect of constitutive active myr-Akt and downstream proteins. E. Contribution of Akt to MPT0E028-induced cell apoptosis. In D and E, BJAB cells were transiently transfected with plasmids encoding vector or myr-Akt by using nucleofection described in Materials and Methods and treated with or without MPT0E028 or SAHA (10 μ M) for 24 h. Whole cell lysates were subjected to western blotting for Akt, downstream proteins, casepase 3, and PARP detection.

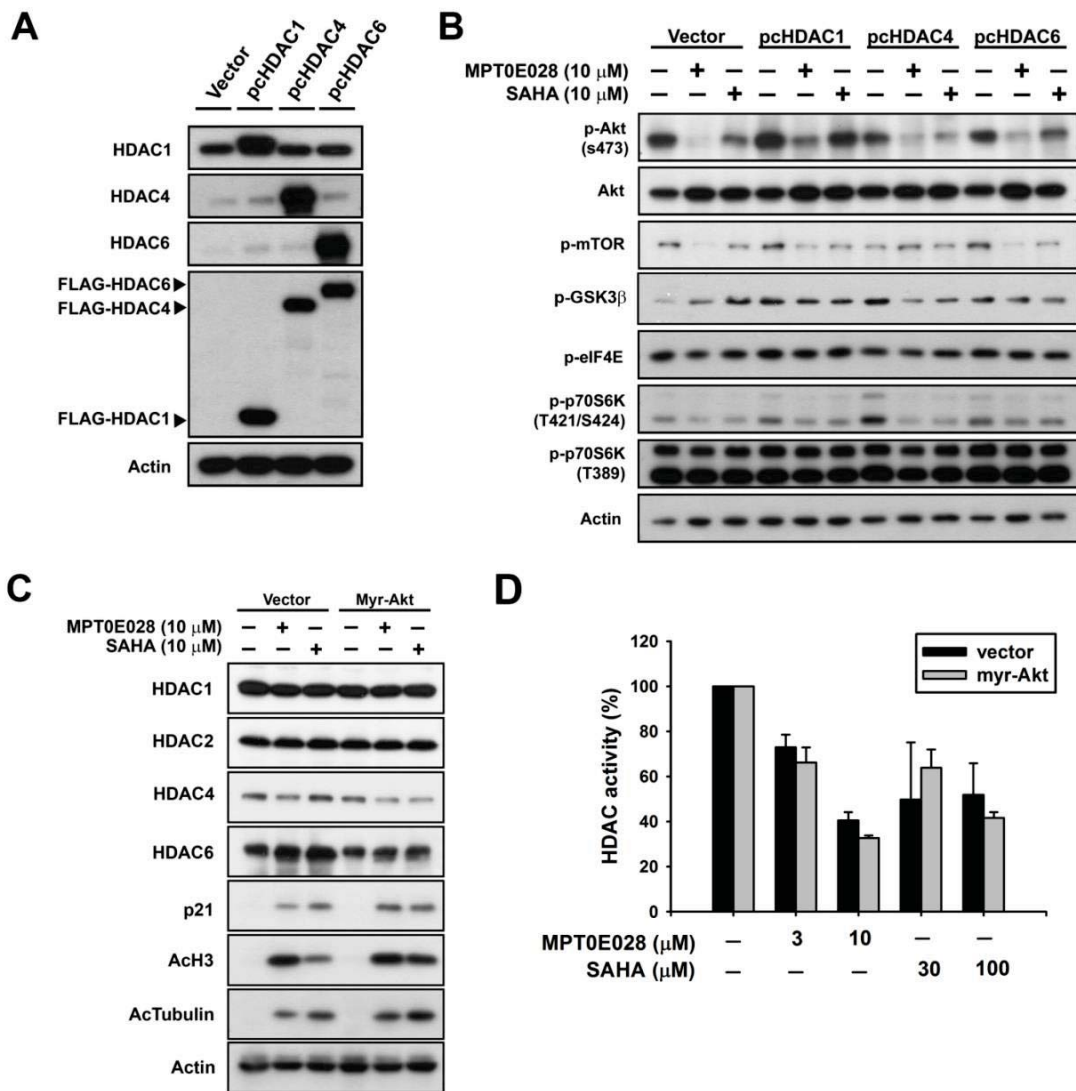
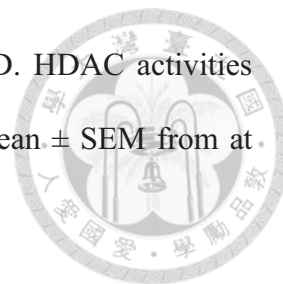


Figure 4-4. The relationship between HDACs and Akt under the effect of MPT0E028. A. Confirmation of transfection efficiency of HDACs. B. Contribution of HDACs to MPT0E028-inhibited Akt phosphorylation. C. Contribution of Akt to MPT0E028-regulated HDAC protein, marker expression, and D. MPT0E028-inhibited HDAC enzyme activity. BJAB cells were transiently transfected with plasmids encoding vector (pcDNA 3.1), flag-tagged human HDAC1, 4, and 6 or myr-Akt by using nucleofection described in Materials and Methods. Cells were treated with indicated concentration of MPT0E028 or SAHA for 24 h and whole cell lysates were subjected to western blotting for A. HDAC proteins, flag, B. Akt, Akt downstream

proteins, C. HDACs and HDAC inhibition marker detection and D. HDAC activities detection as described in Materials and Methods. Data represent mean \pm SEM from at least three independent experiments.



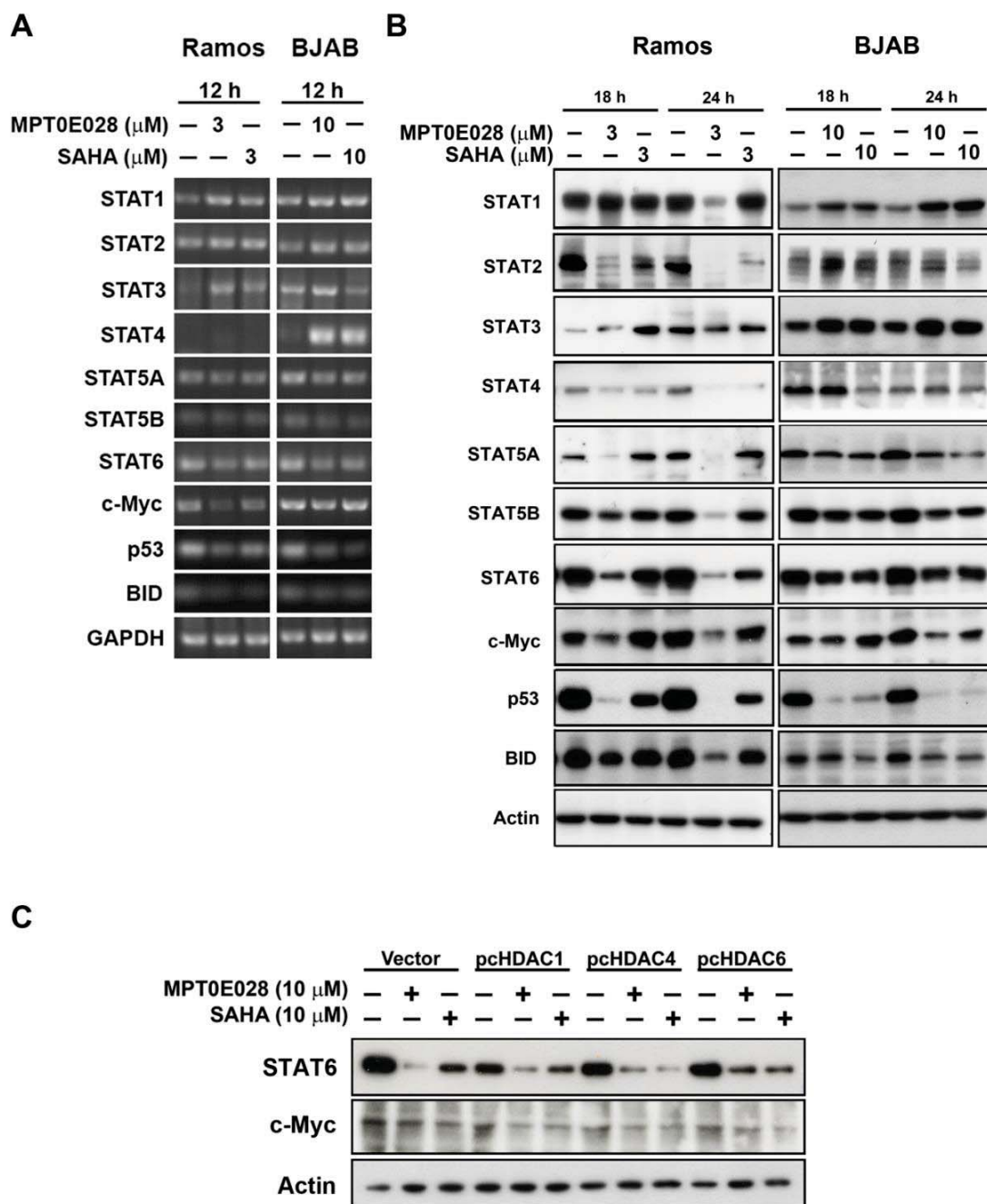
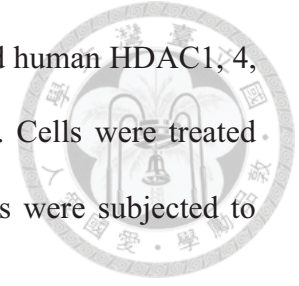


Figure 4-5. MPT0E028 affects the gene expression in multiple ways in lymphoma cells. A. mRNA expression of genes of interest. Cells were treated with MPT0E028 or SAHA for 12 h and then harvest for mRNA detection. B. Protein expression of genes of interest. Cells were treated with MPT0E028 or SAHA for the indicated time interval and then harvested for western blotting detection. C. the role of HDACs in MPT0E028-inhibited STAT6 and c-myc expression. BJAB cells were transiently

transfected with plasmids encoding vector (pcDNA 3.1), flag-tagged human HDAC1, 4, and 6 by using nucleofection described in Materials and Methods. Cells were treated with 10 μ M MPT0E028 or SAHA for 24 h and whole cell lysates were subjected to western blotting.



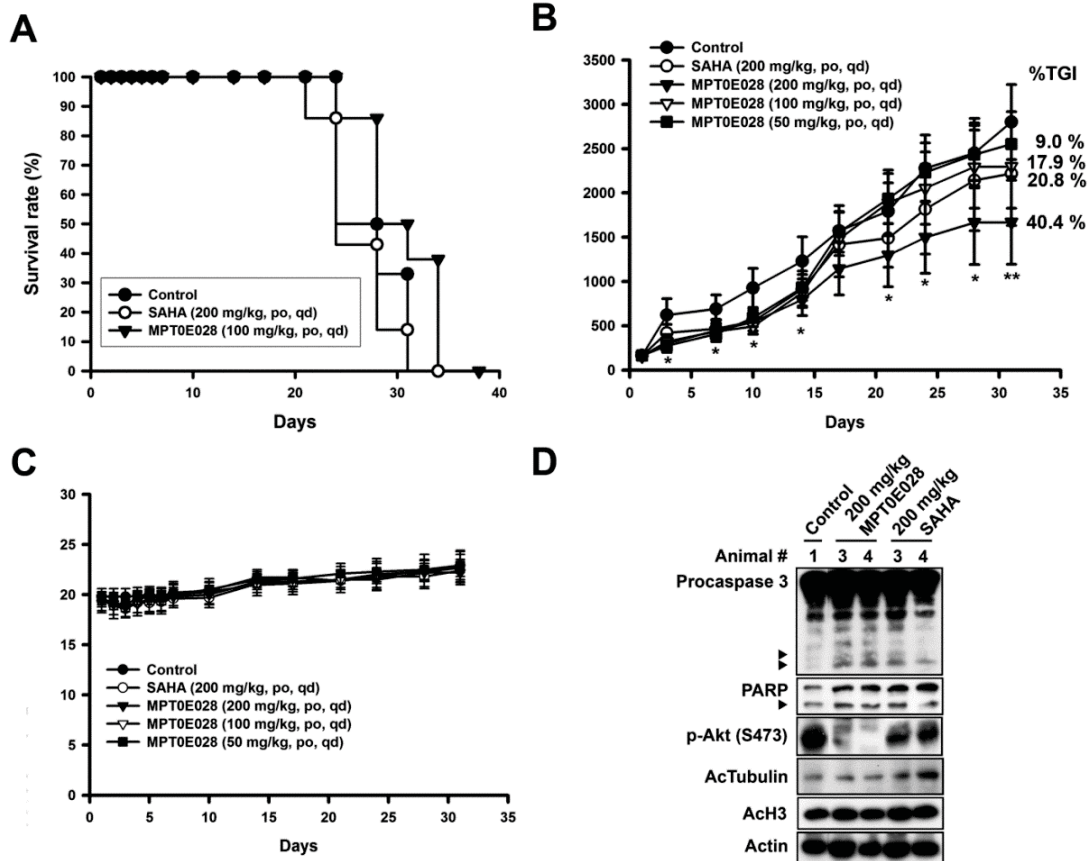
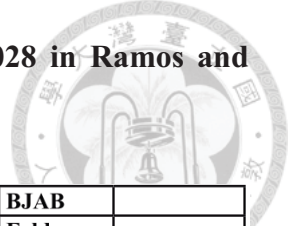


Figure 4-6. Antitumor effect of MPT0E028 *in vivo*. A. MPT0E028-prolonged survival rate in Ramos engraftment model. NOD/SCID mice were engrafted with Ramos cells via tail vein injection. Mice were treated with vehicle, MPT0E028 (100 mg/kg) or SAHA (200 mg/kg) daily by oral gavage. B. MPT0E028-inhibited tumor growth in nude mice bearing the BJAB tumors. Nude mice were treated with vehicle or 50-200 mg/kg of MPT0E028 or 200 mg/kg of SAHA daily by oral gavage for 31 days. Seven mice per group were used in the xenograft experiment (* $P < 0.05$; ** $P < 0.01$). C. Body weight of the BJAB tumor bearing mice under the treatment during the study. Data represent mean \pm SEM from seven mice in each group. D. BJAB xenograft tumors were subjected to western analysis for caspase 3, PARP, p-Akt (S473), acetyl-histone 3, and acetyl- α -tubulin detection.

Table 4-1. Expressed genes of interest in response to MPT0E028 in Ramos and BJAB cells.



Accession #	Gene symbol	Gene name	Ramos		BJAB	
			Fold change	P-value	Fold change	P-value
NM_007315.3	STAT1	signal transducer and activator of transcription 1, 91kDa	1.66	2.87E-8	1.77	2.57E-12
NM_005419.3*	STAT2	signal transducer and activator of transcription 2, 113kDa	1.16	9.46E-8	1.39	0.013
NM_213662.1 [§]	STAT3	signal transducer and activator of transcription 3 (acute-phase response factor)	1.71	7.64E-10	1.39	5.40E-10
NM_003151.2	STAT4	signal transducer and activator of transcription 4	N/A	N/A	4.05	1.94E-15
NM_003152.3	STAT5A	signal transducer and activator of transcription 5A	N/A	N/A	-2.15	8.23E-15
NM_012448.3	STAT5B	signal transducer and activator of transcription 5B	N/A	N/A	-1.23	7.61E-8
NR_033659.1 [†]	STAT6	signal transducer and activator of transcription 6	-1.57	2.59E-7	-1.71	2.62E-10
NM_002467.4	MYC	v-myc myelocytomatosis viral oncogene homolog (avian)	-3.40	1.68E-28	N/A	N/A
NM_001196.2 [‡]	BID	BH3 interacting domain death agonist	-2.19	1.19E-22	-1.78	1.61E-11
NM_000546.4 [£]	TP53	tumor protein p53	-2.95	2.78E-16	-2.06	2.17E-14

Ramos and BJAB cells were treated with 3 μ M and 10 μ M MPT0E028 respectively for 12 h, and then total cellular RNA was extracted for microarray analysis. Each unique splice variant of specific gene was also tested. Different accession numbers are given.

*STAT2: NM_198332.1; [§]STAT3: NM_003150.3, NM_139276.2; [†]STAT6: NM_001178079.1, NM_001178080.1, NM_003153.4, NM_001178081.1, NM_001178078.1; [‡]BID: NM_197967.1, NM_197966.1; [£]TP53: NM_001126115.1, NM_001126116.1, NM_001126113.1, NM_001126117.1, NM_001126114.1

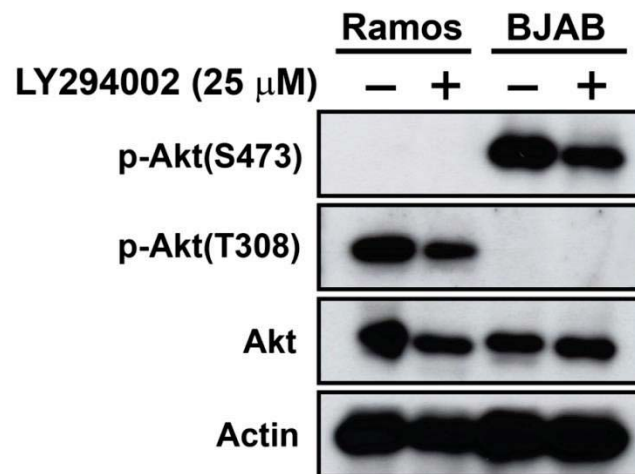
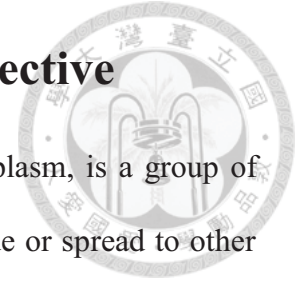


Figure 4-S1. Basal expression of p-Akt in Ramos and BJAB cells. Both cells were treated with 25 μ M of LY294002 for 24 h and harvested for p-Akt (S473), p-Akt (T308), and Akt detection using western blotting.



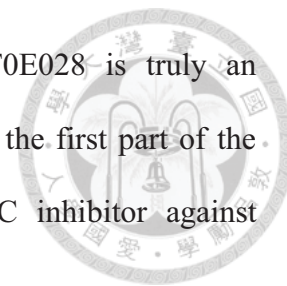
Chapter 5 Conclusions and Perspective



Cancer, also known as a malignant tumor or malignant neoplasm, is a group of diseases involving abnormal cell growth with the potential to invade or spread to other parts of the body. Owing to the heterogeneity and recurrent relapse of cancer, it becomes the tough problem affecting human health. Curing cancer and improve quality of life become the urgent need in recent years but somehow there are no satisfactory therapies to date. Targeting therapy against oncoproteins involved in cancer pathogenesis has emerged its role in cancer treatment, one of these are HDAC inhibitors. Although there are many HDAC inhibitors in clinical trials, we want to provide an oral and potent HDAC inhibitor with dual functions targeting both HDAC and Akt to be a promising agent against human colorectal carcinoma and B cell lymphoma.

Colorectal cancer is the third most common type of cancer diagnosed and common cause of cancer-related deaths both in Taiwan and the United States. Although detailed treatment guideline has been established using surgery and chemotherapy, people still looking for promising new therapy due to high mortality rate. HDAC inhibitor target therapy is one of the investigated options. In the first part of the thesis, we evaluated the anticancer mechanism of the novel oral HDAC inhibitor, MPT0E028, in human colorectal cancer. According to NCI-60 screening assay, MPT0E028 exert its potency most against HCT116 human colorectal cancer cells. Our results showed that MPT0E028 can induce apoptosis stronger than SAHA *in vitro* and *in vivo*, the first HDAC inhibitor approved by the FDA. We determined the antitumor effect of MPT0E028 *in vivo* using HCT116 xenograft model. Results showed that MPT0E028 could inhibit colorectal cancer growth *in vivo*. By detecting HDAC enzyme activity using recombinant proteins and whole cell proteins, as well as the expression of

well-known HDAC-targeted markers, we determined that MPT0E028 is truly an effective anticancer drug against HDAC. According to our data in the first part of the thesis, we demonstrated that MPT0E028 is a promising HDAC inhibitor against colorectal malignancy.



Clinical approved HDAC inhibitors are approved as orphan drugs to treat cutaneous T-cell lymphoma (CTCL), peripheral T-cell lymphoma (PTCL) and multiple myeloma (MM). However, there were no potent HDAC inhibitors against human B-cell lymphomas. In the second part of this thesis, we evaluate the antitumor effect of MPT0E028 in this kind of disease. MPT0E028 could also induce significant apoptosis effect in B-cell lymphoma cells, whereas inhibit HDAC enzyme activity stronger than SAHA. We also found that MPT0E028 could significantly inhibit Akt phosphorylation, which serve as an important survival signal. Based on kinome diversity screening assay, we found that MPT0E028 may directly bind and inhibit Akt kinase activity. Transient transfection assay showed that HDAC and Akt both contributed to MPT0E028-induced apoptosis with each function independently. *In vivo* data revealed that MPT0E028 could prolong survival rate of B-cell lymphoma bearing mice and inhibit tumor growth in B-cell lymphoma xenograft model. These data indicated that MPT0E028 exhibit potent antitumor effect against B-cell lymphoma.

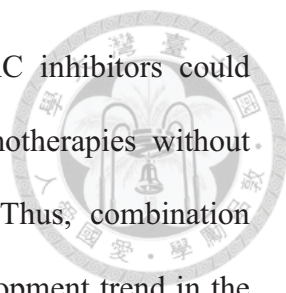
In conclusion, our data suggest that MPT0E028 is a promising and effective anti-cancer HDAC inhibitor against human colorectal carcinoma and B-cell lymphoma. Its antitumor activities include inducing apoptosis, HDAC activity inhibition, Akt pathway deactivation, and regulation of many genes *in vitro* (Fig. 5-1); and prolongation of survival rate and reduction of tumor volume *in vivo*, which showed

greater efficacy compared to SAHA. Taken together, our results provide compelling evidence that MPT0E028 may be a promising HDAC inhibitor for new anticancer therapeutic option.



In addition to the effect of MPT0E028 on colorectal cancer and B-cell lymphoma, MPT0E028 also showed significant antitumor effect on prostate cancer, hepatic cancer, lung cancer, breast cancer, leukemia and pancreatic cancer *in vivo* animal models. Our lab cooperates with Professor Jing-Ping Liou (Taipei Medical University) and Associate Professor Shioh-Lin Pan (Taipei Medical University) to develop MPT0E028, which made great progress in the early 2014. MPT0E028 has been approved for Investigational New Drug (IND) Application by FDA to enter phase I clinical trial against advanced solid malignancies. Since approved HDAC inhibitors are all for hematological malignancies to date, the possible role of MPT0E028 as a first HDAC inhibitor against solid malignancies is noteworthy. According to this thesis, the antitumor effect of MPT0E028 seems show more profound effect against colon cancer. The possible explanation may due to the c-myc and STATs protein depletion effect and Akt-targeting ability of MPT0E028. All these factors have been found that overexpressed in colon cancer whereas c-myc has shown its role in HDAC inhibitor prediction marker in solid tumors (Talbert, Wappel et al. 2013), which may possibly contribute to the antitumor effect of MPT0E028. However, detailed mechanisms still need to be further elucidated.

According to our previous studies, MPT0E028 also showed significant synergism with tyrosine kinase target therapy inhibitors, such as erlotinib and sorafenib, in non-small cell lung cancer (NSCLC) and liver cancer (Chen, Chen et al. 2013; Chen,



Chen et al. 2014). Many clinical trials also indicated that HDAC inhibitors could synergize with other target therapy inhibitors or traditional chemotherapies without additional toxicity but synergistic clinical activity (Table 5-1). Thus, combination therapy using HDAC inhibitors in cancer treatment may be a development trend in the future, which suggests a promising role of MPT0E028 in cancer combination therapy. In addition to anti-cancer effect, MPT0E028 also shows anti-angiogenesis, anti-metastasis and anti-fibrosis ability (unpublished data), which may also broaden the usage of MPT0E028.

Until now, no differences in the clinical activity and adverse effects could be determined between pan-HDAC inhibitors and isoform-selective HDAC inhibitors. Therefore, the hypothesis that isoform-selective HDAC inhibitors could reveal a greater clinical benefit with less toxicity has yet to be proven. However, developments of isoform-selective HDAC inhibitors still make contribution no matter to research field or to clinical. MGCD0103, a class I isoform selective HDAC inhibitor, also shows significant antitumor effect and has entered phase II clinical trial. Recently, HDAC6-selective inhibitors are emerging interest because the relation to the modulation of acetylated non-histone proteins implicated in cancer-relevant processes, including cell migration, metastasis, angiogenesis and apoptosis pathways. Therefore, developing isotype-specific HDAC inhibitors may play some role in cancer therapy in the future.

In order to develop HDAC inhibitors successfully, there are some roadblocks for HDAC inhibitors that need to overcome, which are poor bioavailability, ineffectiveness for solid tumors and off-target toxicity (Gryder, Sodji et al. 2012) (Fig. 5-2).

MPT0E028 has been formulated and successfully increased bioavailability from 10% to around 30%. According to this thesis, MPT0E028 also showed significant antitumor effect against solid tumor and showed no significant toxicity. In conclusion, MPT0E028 is a promising anticancer agent. It is the first local new drug candidate designed, researched and developed by local academic circle in Taiwan, representing a milestone for local biotechnology industry. Our main purpose is to develop anticancer agents to become therapeutic medication in cancer therapy. Look forward to the report of success from MPT0E028 to be a new therapeutic option in cancer treatment in the near future.

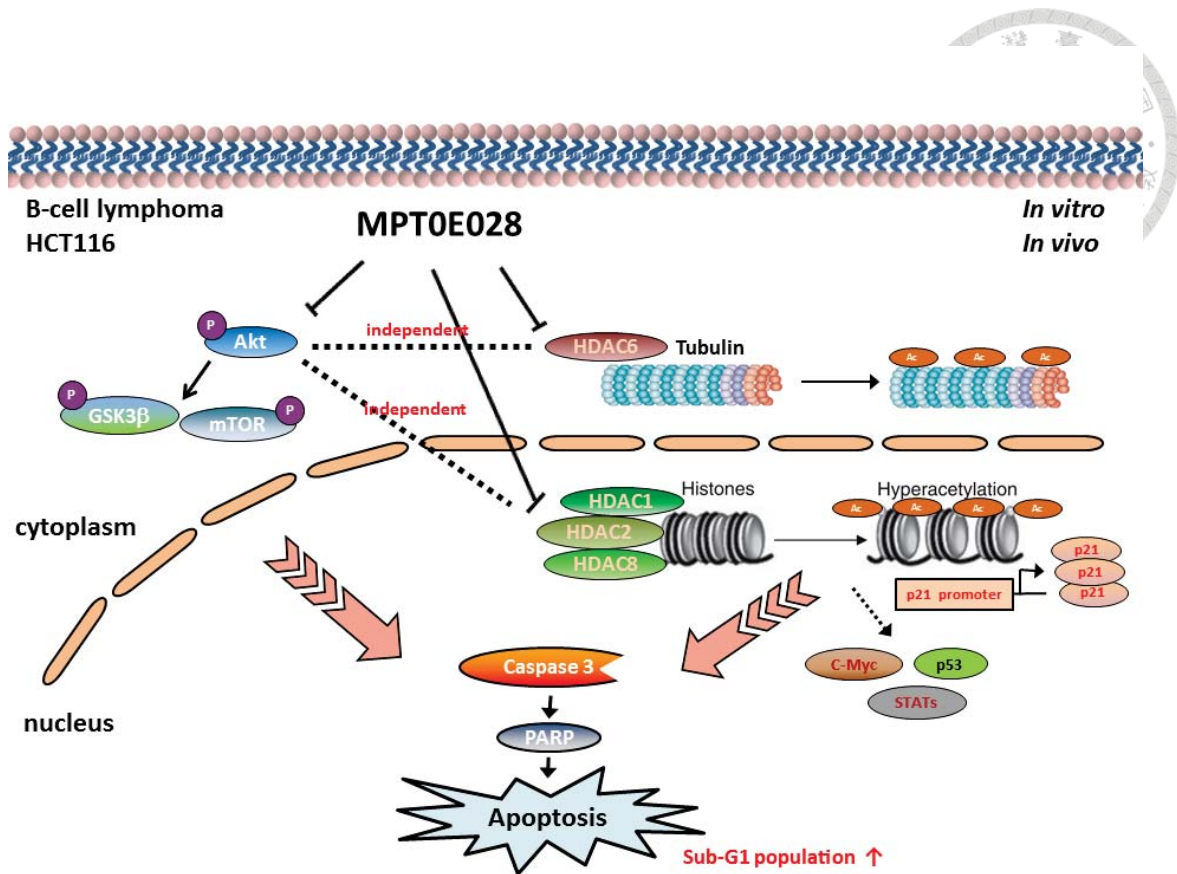


Figure 5-1. Summary of anticancer mechanisms of MPT0E028 in human colorectal cancer and B-cell lymphoma.

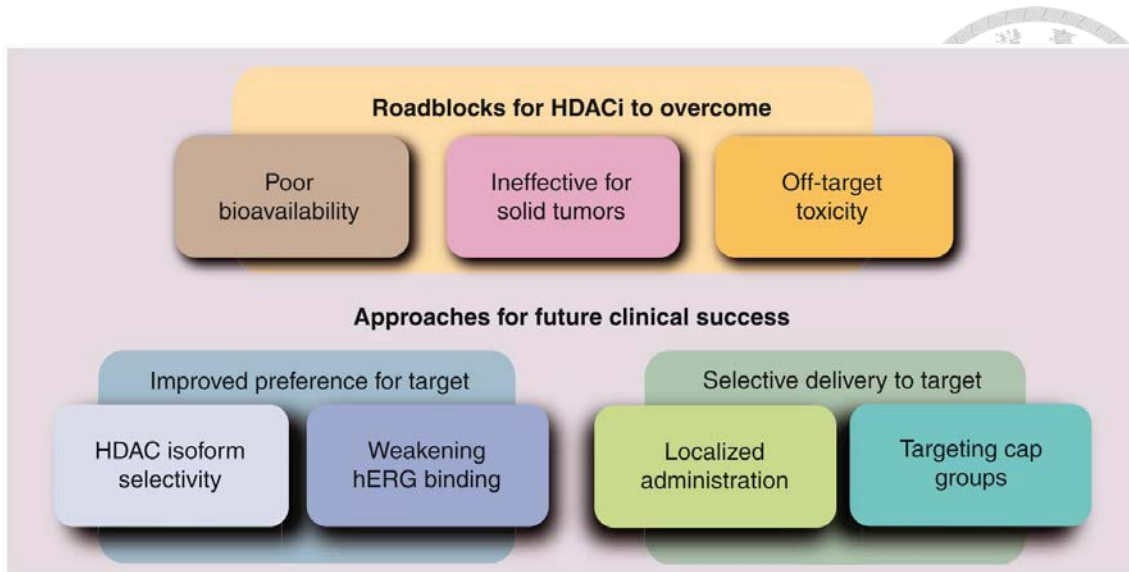


Figure 5-2. Overcoming clinical roadblocks to histone deacetylase inhibitor cancer therapy. (Gryder, Sodji et al. 2012)

Table 5-1. Rational combinations with histone deacetylase inhibitors: current Phase II/III clinical trials.



HDACi	Cancer	Combination(s)
Vorinostat	Breast	Paclitaxel/trastuzumab/doxorubicin/cyclophosphamide; carboplatin/nab-paclitaxel; bevacizumab/paclitaxel; capecitabine; lapatinib
	Glioma	Bevacizumab/temozolomide; temozoloamide/radiation therapy
	Glioblastoma multiforme	Carboplatin/isotretinoin; erlotinib/carboplatin
	NSCLC	Gefitinib; paclitaxel/radiation therapy
	Pancreatic	Fluorouracil/radiation therapy
	Ovarian	Carboplatin/paclitaxel
	Ovarian, fallopian tube or peritoneal	Carboplatin/gemcitabine
	Colorectal	Fluorouracil/leucovorin
	Renal	Carboplatin/isotretinoin
	Lymphoma	Pegylated liposomal doxorubicin
	T-cell lymphoma	Cyclophosphamide/vincristine/doxorubicin/prednisone
	DLBCL	Rituximab/cyclophosphamide/vincristine/prednisone
	Large B-cell lymphoma	Rituximab/cyclophosphamide/etoposide/prednisone
	HIV-associated DLBCL	Rituximab/cyclophosphamide/vincristine/doxorubicin/prednisone
Panobinostat	Breast	Trastuzumab; letrozole
	Prostate	Bicalutamide
	Renal cell	Everolimus
	Melanoma	Decitabine/temozolomide
	Multiple myeloma and lymphomas	Everolimus
Valproic acid	Breast	5-fluorouracil/epirubicin/cyclophosphamide
	Gliomas	Temozolomide/radiation therapy; bevacizumab/radiation therapy
	Ovarian	Azacytidine/carboplatin; hydralazine
	Cervical	Hydralazine
	Small-cell lung carcinoma	Adriamycin/cyclophosphamide/vindesine
	Mesothelioma	Doxorubicin
	Sarcomas	Bevacizumab/gemcitabine/docetaxel
	MDS	5-azacytidine/ATRA
	MDS/AML	Decitabine; 5-azacytidine/ATRA
	AML	Decitabine/ATRA
Belinostat	NSCLC	Carboplatin/paclitaxel/bevacizumab; erlotinib
	Ovarian, fallopian tube or primary peritoneal cancer	Carboplatin
	Cancer of unknown primary	Carboplatin/paclitaxel
	Soft tissue sarcoma	Doxorubicin
	Thymic malignancies	Cisplatin/doxorubicin/cyclophosphamide
Entinostat	NSCLC	Azacitadine
	Colorectal	Azacitadine
PCI-24781	Soft tissue sarcoma	Doxorubicin

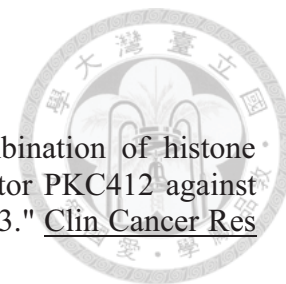
(Thurn, Thomas et al. 2011)

Publications

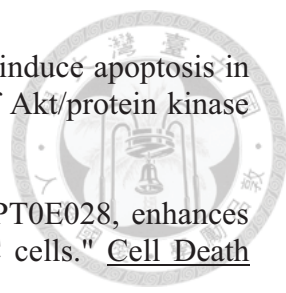


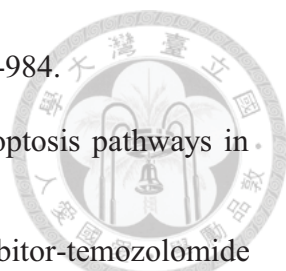
1. **Huang HL**, Peng CY, Lai MJ, Chen CH, Lee HY, Wang JC, Liou JP, Pan SL, Teng CM. Novel oral histone deacetylase inhibitor, MPT0E028, displays potent growth-inhibitory activity against human B-cell lymphoma in vitro and in vivo. *Oncotarget*. 2014 Dec 31. [Epub ahead of print]
2. Lee HY, Yang CR, Lai MJ, **Huang HL**, Hsieh YL, Liu YM, Yeh TK, Li YH, Mehndiratta S, Teng CM, Liou JP. 1-arylsulfonyl-5-(N-hydroxyacryl-amide)indoles histone deacetylase inhibitors are potent cytokine release suppressors. *Chembiochem*. 2013 Jul 8;14(10):1248-54.
3. **Huang HL**, Lee HY, Tsai AC, Peng CY, Lai MJ, Wang JC, Pan SL, Teng CM, Liou JP. Anticancer activity of MPT0E028, a novel potent histone deacetylase inhibitor, in human colorectal cancer HCT116 cells in vitro and in vivo. *PLoS One*. 2012;7(8):e43645.
4. Lai MJ*, **Huang HL***, Pan SL*, Liu YM, Peng CY*, Lee HY, Yeh TK, Huang PH, Teng CM, Chen CS, Chuang HY, Liou JP. Synthesis and biological evaluation of 1-arylsulfonyl-5-(N-hydroxyacrylamide)indoles as potent histone deacetylase inhibitors with antitumor activity in vivo. *J Med Chem*. 2012 Apr 26;55(8):3777-91.
(*Contributed equally)

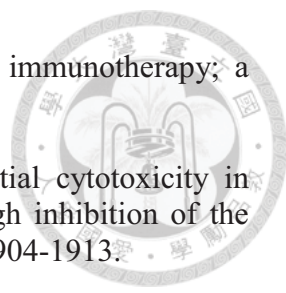
References




- Bali, P., P. George, et al. (2004). "Superior activity of the combination of histone deacetylase inhibitor LAQ824 and the FLT-3 kinase inhibitor PKC412 against human acute myelogenous leukemia cells with mutant FLT-3." Clin Cancer Res **10**(15): 4991-4997.
- Bali, P., M. Pranpat, et al. (2005). "Inhibition of histone deacetylase 6 acetylates and disrupts the chaperone function of heat shock protein 90: a novel basis for antileukemia activity of histone deacetylase inhibitors." J Biol Chem **280**(29): 26729-26734.
- Blagosklonny, M. V., R. Robey, et al. (2002). "Histone Deacetylase Inhibitors All Induce p21 but Differentially Cause Tubulin Acetylation, Mitotic Arrest, and Cytotoxicity." Mol Cancer Ther **1**(11): 937-941.
- Blagosklonny, M. V., S. Trostel, et al. (2005). "Depletion of mutant p53 and cytotoxicity of histone deacetylase inhibitors." Cancer Res **65**(16): 7386-7392.
- Boland, C. R. and A. Goel (2005). "Somatic evolution of cancer cells." Semin Cancer Biol **15**(6): 436-450.
- Bolden, J. E., M. J. Peart, et al. (2006). "Anticancer activities of histone deacetylase inhibitors." Nat Rev Drug Discov **5**(9): 769-784.
- Bruserud, O., C. Stapnes, et al. (2007). "Histone deacetylase inhibitors in cancer treatment: a review of the clinical toxicity and the modulation of gene expression in cancer cells." Current Pharmaceutical Biotechnology **8**(6): 388-400.
- Buglio, D., G. V. Georgakis, et al. (2008). "Vorinostat inhibits STAT6-mediated TH2 cytokine and TARC production and induces cell death in Hodgkin lymphoma cell lines." Blood **112**(4): 1424-1433.
- Chang, J.-Y., H.-P. Hsieh, et al. (2006). "7-Aroyl-aminoindoline-1-sulfonamides as a Novel Class of Potent Antitubulin Agents." Journal of Medicinal Chemistry **49**(23): 6656-6659.
- Chang, J.-Y., M.-J. Lai, et al. (2010). "Synthesis and biological evaluation of 7-arylindoline-1-benzenesulfonamides as a novel class of potent anticancer agents." MedChemComm **1**(2): 152.
- Chen, C. H., M. C. Chen, et al. (2014). "Synergistic interaction between the HDAC inhibitor, MPT0E028, and sorafenib in liver cancer cells in vitro and in vivo." Clin Cancer Res **20**(5): 1274-1287.
- Chen, C. S., S. C. Weng, et al. (2005). "Histone acetylation-independent effect of histone deacetylase inhibitors on Akt through the reshuffling of protein phosphatase 1 complexes." J Biol Chem **280**(46): 38879-38887.

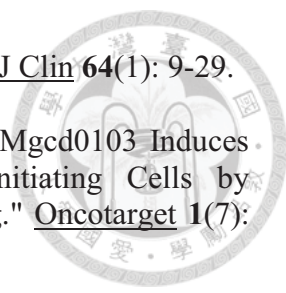
- 
- Chen, J., F. M. Ghazawi, et al. (2006). "Valproic acid and butyrate induce apoptosis in human cancer cells through inhibition of gene expression of Akt/protein kinase B." Mol Cancer **5**: 71.
- Chen, M. C., C. H. Chen, et al. (2013). "The HDAC inhibitor, MPT0E028, enhances erlotinib-induced cell death in EGFR-TKI-resistant NSCLC cells." Cell Death Dis **4**: e810.
- Cheng, G., S. Park, et al. (2008). "Advances of Akt pathway in human oncogenesis and as a target for anti-cancer drug discovery." Current Cancer Drug Targets **8**(1).
- Chi, X. Z., J. O. Yang, et al. (2005). "RUNX3 suppresses gastric epithelial cell growth by inducing p21(WAF1/Cip1) expression in cooperation with transforming growth factor {beta}-activated SMAD." Mol Cell Biol **25**(18): 8097-8107.
- Cross, D. A. E., D. R. Alessi, et al. (1995). "Inhibition of glycogen synthase kinase-3 by insulin mediated by protein kinase B." Nature **378**(6559): 785-789.
- Darvas, K., S. Rosenberger, et al. (2010). "Histone deacetylase inhibitor-induced sensitization to TNFalpha/TRAIL-mediated apoptosis in cervical carcinoma cells is dependent on HPV oncogene expression." Int J Cancer **127**(6): 1384-1392.
- Denlinger, C. E., B. K. Rundall, et al. (2005). "Inhibition of phosphatidylinositol 3-kinase/Akt and histone deacetylase activity induces apoptosis in non-small cell lung cancer in vitro and in vivo." J Thorac Cardiovasc Surg **130**(5): 1422-1429.
- Dokmanovic, M., C. Clarke, et al. (2007). "Histone deacetylase inhibitors: overview and perspectives." Mol Cancer Res **5**(10): 981-989.
- Ellis, L., S. Ku, et al. (2013). "Combinatorial antitumor effect of HDACs and the PI3K-Akt-mTOR pathway inhibition in a Pten deficient model of prostate cancer." Oncotarget **4**(12): 2225-2236.
- Engelman, J. A. (2009). "Targeting PI3K signalling in cancer: opportunities, challenges and limitations." Nat Rev Cancer **9**(8): 550-562.
- Falkenberg, K. J. and R. W. Johnstone (2014). "Histone deacetylases and their inhibitors in cancer, neurological diseases and immune disorders." Nat Rev Drug Discov **13**(9): 673-691.
- Fearnhead, N. S., J. L. Wilding, et al. (2002). "Genetics of colorectal cancer: hereditary aspects and overview of colorectal tumorigenesis." British Medical Bulletin **64**(1): 27-43.
- Fearon, E. R. and B. Vogelstein (1990). "A genetic model for colorectal tumorigenesis." Cell **61**(5): 759-767.
- Fuino, L., P. Bali, et al. (2003). "Histone deacetylase inhibitor LAQ824 down-regulates Her-2 and sensitizes human breast cancer cells to trastuzumab, taxotere,

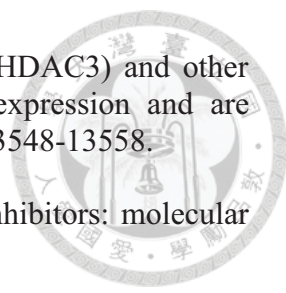
- 
- gemcitabine, and epothilone B." Mol Cancer Ther **2**(10): 971-984.
- Fulda, S. and K. M. Debatin (2006). "Extrinsic versus intrinsic apoptosis pathways in anticancer chemotherapy." Oncogene **25**(34): 4798-4811.
- Gatti, L., A. Sevko, et al. (2014). "Histone deacetylase inhibitor-temozolomide co-treatment inhibits melanoma growth through suppression of Chemokine (C-C motif) ligand 2-driven signals." Oncotarget **5**(12): 4516-4528.
- Glozak, M. A., N. Sengupta, et al. (2005). "Acetylation and deacetylation of non-histone proteins." Gene **363**: 15-23.
- Gryder, B. E., Q. H. Sodji, et al. (2012). "Targeted cancer therapy: giving histone deacetylase inhibitors all they need to succeed." Future Medicinal Chemistry **4**(4): 505-524.
- Gueugnon, F., P.-F. Cartron, et al. (2014). "New histone deacetylase inhibitors improve cisplatin antitumor properties against thoracic cancer cells." Oncotarget **5**(12): 4504-4515.
- Ha, K., W. Fiskus, et al. (2014). "Histone deacetylase inhibitor treatment induces 'BRCAness' and synergistic lethality with PARP inhibitor and cisplatin against human triple negative breast cancer cells." Oncotarget **5**(14): 5637-5650.
- Hassig, C. A., K. T. Symons, et al. (2008). "KD5170, a novel mercaptoketone-based histone deacetylase inhibitor that exhibits broad spectrum antitumor activity in vitro and in vivo." Mol Cancer Ther **7**(5): 1054-1065.
- Hennessy, B. T., D. L. Smith, et al. (2005). "Exploiting the PI3K/AKT pathway for cancer drug discovery." Nat Rev Drug Discov **4**(12): 988-1004.
- Huang, H.-L., H.-Y. Lee, et al. (2012). "Anticancer Activity of MPT0E028, a Novel Potent Histone Deacetylase Inhibitor, in Human Colorectal Cancer HCT116 Cells In Vitro and In Vivo." PLoS One **7**(8): e43645.
- Johnston, P. B., R. Yuan, et al. (2010). "Targeted therapy in lymphoma." J Hematol Oncol **3**: 45.
- Juan, L. J., W. J. Shia, et al. (2000). "Histone deacetylases specifically down-regulate p53-dependent gene activation." J Biol Chem **275**(27): 20436-20443.
- Kazantsev, A. G. and L. M. Thompson (2008). "Therapeutic application of histone deacetylase inhibitors for central nervous system disorders." Nat Rev Drug Discov **7**(10): 854-868.
- Khosravi-Far, R., E. White, et al. (2007). Histone Deacetylase Inhibitors: Mechanisms and Clinical Significance in Cancer: HDAC Inhibitor-Induced Apoptosis Programmed Cell Death in Cancer Progression and Therapy, Springer Netherlands. **615**: 261-298.

- 
- Kroesen, M., P. R. Gielen, et al. (2014). "HDAC inhibitors and immunotherapy; a double edged sword?" Oncotarget; Vol 5, No 16.
- Li, D., N. D. Marchenko, et al. (2011). "SAHA shows preferential cytotoxicity in mutant p53 cancer cells by destabilizing mutant p53 through inhibition of the HDAC6-Hsp90 chaperone axis." Cell Death Differ **18**(12): 1904-1913.
- Liu, P., H. Cheng, et al. (2009). "Targeting the phosphoinositide 3-kinase pathway in cancer." Nat Rev Drug Discov **8**(8): 627-644.
- LoPiccolo, J., G. M. Blumenthal, et al. (2008). "Targeting the PI3K/Akt/mTOR pathway: effective combinations and clinical considerations." Drug Resist Updat **11**(1-2): 32-50.
- Ma, X., H. H. Ezzeldin, et al. (2009). "Histone Deacetylase Inhibitors: Current Status and Overview of Recent Clinical Trials." Drugs **69**(14): 1911-1934
1910.2165/11315680-000000000-000000000.
- Mahadevan, D. and R. I. Fisher (2011). "Novel therapeutics for aggressive non-Hodgkin's lymphoma." J Clin Oncol **29**(14): 1876-1884.
- Mann, B. S., J. R. Johnson, et al. (2007). "FDA approval summary: vorinostat for treatment of advanced primary cutaneous T-cell lymphoma." Oncologist **12**(10): 1247-1252.
- Manning, B. D. and L. C. Cantley (2007). "AKT/PKB signaling: navigating downstream." Cell **129**(7): 1261-1274.
- Mariadason, J. M. (2008). "HDACs and HDAC inhibitors in colon cancer." Epigenetics **3**(1): 28-37.
- Marks, P. A. and R. Breslow (2007). "Dimethyl sulfoxide to vorinostat: development of this histone deacetylase inhibitor as an anticancer drug." Nat Biotechnol **25**(1): 84-90.
- Marks, P. A. and W. S. Xu (2009). "Histone deacetylase inhibitors: Potential in cancer therapy." J Cell Biochem **107**(4): 600-608.
- Mehrotra, P., J. P. Riley, et al. (2011). "PARP-14 functions as a transcriptional switch for Stat6-dependent gene activation." J Biol Chem **286**(3): 1767-1776.
- Mercurio, C., S. Minucci, et al. (2010). "Histone deacetylases and epigenetic therapies of hematological malignancies." Pharmacol Res **62**(1): 18-34.
- Nakagawa, M., Y. Oda, et al. (2007). "Expression profile of class I histone deacetylases in human cancer tissues." Oncol Rep **18**: 769-774.
- Nishioka, C., T. Ikezoe, et al. (2008). "Blockade of mTOR signaling potentiates the ability of histone deacetylase inhibitor to induce growth arrest and differentiation of acute myelogenous leukemia cells." Leukemia **22**(12):

2159-2168.

- 
- Nogai, H., B. Dorken, et al. (2011). "Pathogenesis of non-Hodgkin's lymphoma." J Clin Oncol **29**(14): 1803-1811.
- Pal, S. K., K. Reckamp, et al. (2010). "Akt inhibitors in clinical development for the treatment of cancer." Expert Opinion on Investigational Drugs **19**(11): 1355-1366.
- Patel, J. H., Y. Du, et al. (2004). "The c-MYC oncoprotein is a substrate of the acetyltransferases hGCN5/PCAF and TIP60." Mol Cell Biol **24**(24): 10826-10834.
- Paull, K., E. Hamel, et al. (1995). Prediction of biochemical mechanism of action from the in vitro antitumor screen of the National Cancer Institute, in Cancer Chemotherapeutic Agents. Cancer chemotherapeutic agents. W. Foye. Washington, DC, American Chemical Society.
- Peart, M. J., G. K. Smyth, et al. (2005). "Identification and functional significance of genes regulated by structurally different histone deacetylase inhibitors." Proc Natl Acad Sci U S A **102**(10): 3697-3702.
- Price, T. J., E. Segelov, et al. (2013). "Current opinion on optimal treatment for colorectal cancer." Expert Review of Anticancer Therapy **13**(5): 597-611.
- Prince, H. M., M. J. Bishton, et al. (2009). "Clinical studies of histone deacetylase inhibitors." Clin Cancer Res **15**(12): 3958-3969.
- Rahmani, M., E. Reese, et al. (2005). "Coadministration of histone deacetylase inhibitors and perifosine synergistically induces apoptosis in human leukemia cells through Akt and ERK1/2 inactivation and the generation of ceramide and reactive oxygen species." Cancer Res **65**(6): 2422-2432.
- Richon, V. M., T. W. Sandhoff, et al. (2000). "Histone deacetylase inhibitor selectively induces p21WAF1 expression and gene-associated histone acetylation." Proc Natl Acad Sci U S A **97**(18): 10014-10019.
- Sato, S., N. Fujita, et al. (2000). "Modulation of Akt kinase activity by binding to Hsp90." Proc Natl Acad Sci U S A **97**(20): 10832-10837.
- Sawas, A., C. Diefenbach, et al. (2011). "New therapeutic targets and drugs in non-Hodgkin's lymphoma." Curr Opin Hematol **18**(4): 280-287.
- Shelley L, B. (2002). "Histone modifications in transcriptional regulation." Current Opinion in Genetics & Development **12**(2): 142-148.
- Shimizu, R., J. Kikuchi, et al. (2010). "HDAC inhibitors augment cytotoxic activity of rituximab by upregulating CD20 expression on lymphoma cells." Leukemia **24**(10): 1760-1768.

- 
- Siegel, R., J. Ma, et al. (2014). "Cancer statistics, 2014." CA Cancer J Clin **64**(1): 9-29.
- Sikandar, S., D. Dizon, et al. (2010). "The Class I Hdac Inhibitor Mgcd0103 Induces Cell Cycle Arrest and Apoptosis in Colon Cancer Initiating Cells by Upregulating Dickkopf-1 and Non-Canonical Wnt Signaling." Oncotarget **1**(7): 596-605.
- Spange, S., T. Wagner, et al. (2009). "Acetylation of non-histone proteins modulates cellular signalling at multiple levels." Int J Biochem Cell Biol **41**(1): 185-198.
- Stimson, L., V. Wood, et al. (2009). "HDAC inhibitor-based therapies and haematological malignancy." Ann Oncol **20**(8): 1293-1302.
- Takai, N. and H. Narahara (2007). "Human endometrial and ovarian cancer cells: histone deacetylase inhibitors exhibit antiproliferative activity, potently induce cell cycle arrest, and stimulate apoptosis." Curr Med Chem. **14**(24): 2548-2553.
- Talbert, D. R., R. L. Wappel, et al. (2013). "The Role of Myc and the miR-17~92 Cluster in Histone Deacetylase Inhibitor Induced Apoptosis of Solid Tumors." Journal of Cancer Therapy **04**(04): 907-918.
- Taub, R., I. Kirsch, et al. (1982). "Translocation of the c-myc gene into the immunoglobulin heavy chain locus in human burkitt lymphoma and murine plasmacytoma cells." Proc Natl Acad Sci U S A **79**: 7837-7841.
- Taylor, R. C., S. P. Cullen, et al. (2008). "Apoptosis: controlled demolition at the cellular level." Nat Rev Mol Cell Biol **9**(3): 231-241.
- Thurn, K. T., S. Thomas, et al. (2011). "Rational therapeutic combinations with histone deacetylase inhibitors for the treatment of cancer." Future Oncol **7**(2): 263-283.
- Tsapis, M., M. Lieb, et al. (2007). "HDAC inhibitors induce apoptosis in glucocorticoid-resistant acute lymphatic leukemia cells despite a switch from the extrinsic to the intrinsic death pathway." Int J Biochem Cell Biol **39**(7-8): 1500-1509.
- Verheul, H. M., B. Salumbides, et al. (2008). "Combination strategy targeting the hypoxia inducible factor-1 alpha with mammalian target of rapamycin and histone deacetylase inhibitors." Clin Cancer Res **14**(11): 3589-3597.
- Vivanco, I. and C. L. Sawyers (2002). "The phosphatidylinositol 3-Kinase AKT pathway in human cancer." Nat Rev Cancer **2**(7): 489-501.
- Wedel, S., L. Hudak, et al. (2011). "Impact of combined HDAC and mTOR inhibition on adhesion, migration and invasion of prostate cancer cells." Clin Exp Metastasis **28**(5): 479-491.
- Whittaker, S. J., M. F. Demierre, et al. (2010). "Final results from a multicenter, international, pivotal study of romidepsin in refractory cutaneous T-cell lymphoma." J Clin Oncol **28**(29): 4485-4491.

- 
- Wilson, A. J., D. S. Byun, et al. (2006). "Histone deacetylase 3 (HDAC3) and other class I HDACs regulate colon cell maturation and p21 expression and are deregulated in human colon cancer." J Biol Chem **281**(19): 13548-13558.
- Xu, W. S., R. B. Parmigiani, et al. (2007). "Histone deacetylase inhibitors: molecular mechanisms of action." Oncogene **26**(37): 5541-5552.
- Zhang, X., X. Chen, et al. (14 June 2012). "Myc represses miR-15a/miR-16-1 expression through recruitment of HDAC3 in mantle cell and other non-Hodgkin B-cell lymphomas." Oncogene **31**: 3002-3008.
- Zhu, P., E. Martin, et al. (2004). "Induction of HDAC2 expression upon loss of APC in colorectal tumorigenesis." Cancer Cell **5**(5): 455-463.
- Zopf, S., D. Neureiter, et al. (2007). "Differential response of p53 and p21 on HDAC inhibitor-mediated apoptosis in HCT116 colon cancer cells in vitro and in vivo." Int J Oncol. **31**: 1391-1402.